APPENDIX F
EROSION STUDIES

APPENDIX F
EROSION STUDIES

Erosional processes are actively changing the glacial till landscape at the Western New York Nuclear Service Center (WNYNSC), including the vicinity of the Project Premises and the New York State-licensed Disposal Area (SDA). The North and South Plateaus are being modified through stream downcutting, slope movement, gully migration, and sheet and rill erosion. The rate at which the plateaus are eroding has been the subject of numerous studies at WNYNSC over the last 30 years (WVNS 1993a, 1993b).

The objective of this appendix is to describe current understanding of the erosion processes affecting WNYNSC and the experimental observations and predictive modeling used to relate erosional process effects and rates to the site's waste isolation capability. It summarizes erosion study results and presents short- and long-term erosion rate estimates. Most of these analyses assume no engineering changes to the site drainage pattern and no erosion control measures, though two long-term model simulations were developed to examine the potential impacts of the engineered structures proposed as part of the Sitewide Close-In-Place Alternative. Long-term erosion predictions are estimated using the CHILD and SIBERIA landscape evolution models and validated using the limited amount of available site-specific data. Two sets of predictions are presented in this appendix. Section F.1 presents an overview of the processes affecting erosion at WNYNSC and the geologic context in which those processes are acting. Section F.2 discusses observations of environmental conditions related to erosion and summarizes erosion rate estimates based solely on these observations. Section F.3 describes approaches to mathematical modeling of erosion processes and presents erosion rate estimates for both short and long periods of time.

F.1   Overview of Western New York Nuclear Service Center Erosional Processes and History

F.1.1   Overview of Erosional Processes

Erosion is the loosening and removal of soil by running water, moving ice, wind, or gravity. At WNYNSC, running water is the predominate mechanism that causes erosion. Development of the topography and stream drainage patterns currently observed at WNYNSC began with the glaciation and retreat process that ended approximately 17,000 years ago. Erosion processes have affected the WNYNSC topography due to gravitational forces and water flow within the Buttermilk Creek watershed. A portion of the watershed is represented schematically in the topographic map presented as **Figure F–1**. Buttermilk Creek flows in a northwesterly direction close to the central axis of WNYNSC at an elevation approximately 30.5 meters (100 feet) below the plateau on which most of the facilities are located. On the plateau, Erdman Brook divides the Project Premises and the SDA into two areas: the North Plateau, containing the industrial area, and the South Plateau, containing the disposal areas. The entire watershed is shown in **Figure F–2**. This figure shows the Project Premises and the SDA as a small area in the central portion of the watershed.

Major erosion processes affecting WNYNSC include stream channel downcutting, stream valley rim-widening, gully advance, and, in disturbed areas, sheet and rill erosion. Each of these processes is discussed in the following paragraphs.

During precipitation events, surface water runoff can create sheet and rill flow, which can entrain and transport sediment particles. Sheet flow is a continuous film of water moving over smooth soil surfaces. Rill flow consists of a series of small rivulets connecting one water-filled hollow with another on the rougher terrain. Sheet and rill erosion occurs when the stress exerted by flow is sufficient to entrain and remove soil and sediment particles. This form of erosion is generally rare on well-vegetated surfaces, but can be significant when vegetation is sparse or absent.
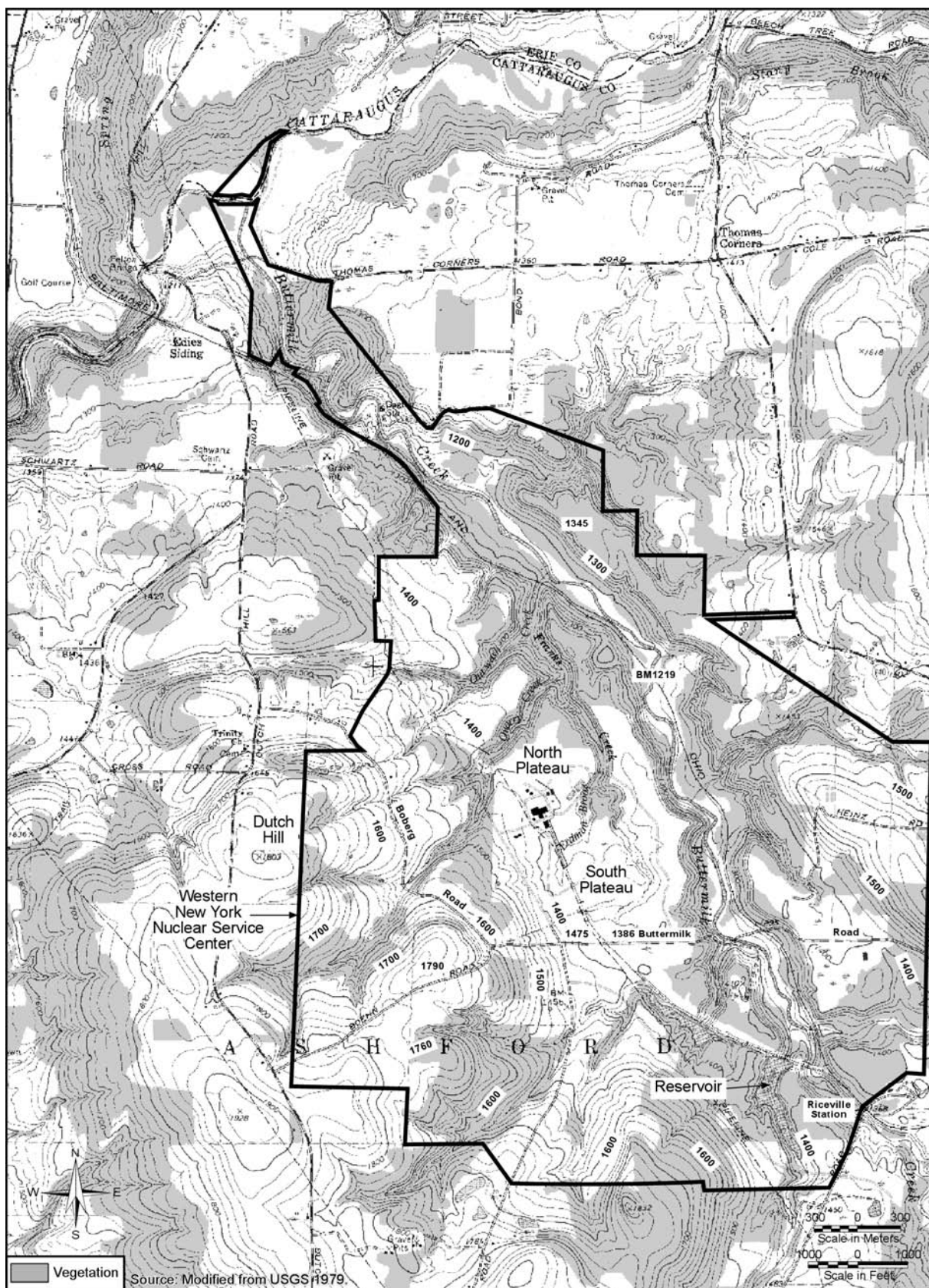
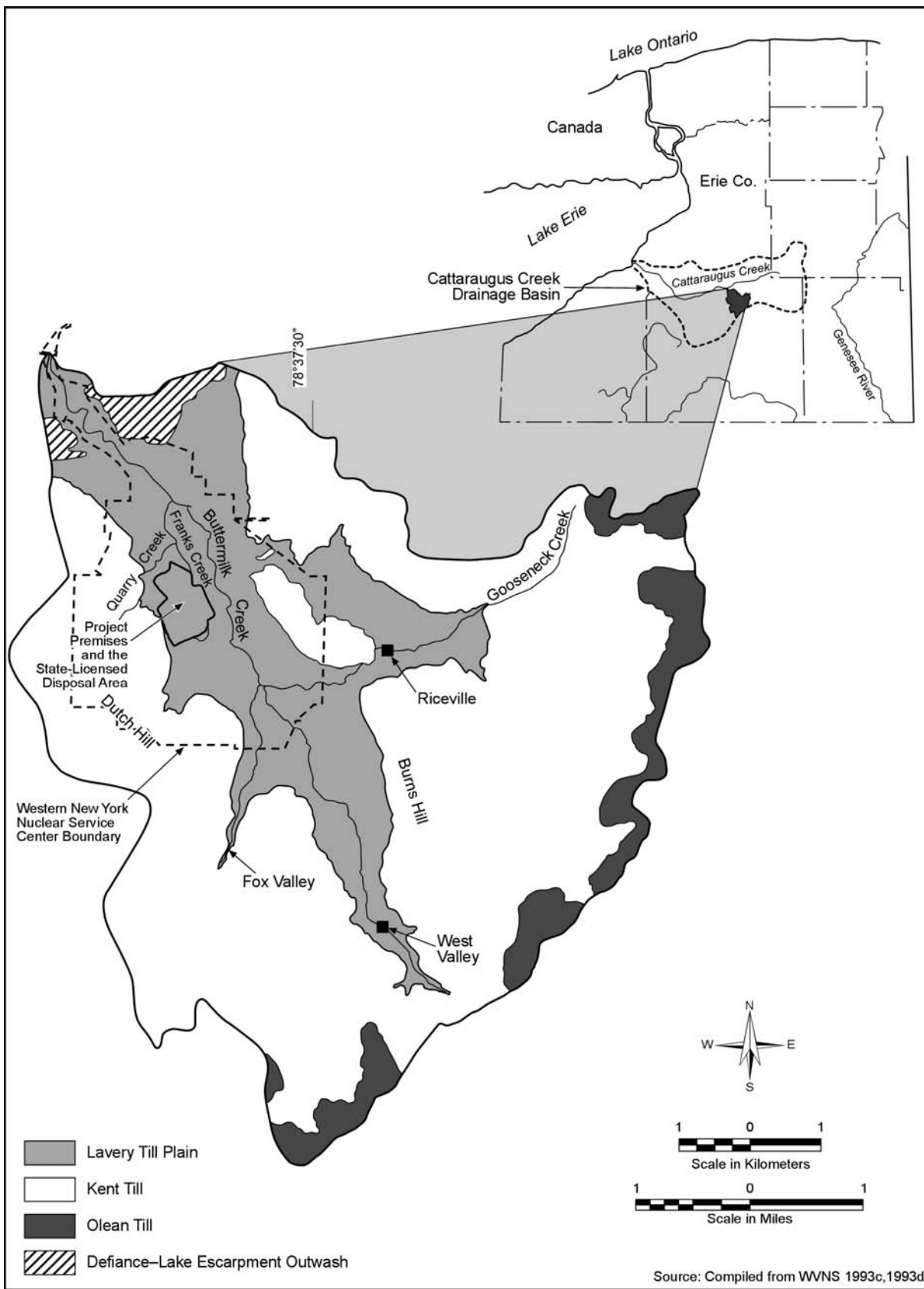**Figure F–1 Western New York Nuclear Service Center Topography**

Figure F–2 Buttermilk Creek Drainage Basin

The three small stream channels (Erdman Brook, Quarry Creek, and Franks Creek) that drain the Project Premises and the SDA are being eroded by the stream channel downcutting and valley rim-widening processes. The streams appear to be incising rapidly, as suggested by convex-upward longitudinal profiles, steep V-shaped valley-side profiles, and the paucity of floodplains over a major portion of their length. The streams within the plateau areas flow over glacial till material that is highly erodible. As channel downcutting progresses, two specific mechanisms contribute to stream rim-widening. Streambanks are undercut, causing localized slope failures (i.e., slumps and landslides). This process commonly occurs at the outside of the meander loops and produces a widening of the stream valley rim. Even in locations where there is no bank undercutting, downcutting of the stream will produce a steeper creek bank that is subject to slumping. This second mechanism also produces widening of the floodplain.

Gully advance is the third type of erosion process that results from local runoff and reflects soil characteristics. Gullies are most likely to form in areas along streambanks where slumps and deep fractures are present, seeps are flowing, and the toe of the slope intersects the outside of the meander loop. Gully growth is not a steady-state process; it occurs in response to episodic events, such as during thaws and after thunderstorms in areas where a concentrated stream of water flows over the side of a plateau, as well as in areas where groundwater pore pressure is high enough for seepage to promote grain-by-grain entrainment and removal of soil particles from the base of the gully scarp (a process sometimes known as "sapping"). Sapping causes small tunnels (or "pipes") to form in the soil at the gully base, which contributes to gully growth by undermining and weakening the scarp until it collapses. Surface water runoff into the gully also contributes to gully growth by removing fallen debris at the scarp base, undercutting side walls, and scouring the base of a head scarp. Although human-induced changes to the surface water drainage pattern can control the growth of some gullies, other natural processes that induce gully formation, such as the development of animal trails or tree falls, cannot be readily controlled.

F.1.2   Overview of Geomorphic History

The postglacial geomorphic history of the site is relevant to calibrating long-term erosion models, so it is useful to briefly review what is known about that history. The Cattaraugus Creek drainage basin empties into Lake Erie. The bedrock geology consists of late Paleozoic sedimentary rocks that dip 0.5 to 0.8 degrees to the south. Within the larger valleys, the bedrock is buried beneath a thick sequence of glacial, lacustrine, and alluvial deposits (LaFleur 1979; Boothroyd et al. 1979, 1982; Fakundiny 1985). These deposits, which are now partly dissected by stream incision, form an extensive set of low-relief, terrace-like surfaces inset into the bedrock topography. Thus, the catchment has three distinct topographic elements: (1) rounded bedrock hills with peak altitudes on the order of 550 meters (1,805 feet), (2) mid-level inset glacial terraces at an altitude of approximately 400 meters (1,312 feet), and (3) modern valley floors etched several tens of meters below the glacial terraces (see **Figure F–3**). The glacial terraces that form the "second story" in this landscape owe their existence to deposition during repeated advances of the Wisconsin ice sheet. Glacial deposits within the Buttermilk Creek Valley are composed of a series of till units representing the Olean, Kent, and Lavery advances, together with interstadial deltaic, lacustrine facies, and alluvial facies (LaFleur 1979). At its maximum extent, the ice margin reached a position several kilometers south of the Cattaraugus basin (e.g., Millar 2004). The ice margin in this area is demarcated in part by the Kent moraine, which has been correlated with the maximum ice advance some time later than 24,000 years ago (Muller and Calkin 1993).

The best constraints on the timing of glacial recession in western New York State appear to come from stratigraphic studies in the Finger Lakes region. A seismic stratigraphic study by Mullins et al. (1996) showed that the Finger Lakes were last eroded by a surge of ice at approximately 14,500 carbon-14 years before present (about 17,000 calendar years ago) that is correlated with Heinrich event H-1 (the most recent of the
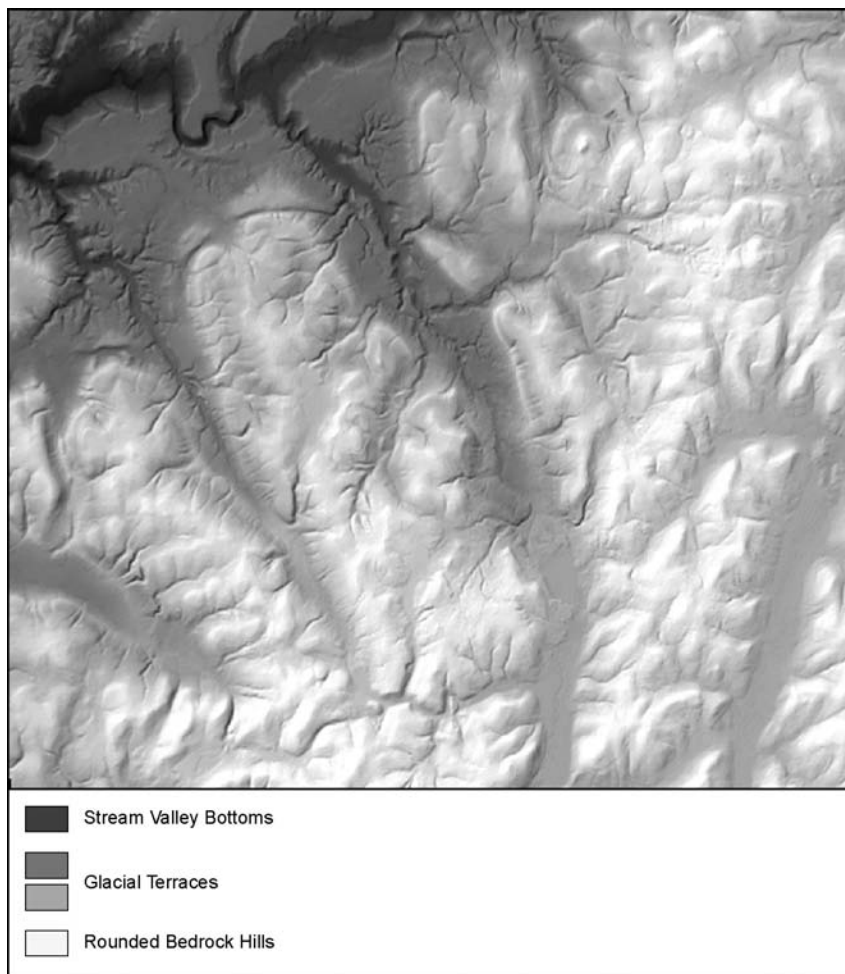
Stream Valley Bottoms

Glacial Terraces

Rounded Bedrock Hills

**Figure F–3 Shaded Relief Image of Buttermilk Creek and Vicinity, Showing
Rounded Bedrock Hills, Glacial Terraces, and Stream Valley Bottoms**

glacial North Atlantic large iceberg discharges). Radiocarbon-dated cores from Seneca Lake reveal that ice retreated rapidly from the north end of the lake at about 14,000 carbon-14 years before present (approximately 16,600 calendar years ago) (Anderson et al. 1997, Ellis et al. 2004). (Note that the difference between measured carbon-14 years and actual calendar years represents a correction applied to compensate for natural variations through time in both the production rate and concentration of carbon-14 in the earth's atmosphere; see for example Fairbanks et al. 2005 for details on calibration methods).

Cattaraugus Creek and many of its tributaries are deeply incised into the complex of unconsolidated, glacially derived sediments that fill the bedrock valleys. The depth of incision varies but is typically on the order of 60 to 70 meters (197 to 230 feet). Near the outlet of Buttermilk Creek, for example, the modern channel lies about 60 meters (197 feet) below the adjacent glacial terrace. The incision is clearly postglacial because it cuts late Wisconsinan valley fills. Although some incision during one of the later interstadials (post-Erie) cannot definitely be ruled out, the geometry of the incised portion of drainage network makes this unlikely. Incision along Cattaraugus Creek extends downstream through the Zoar Valley, a narrow, deep (approximately 150 meters [492 feet]) bedrock canyon just east of Gowanda, New York. Downstream of the Zoar Valley, relief drops markedly as the creek enters a broad, tongue-shaped valley that appears to reflect the position of a former ice lobe. It is hypothesized that incision of the Zoar Valley and the valley fills upstream of it was triggered by baselevel lowering as the ice margin retreated north from the Gowanda area. Results from optically stimulated luminescence (OSL) dating in and near Buttermilk Creek, discussed in Section F.2.2, are

consistent with this hypothesis, though additional dates from terraces along the Cattaraugus Valley upstream and downstream of the Zoar Valley would be necessary to confirm it.

F.2   Summary of Site Erosion Measurements

Site-specific historical erosion rates are important for testing the validity of any erosion predictions. Rates for the four dominant erosion processes (sheet and rill erosion, stream channel downcutting, stream valley widening, and gully advancement) for the Project Premises and the SDA have been estimated from measurements at the site. Sheet and rill erosion rates were directly measured using erosion frames at 23 locations along the stream valley banks adjacent to the Project Premises. Stream downcutting rates were determined from the age dating of terraces using carbon-14 and OSL methods and stream channel longitudinal profile measurements. The downcutting rates were translated into stream valley rim-widening rates using an estimate of the stable slope angle and geometric considerations. Gully migration rates were determined using aerial photographs and the Soil Conservation Service Technical Release 32 Method (USDA 1976). Observation of other geomorphic processes, including meandering and knickpoint advance, provides perspective but no additional quantitative information for erosion rate estimates.

These historical measurements provide perspective by which to judge the reasonableness of current erosion projections. All of these measurements, with the exception of OSL terrace dating, were collected before the current long-term erosion modeling effort was initiated and, therefore, were not designed as calibration measurements with quantifiable uncertainties. Thus, with the exception of the OSL age-dating data, specific measurements reported in this section were not directly used in the long-term modeling projections discussed in Section F.3.2.

F.2.1   Sheet and Rill Erosion Measurement

Field measurements of sheet and rill erosion on overland flow areas and mass wasting on hillslopes were taken at 23 locations along Erdman Brook, Franks Creek, and Quarry Creek using erosion frames (WVNS 1993a) (see **Figure F–4**). Each erosion frame was composed of a triangular steel structure designed to detect changes in soil depth at the point of installation. Twenty-one frames were placed on hillslopes that are close to plant facilities and contain a variety of soil types and slope angles. Two frames (EF-5 and EF-9) were placed near the edges of stream valley walls to monitor the potential slumping of large soil blocks. The frames were installed in September 1990 and initially monitored every month and subsequently, monitored at 6-month to 1-year intervals between 1993 and September 2001. In September 1995, SDA construction activities necessitated removal of frames EF-3, -4, and -5 to allow for the construction of erosion controls in the SDA gully. Also, EF-12 was removed from the monitoring program in June 1998 because it had been displaced due to a gross slump (block) failure.

The sheet and rill erosion results are shown in **Table F–1**. These results show that soil buildup (aggradation) ranging from 0.003 to 0.16 meters (0.01 to 0.52 feet) was occurring at eight locations along Erdman Brook (EF-1, -2, -7, -8, -9, -21, -22, and -23), three locations along Franks Creek (EF-16, -19, and -20), and one location along Quarry Creek (EF-10) (WVNS 1993a). Soil depletion (degradation) ranging from -0.0003 to -0.015 meters (-0.001 to -0.05 feet) was observed at one location along Quarry Creek (EF-11) and five locations on Franks Creek (EF-6, -13, -15, -17, and -18). The Quarry Creek location (EF-11) is on the slope of the NP-1 gully (see **Figure F–5**), where a stormwater outfall (SO-4) is also located. The management practice of directing runoff to this location likely accelerated the gully development; however, none of the five locations on Franks Creek where degradation occurred are near stormwater outfall locations or appear to have been influenced by stormwater management practices. No soil aggradation or degradation was measured at the EF-14 location. The largest measured erosion rate over the 11-year period was measured at frame EF-17 with an elevation change of 0.05 feet per eleven years, which is equal to a rate of 0.0014 meters (0.0046 feet) per year or 1,400 millimeters (4.6 feet) per 1,000 years.
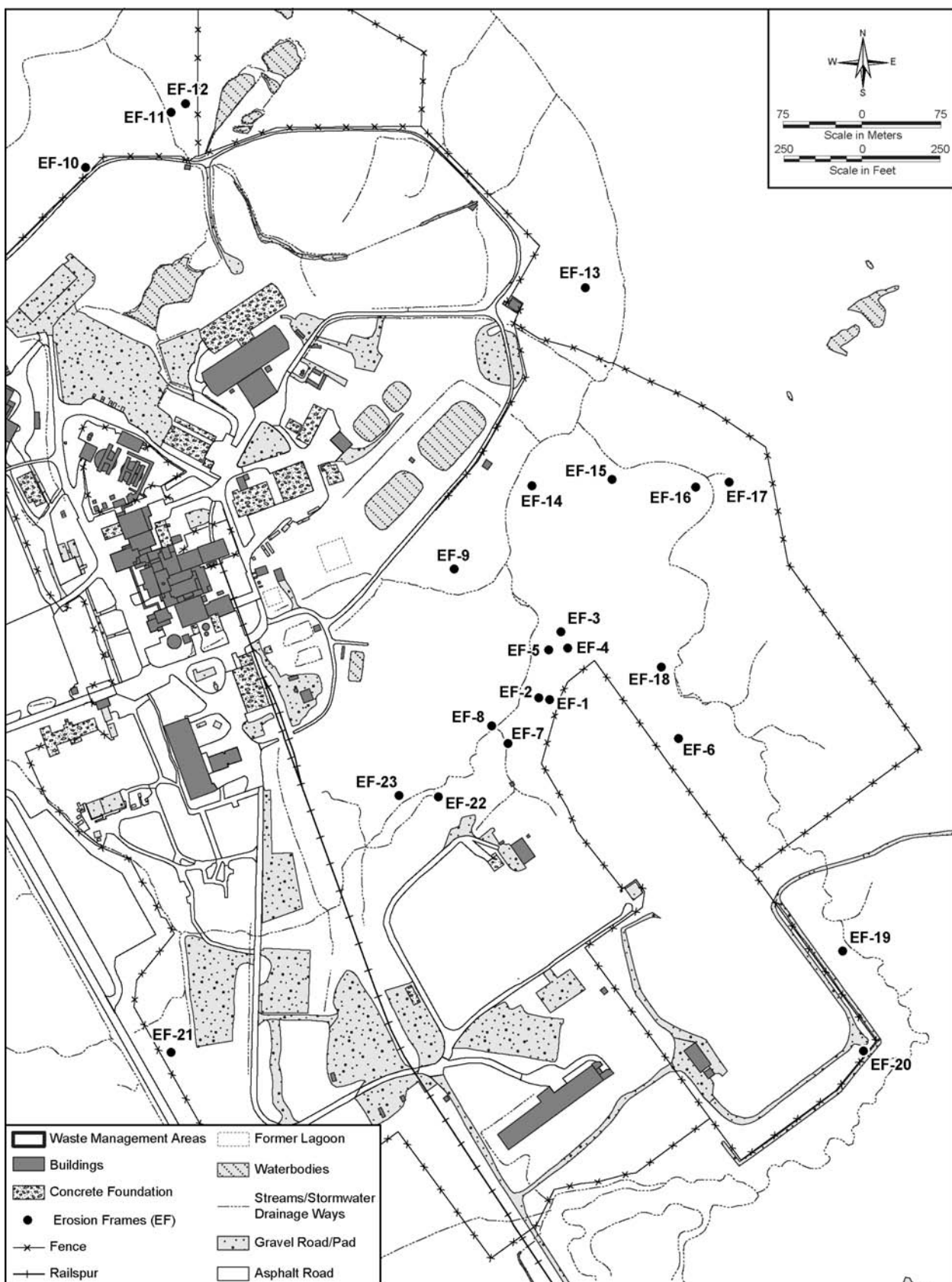
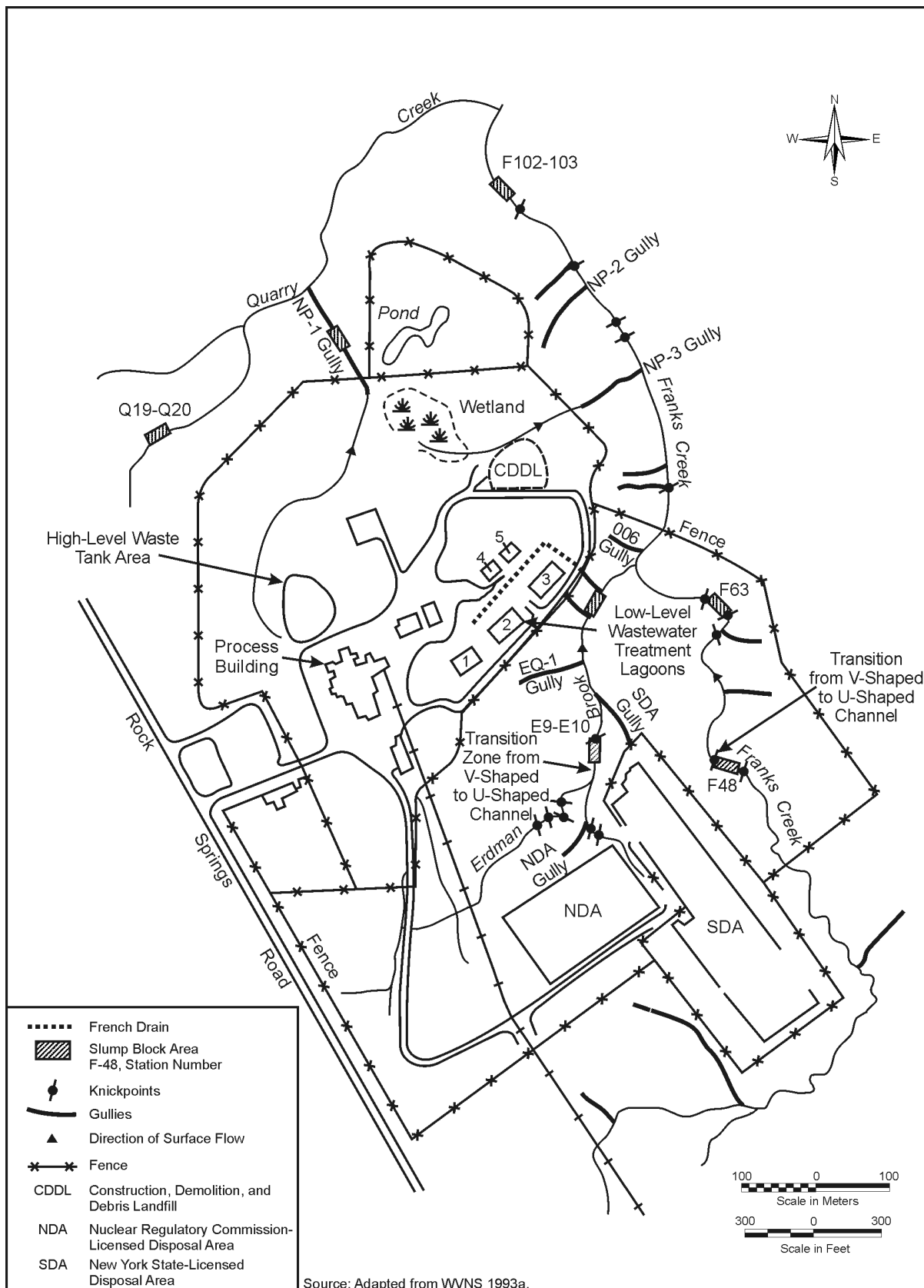**Figure F–4 Sheet and Rill Erosion Frame Measurement Locations**

Figure F–5 North and South Plateau Gully Locations

Table F–1 Sheet and Rill Erosion Measurements

Frame Number	*Frame Location*	*Elevation Change between 1990 and 2001 (feet)*
EF-1	At north end of SDA on slope to Erdman Brook	+0.39
EF-2	On slope to Erdman Brook downgradient of EF-1 location	+0.03
EF-3	Adjacent to gully located northeast of SDA	N/A
EF-4	In stream channel near northeast corner of SDA	N/A
EF-5	On flat ground near northeast corner of SDA	N/A
EF-6	At crest of a hillslope on the eastern slope of SDA	-0.02
EF-7	On ridge near northwest corner of NDA	+0.11
EF-8	On ridge along Erdman Brook	+0.10
EF-9	On flat ground south of lagoon 2	+0.04
EF-10	On plateau at north end of facilities near Quarry Creek	+0.01
EF-11	On west slope of the NP-1 gully	-0.04
EF-12	In gully NP-1 north of the security fence	N/A
EF-13	On western slope of lower Franks Creek	-0.001
EF-14	South of lagoon 3 on eastern slope of Erdman Brook	-0.000
EF-15	On south slope of Franks Creek	-0.04
EF-16	On west slope of Franks Creek	+0.07
EF-17	On eastern slope of Franks Creek	-0.05
EF-18	On west slope of Franks Creek	-0.004
EF-19	On slope outside the southeastern end of SDA	+0.52
EF-20	On slope outside the south end of SDA	+0.13
EF-21	At southwest end of site along Rock Springs Road	+0.06
EF-22	On south bank of Erdman Brook north of NDA	+0.09
EF-23	On north bank of Erdman Brook north of NDA	+0.24

SDA = State-licensed Disposal Area, N/A = frames removed due to construction activities in SDA and gross slump block failures, NDA = NRC-licensed Disposal Area, + = aggradation, - = degradation.
Note: To convert meters to feet, multiply by 3.281.

F.2.2   Stream Downcutting

Estimates of past rates of channel incision serve three purposes: they give an indication of potential future incision rates, they enable estimates of valley rim-widening (using a geometric approach described in Section F.2.3), and they provide data for testing and calibrating long-term erosion models. Rates of stream incision were estimated using two complementary methods. The first method uses dated stream terraces to estimate average incision rates during the time period since terrace abandonment. The second relies on repeated surveys of channel cross sections to assess rates of channel lowering on annual to decadal time scales.

LaFleur and Boothroyd calculated an average stream downcutting rate of approximately 6.0 meters (20 feet) per 1,000 years by means of the carbon-14 age dating of one wood fragment sample collected from the highest of 14 terrace levels on the west side of Buttermilk Creek (LaFleur 1979). The sample was extracted from a trench where wood fragments were buried 50 centimeters (20 inches) below the river gravel surface, and was determined to have an age of $9,920 \pm 240$ years before present (before present uncorrected carbon-14 years, dated by Richard Pardi, Queens College) (Boothroyd et al. 1979). Using the CalPal online radiocarbon calibration curve (http://www.calpal-online.de/), the corresponding calendar age is $11,502 \pm 507$ years before present. This age was assumed to be close to the time of initial incision and downcutting of Buttermilk Creek. Because Buttermilk Creek has eroded to a depth of 55 meters (180 feet) at the Bond Road Bridge near the

confluence with Cattaraugus Creek, Boothroyd et al. (1979) calculated a stream downcutting rate of 5.5 meters (18 feet) per 1,000 years as determined by dividing 55 meters by 10,000 years (the approximate uncalibrated age). The equivalent calculation using the calibrated age yields an average downcutting rate of 4.8 meters (15.7 feet) per 1,000 years.

In November 2006, samples for OSL dating were collected from ten locations along and near Buttermilk Creek, as shown in **Figure F–6** and **Table F–2**. Three pairs of samples (OSL 4, 8, and 9) were collected from fluvial gravels deposited on or near the plateau surface in areas isolated from tributary sediment sources. Five pairs (OSL 1, 2, 3, 5, and 6) were collected from fluvial terraces mapped by LaFleur (1979) and Boothroyd et al. (1982). An additional sample pair (OSL 7) was collected from a mid-level strath terrace in the Cattaraugus Valley near the Buttermilk confluence. The final sample pair (OSL 10), which is not shown in Figure F-6, was obtained from a high-level strath terrace in the adjacent Connoisarauley Creek Valley, which lies just to the southwest of the Buttermilk Creek watershed. Sample collection followed standard procedures for OSL sampling (http://crustal.usgs.gov/laboratories/luminescence_dating/prospective.html). The samples were processed at the U.S. Geological Survey (USGS) Luminescence Laboratory (Mahan 2007).

The OSL sample results shown in **Table F–3** were obtained using a central-age model, which is most appropriate for well-bleached samples (i.e., those with a narrow equivalent-dose histogram). Three of the samples (OSL 1A, 5A, and 8A) show tight dose-equivalent clusters, indicating that the grains within them are likely to have been well bleached. These samples are considered to be the most reliable of the group. Sample 9A suggests a date of 17,100 ± 1,390 years before present for initial incision of Buttermilk Creek; this date overlaps within one-sigma error the age estimates for the other two high-surface samples (4A and 9A; Table F–3). Of the Buttermilk Creek terrace samples, the most reliable are considered to be samples 1A and 5A (due to their narrow single-aliquot distributions, which are indicative of good bleaching). Both samples were obtained from terraces with treads lying roughly midway between the plateau surface and the modern valley floor. The central-age estimates of 14,800 ± 1,330 and 14,500 ± 1,080 years before present for samples 1A and 5A, respectively, suggest that roughly half of the incision had occurred by 13,000 to 16,000 years before present, and that the remaining incision has occurred since that time. Thus, the incision rate along Cattaraugus Creek has evidently slowed down over time. Collectively, the OSL dates suggest rapid incision from about 17,000 to 15,000 years before present and a slower incision rate from approximately 15,000 years before present to the present. The estimated rates vary somewhat with location, but are on the order of 0.01 meters (0.03 feet) per year during the early period and 0.001 meters (0.003 feet) per year during the later period.

The origin of the discrepancy between the carbon-14 age and the OSL ages is not known. One possibility is that the carbon-14 was contaminated with younger carbon. Another possibility is that the OSL samples are biased toward older ages by incompletely bleached grains, though if this were the case it would have to apply to all the samples. Resolution of the discrepancy would require additional data collection and/or analysis, such as collection of additional carbon-14 samples and/or application of alternative-age models to the OSL dose-equivalent data (e.g., the minimum-age model of Galbraith and Laslett [1993]).

The second measurement for downcutting involves comparison of elevation changes in cross-sections after 10 years. In 1980 a longitudinal profile survey was conducted by Dames and Moore (WVNS 1993a) on a section of Franks Creek starting at the Quarry Creek confluence and proceeding upstream to a point on the east side of the SDA. In 1990 a second survey was completed along the same section of Franks Creek, and a comparison of resulting data indicated a downcutting rate of approximately 0.6 meters (2 feet) per 10-year period, which is equivalent to 60 meters (200 feet) per 1,000 years. This downcutting rate is the result of direct measurement of the change in thalweg, which is the locus of the lowest points in a stream or valley depth over the 10-year period. Because this rate is based on a short (10-year) projection, it does not take into account the wider range of precipitation values that are likely to occur over the long term, and thus, is not considered to be
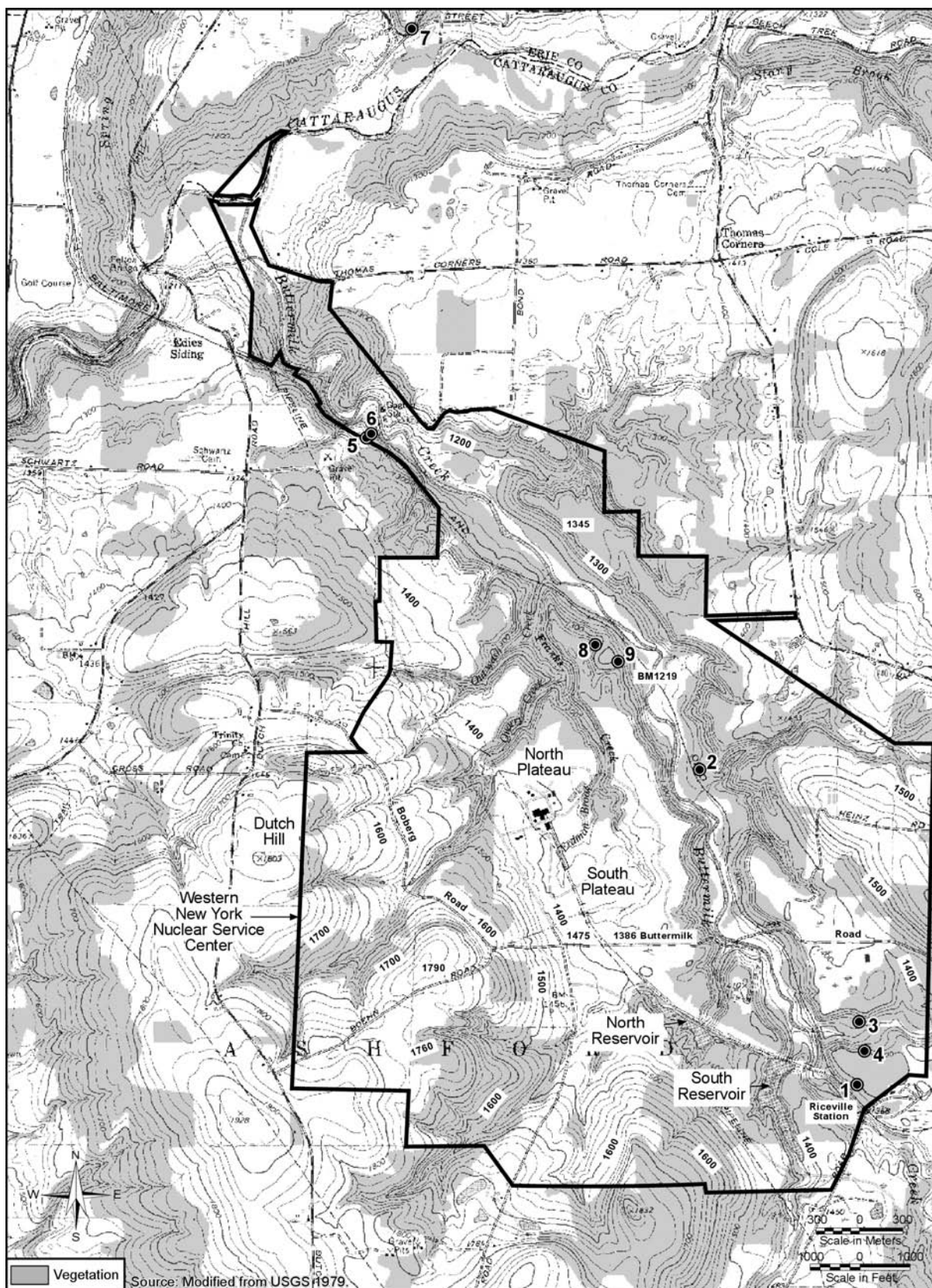
Figure F–6 Contour Map of Buttermilk Creek Showing Optically Stimulated Luminescence Sample Locations

Table F–2 Optically Stimulated Luminescence Sample Locations

Site Number	Coordinates	Altitude (meters)	Location Notes
WV-OSL-1	42.43542 N, 78.63179 W	414	Right-bank strath terrace, upper Buttermilk valley
WV-OSL-2	42.45270 N, 78.64275 W	382	Right-bank terrace, middle Buttermilk valley
WV-OSL-3	42.43885 N, 78.63079 W	410	Right-bank terrace in tributary valley
WV-OSL-4	42.43709 N, 78.63091 W	425	Gravel quarry on plateau surface, upper Buttermilk valley
WV-OSL-5	42.47130 N, 78.66745 W	379	Left-bank terrace, lower Buttermilk valley
WV-OSL-6	42.47155 N, 78.66703 W	367	Left-bank strath terrace, lower Buttermilk valley
WV-OSL-7	42.49426 N, 78.66277 W	365	Right-bank terrace, Cattaraugus valley
WV-OSL-8	42.45938 N, 78.65047 W	408	Plateau-top terrace between Franks and Buttermilk
WV-OSL-9	42.45874 N, 78.64859 W	394	Fluvial gravel over till, south end of abandoned meander loop
WV-OSL-10	42.42475 N, 78.69410 W	440	Plateau sand/gravel over till, Connoisarauley valley

Altitude represents terrace tread height rather than sample height.
Note: To convert meters to feet, multiply by 3.281.

Table F–3 Optically Stimulated Luminescence Sample Ages and Average Incision Rates

Sample Number	Central-Age Model Date (ky ± 1σ)	Depth Below Plateau (meters)	Height Above Valley Floor (meters)	Pre-terrace Incision Rate (meters per 1,000 years)	Post-terrace Incision Rate (meters per 1,000 years)
1A	14.8 ± 1.33	14	18	6.5	1.2
2A	16.2 ± 1.31	42	9	52	0.56
3A	16.7 ± 0.88	20	10	66	0.60
4A	16.1 ± 2.01	5	25	5.3	1.6
5A	14.5 ± 1.08	32	28	13	1.9
6A	15.0 ± 2.04	44	16	22	1.1
7A	15.2 ± 1.82	40	25	22	1.6
8A	16.8 ± 1.53	7	45	N/A	2.7
9A	17.1 ± 1.39	21	31	N/A	1.8
10A	21.2 ± 1.17	N/A	N/A	N/A	N/A

Depth below plateau and height above valley floor estimated from contour map and/or digital elevation model.
Post-terrace incision rate based on assumed start time of incision of 17 thousand years before AD 1950.
ky = 1,000 years, 1σ = one standard deviation.
Note: To convert meters to feet, multiply by 3.281.

representative of long-term conditions. The 10-year projection also relies heavily on the current status of land use in the watershed, which is industrial in the vicinity of WNYNSC. The larger percentage of impervious areas associated with the industrial complex results in higher surface water runoff rates than are expected to occur following decommissioning.

F.2.3   Historical Stream Valley Rim-Widening

Stream valley rim-widening rates were calculated using estimates of the stream channel downcutting rates and the stream valley stable slope angle. The estimate of stable slope angle was determined from measurements of slope movement rates on several stream valley slopes that are actively slumping. The average downcutting rate, as estimated from dated terraces and the longitudinal profile study, was translated into a rim-widening rate by dividing the downcutting rate by the tangent of the stable slope angle.

F.2.3.1   Rim-Widening Estimates Based on Stream Downcutting Measurements

Dames and Moore studied the ravine angle of slopes within the Buttermilk Creek Drainage Basin to estimate the angle of stable slopes. They measured 21 cross-sections along Quarry Creek, Franks Creek, and Erdman Brook using the 0.61-meter (2-foot) contour interval on a topographic map compiled by stereo-photogrammetric methods from 1:6,000-scale aerial photographs taken on May 17, 1989, and compiled by Tallamy, Van Kuren, Gertis, and Associates of Orchard Park, New York (WVNS 1993a). The cross-sections were taken in areas having rather stable stream valley walls (no evidence of active landsliding), and an average slope angle was calculated. The slope angle, approximately 21 degrees, is considered to be representative of an "at-rest" slope condition, meaning the valley walls have reached equilibrium. Slopes with angles greater than 21 degrees are viewed as potentially unstable.

A second method confirmed the estimate of a 21-degree stable-slope angle. In this second study, force balance analysis was applied to estimate the slope angles for eight areas along Erdman Brook and Franks Creek (WVNS 1993a). Five of the areas, with slope angles ranging from 18.4 to 24.9 degrees, were found to be stable. One of the areas, with a slope angle of 27 degrees, was found subject to creep. The remaining two areas, with slope angles of 26 and 38 degrees, were found to be unstable.

Using the stable-slope estimate of 21 degrees and an average downcutting rate of 5,500 millimeters (18 feet) per 1,000 years computed from the uncalibrated carbon-14 age of the high-terrace sample, the average rim-widening rate for Buttermilk Creek is 0.0143 meters (0.05 feet) per year. The equivalent figure for the calibrated carbon-14 age is 0.0125 meters (0.04 feet) per year. The same calculation can be made using rates of downcutting estimated from OSL terrace ages. Dividing the height of mid-level Buttermilk Creek terraces (sample locations 1, 2, 3, 5, and 6) by their ages yields average downcutting rates ranging from 0.6 to 1.9 meters (2.0 to 6.2 feet) per 1,000 years (Table F–3). Of these, the most reliable figures are thought to come from the well bleached samples 1A and 5A, with estimated post-15,000 years ago downcutting rates of 1.2 and 1.6 meters (3.9 to 5.2 feet) per 1,000 years, respectively. The corresponding rim-widening rates are 3.1 and 4.2 meters (10.2 to 13.8) per 1,000 years, respectively. Note, however, that downcutting estimates based on Buttermilk Creek would likely underestimate the current downcutting rate along Franks Creek, which has a partly convex-upward longitudinal profile that may indicate that it is still in a state of transient response to base-level lowering in the Buttermilk Creek Valley, and therefore incising faster than Buttermilk Creek.

The rim-widening rate was also estimated using the measured short-term downcutting rate from the longitudinal profile study of approximately 0.6 meters (2 feet) per 10 years in conjunction with an assumed 21-degree stable slope. This approach results in a rim-widening rate of 0.156 meters (0.5 feet) per year for Franks Creek (see **Table F–4**).

Table F–4 Estimates of Stream Valley Rim-Widening Based on Stream Downcutting

Location and Method	*Stream Downcutting Rate (meters per 1,000 years)*	*Stream Valley Rim-Widening Rate (meters per year)*
Buttermilk Creek (calibrated carbon-14 age dating of wood fragment)	4.8	0.0125
Buttermilk Creek (OSL dating of terrace alluvium, samples 1A and 5A)	1.2 (1A) 1.6 (5A)	0.0031 0.0042
Franks Creek (longitudinal profile survey)	60	0.156

OSL = optically stimulated luminescence.
Note: To convert meters to feet, multiply by 3.281.

F.2.3.2   Rim-Widening Estimates Based on Slope Movement Measurements

The slope movement rate was measured on active slump areas along Buttermilk Creek and Erdman Brook. In 1978 movement of a slump block on the Buttermilk Creek ravine, referred to as the "BC-6" landslide, approximately 426 meters (1,400 feet) east of the Waste Management Area 2 lagoons was analyzed (Boothroyd et al. 1979). Thirty-five steel posts were surveyed at locations on the slump block complex and adjoining slopes. Resurvey of the posts two years later yielded an estimated average downslope movement rate of 7.9 meters (26 feet) per year. This downslope movement rate corresponds to a stream valley rim-widening rate of 4.9 to 5.8 meters (16 to 19 feet) per year based on the angle of the slope (Boothroyd et al. 1982). This movement rate is believed to represent an upper estimate of the annual mass movement that has occurred on the slope because a severe storm (recurrence interval: 10 to 20 years) was recorded during the measurement period and a sand layer 4.6 meters (15 feet) thick was identified near the top of the landslide. The movement rate is also expected to be higher than the long-term average because a moderately severe storm occurred during the short measurement timeframe, inducing rapid movement and potentially skewing results toward the high end. Also, the high rate is not sustainable over the long term because slope movement slows as the slope angle tends to stabilize and eventually stops as that angle attains equilibrium; movement may be rejuvenated, however, by stream incision at the base of the slope. Over the course of a 1,000-year period, many localized areas throughout the stream valley would develop unstable slopes, which would move rapidly over a short time and then stabilize.

Along the section of Erdman Brook referred to as the "North Slope of the SDA," the New York State Geological Survey installed and surveyed 34 posts in 1982 and resurveyed the post elevations in 1983 to assess slope movement. The downslope till movement rate for the first year (1982 to 1983) was reported to be 0.2 meters (0.66 feet) per year, equivalent to a stream valley rim-widening rate of approximately 0.15 meters (0.49 feet) per year (Albanese et al. 1984). The New York State Energy Research and Development Authority (NYSERDA) resumed yearly measurements in 1991 and reported a maximum downslope till movement rate of 0.04 meters (0.12 feet) per year over the last 22 years (1982 to 2004) and a maximum of 0.02 meters (0.07 feet) per year over the last 13 years (1991 to 2004), indicating that the movement rate has slowed down over the last decade (WVNS 1993a). **Table F–5** summarizes these results.

Table F–5 Estimates of Stream Valley Rim-Widening Based on Slope Movement

Location	*Slope Movement Rate (meters per year)*	*Stream Valley Rim-Widening Rate (meters per year)*
BC-6 landslide (on Buttermilk Creek 426 meters east of the lagoons)	7.9	4.9 to 5.8
North Slope of SDA (on Erdman Brook) – first-year rate	0.2	0.15
North Slope of SDA (on Erdman Brook) – 22-year rate	0.02 to 0.04	0.015 to 0.03

SDA = State-licensed Disposal Area.
Note: To convert meters to feet, multiply by 3.281.

F.2.3.3   Measurement of Gully Advance Rates

Several existing gullies in the Buttermilk drainage basin are migrating into the edge of the North and South Plateaus. If natural gully advancement proceeds without mitigation, the gully heads could cut into the areas in which residual radioactivity could be closed in place. To address this concern, studies have been initiated to determine the gully migration rate. As shown in Figure F–5, five gullies have been mapped on the North Plateau extending from Quarry Creek (NP-1), Erdman Brook (EQ-1), and Franks Creek (NP-2, NP-3, and 006) toward the industrial area, and two have been mapped onto the South Plateau (SDA and NRC-licensed disposal Area [NDA]) extending from Erdman Brook toward the disposal facilities.

The headward advance rate of three active gullies (SDA, NP-3, and 006) was calculated (WVNS 1993a) using the Soil Conservation Service Technical Release 32 method (USDA 1976). Aerial photographs taken in 1955, 1961, 1968, 1977, 1978, 1980, 1984, and 1989 were reviewed in support of the calculation. As shown in **Table F–6**, this method indicated that the SDA gully was advancing toward SDA Disposal Trench 1 at a rate of 0.4 meters (1.2 feet) per year, implying that, without mitigation, the gully would reach the SDA fence in approximately 25 years and the trench in about 200 years. In 1995, as part of an effort to control infiltration and runoff at the SDA, the gully was reconstructed to mitigate erosion. The NP-3 gully is advancing toward the Construction and Demolition Debris Landfill at a rate of 0.7 meters (2.2 feet) per year; without mitigation, this gully will encroach upon it in about 100 years. The 006 gully is migrating toward the area between the Construction and Demolition Debris Landfill and the wastewater treatment lagoons at a rate of 0.7 meters (2.3 feet) per year. Without mitigation, this gully is predicted to reach the area in approximately 150 years; however, given the present surface water drainage course, the gully head is not likely to affect the two facilities. Other gullies on the Project Premises have not shown sufficient visible movement of the gully heads to allow for the calculation of migration rates by the Soil Conservation Service Technical Release 32 method.

Table F–6 Gully Advance Rate Measurements

Gully Name	Gully Location	Gully Advance Rate (meters per year)
SDA	On east bank of Erdman Brook north of SDA	0.4 [a]
NP-3	On west bank of lower Franks Creek, east of Construction and Demolition Debris Landfill	0.7
006	On west bank of Franks Creek, just north of confluence with Erdman Brook	0.7

SDA = State-licensed Disposal Area.
[a] The SDA gully was reconstructed in 1995 and the 0.4 meters per year rate was measured before mitigation.
Note: To convert meters to feet, multiply by 3.281.

F.3   Erosion Rate Prediction Methods

Mathematical models are used to predict the nature and rates of erosion processes. A survey of the models shows that they fall into two broad categories. Models in the first category make short-term predictions (projections considered valid for decades). These short-term models are generally based on detailed simulation of one or two distinct erosional processes. Models in the second category use upper-level conservation equations representing the combined effect of multiple erosional processes to make long-term projections (thousands of years). The following paragraphs provide a discussion of the various short- and long-term erosion models and a summary of erosion rate estimates at the West Valley Site developed using these models. Currently no single model provides a detailed representation of the variety of natural processes that, over differing spaces and times, combine to produce observed landform and stream channel configurations.

F.3.1   Short-Term Models

This section presents available, relevant, short-term erosion predictions that were made before the current long-term erosion modeling effort was initiated. The models were used to predict channel downcutting and sheet and rill erosion processes. These historical short-term erosion predictions provide perspective by which to judge the reasonableness of current erosion projections; however, the predictions reported in this section were not directly used in the calibration of the long-term modeling projections discussed in Section F.3.2.

F.3.1.1   Short-Term Sheet and Rill Erosion Prediction

Four methods were used to predict the sheet and rill erosion rate at WNYNSC. First, the Universal Soil Loss Equation (USLE) was used to predict the average annual soil loss from individual subwatershed areas that collectively represent the Franks Creek, Erdman Brook, and Quarry Creek watershed (referred to as the

"Franks Creek watershed"). Then, the Sedimentology by Distributed Model Treatment (SEDIMOT) II model was run to account for soil loss that occurs during major storm events within the same subwatershed areas. Third, the Chemicals, Runoff, and Erosion from Agricultural Management Systems (CREAMS) model was used to predict the average annual sediment yield from a small portion of the South Plateau. And fourth, the Water Erosion Prediction Project (WEPP) model was run to predict the average annual sediment yield from all the subwatershed areas within the Franks Creek watershed and to determine the sediment yield from these subwatershed areas during major storm events.

Universal Soil Loss Equation

The USLE is an empirically derived relationship developed to predict soil loss rates for agricultural conditions. The empirical equation is the product of six major factors that use the quantity of rainfall, length and average gradient of the slopes, type of soil, and type of soil cover (e.g., forest, grass, bare soil). It predicts soil loss caused by overland flow from the point of origin to a channel (Weltz et al. 1992) and does not simulate soil deposition or gully and channel erosion (Foster 1982).

The USLE equation is:

$$A = R \times K \times LS \times C \times P$$

where:

A is the potential long term average annual soil loss in metric tons per hectare per year.

R is the rainfall and runoff factor by geographic location. The greater the intensity and duration of the rainstorm, the higher the erosion potential. The runoff factor takes into account the variation in land-use conditions.

K is the soil erodibility factor. It is the average soil loss per unit area (in metric tons per hectare) for a particular soil in cultivated, continuous fallow with an arbitrarily selected slope length of 72.6 feet and a slope steepness of 9 percent. K is a measure of the susceptibility of soil particles to detachment and transport by rainfall and runoff. Texture is the principal factor affecting K, but structure, organic matter, and permeability also contribute.

LS is the slope length-gradient factor. The LS factor represents a ratio of soil loss under given conditions to soil loss at a site with the "standard" slope steepness of 9 percent and slope length of 72.6 feet. The steeper and longer the slope, the higher is the risk for erosion.

C is the crop/vegetation and management factor. It is used to determine the relative effectiveness of soil and crop management systems in preventing soil loss. The C factor is a ratio of soil loss from land under a specific crop and management system to soil loss from continuously fallow and tilled land.

P is the support practice factor. It reflects the effects of practices that will reduce the amount and rate of water runoff and thus reduce the amount of erosion. The P factor represents the ratio of soil loss by a support practice to soil loss attributable to straight-row farming up and down the slope.

The USLE method was used to predict the rate of soil loss from the hillslopes within the entire Franks Creek watershed. As shown in **Figure F–7**, the Project Premises and the SDA are near the downgradient end of the 440-hectare (1,040-acre) watershed. The watershed was divided into the same 22 subwatershed areas defined in the hydrologic modeling studies conducted by Dames and Moore (WVNS 1993c) to provide consistency in the analyses. Precipitation data were obtained from the site meteorological tower for the 1-year period of

March 1, 1990, to February 28, 1991 (WVNS 1993a). Soil erodibility values were based on standard U.S. Department of Agriculture (USDA) grain-size classifications of each soil unit, as defined in site-specific studies (WVNS 1993a). Vegetation cover values were based on a vegetation survey of the area (WVNS 1993d). Input values for cover management factors were obtained from source document tables (Wischmeier and Smith 1978). **Table F–7** summarizes input parameters used in the USLE for each of the 22 subwatershed areas and the results.
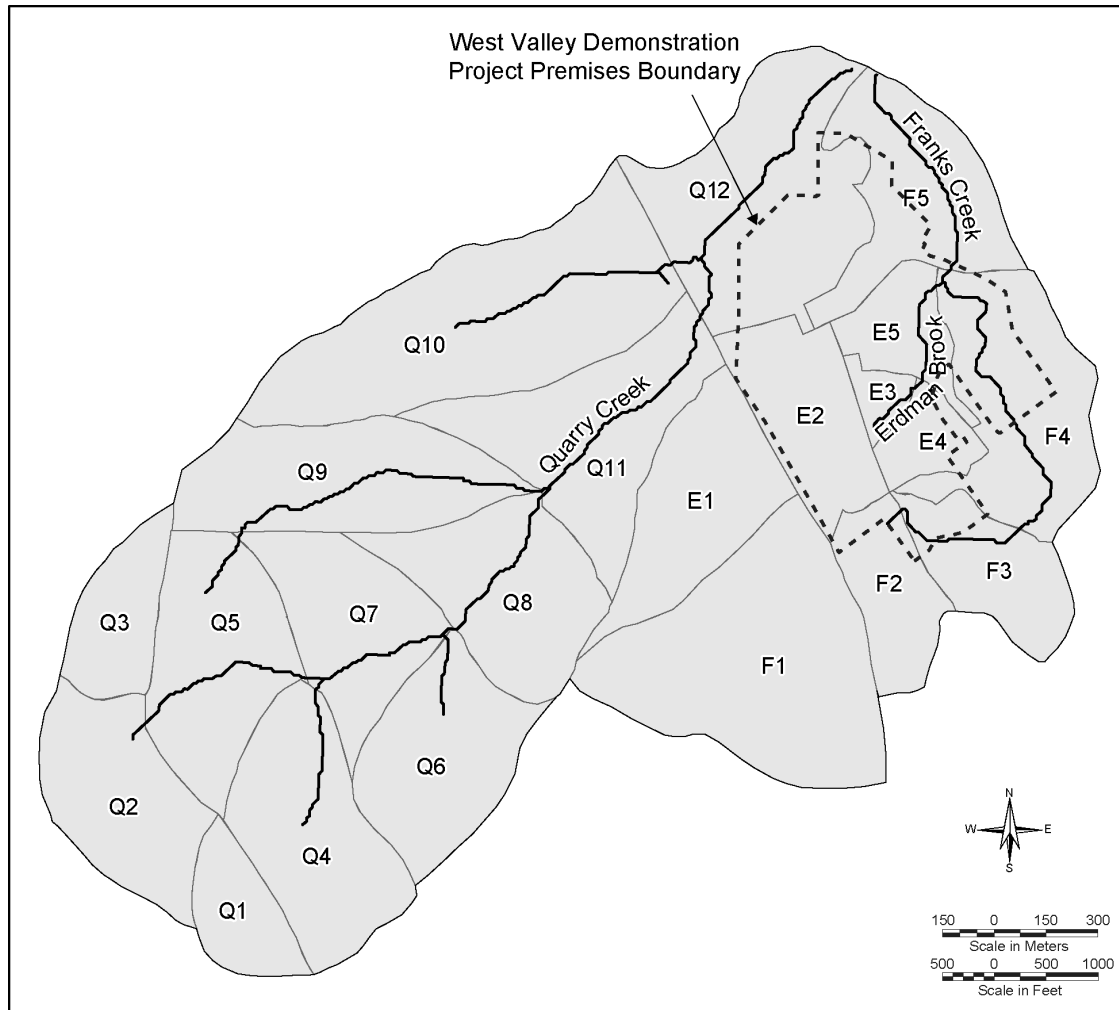

Figure F–7 USLE and SEDIMOT II Modeling Studies Subwatershed Areas

The results indicate that small quantities of soil are being removed from the hillslopes by the sheet and rill erosion process. The correlation indicates that the areas with the greatest soil loss were within the Quarry Creek Drainage Basin west and northwest of the Project Premises and within the Erdman Brook-Franks Creek Drainage Basin west and east of the Project Premises. The average soil loss for the watershed was estimated to be 0.19 metric tons per hectare (0.085 tons per acre) per year. This soil loss rate is equivalent to an average decrease in elevation of 12.8 millimeters (0.04 feet) per 1,000 years. These USLE estimates are based on only 1 year of site-specific precipitation data. USLE estimates are more accurate when applied over a period of at least 30 years, which allows effects of isolated and unpredictable short-term fluctuations to be dampened.

Table F–7 USLE Input Parameters and Results

Sub-area	Area (hectares)	R (MJ × millimeters per hectare × hour × year)	LS	K (metric tons × hectare × hour / hectare × MJ × millimeter)	K Distr. %	C	P	Soil Loss (metric tons per hectare-year)	Soil Loss (metric tons per year)
Q1	10.26	2067.33	3.2	0.0026	100	0.003	0.6	0.03	0.32
Q2	20.63	2067.33	4.3	0.0026	100	0.003	0.6	0.04	0.86
Q3	10.30	2067.33	1.8	0.0026	100	0.003	0.5	0.02	0.15
Q4	26.24	2067.33	11.0	0.0026	100	0.003	0.8	0.14	3.77
Q5	23.01	2067.33	5.0	0.0026	100	0.003	0.6	0.05	1.12
Q6	20.63	2067.33	9.1	0.0026	100	0.003	0.75	0.11	2.30
Q7	17.82	2067.33	5.8	0.0026	100	0.003	0.7	0.07	1.18
Q8	24.30	2067.33	19.2	0.0026	100	0.003	1.0	0.31	7.62
Q9	32.65	2067.33	23.4	0.0026	100	0.003	1.0	0.38	12.48
Q10	45.79	2067.33	16.9	0.0026 / 0.0020	90 / 10	0.003 / 0.003	0.8 / 0.8	0.20 / 0.02	9.14 / 0.76
Q11	26.35	2067.33	27.0	0.0026 / 0.0020	80 / 20	0.003 / 0.003	1.0 / 1.0	0.35 / 0.07	9.28 / 1.74
Q12	34.49	2067.33	3.6	0.0026 / 0.0020	60 / 40	0.003 / 0.003	0.55 / 0.55	0.02 / 0.01	0.66 / 0.34
E1	21.24	2067.33	22.5	0.0026	100	0.003	1.0	0.36	7.81
E2	12.13	2067.33	6.8	0.0026 / 0.0020	50 / 50	0.003 / 0.003	0.8 / 0.8	0.04 / 0.03	0.54 / 0.41
E3	2.99	2067.33	6.4	0.0026 / 0.0020	70 / 30	0.003 / 0.003	0.85 / 0.85	0.05 / 0.03	0.14 / 0.08
E4	6.41	2067.33	1.9	0.0026	100	0.003	0.55	0.02	0.11
E5	9.32	2067.33	1.9	0.0026 / 0.0020	60 / 40	0.003 / 0.003	0.55 / 0.55	0.01 / 0.01	0.07 / 0.06
F1	42.51	2067.33	15.1	0.0026	100	0.003	1.0	0.25	10.49
F2	12.24	2067.33	4.3	0.0026	100	0.003	0.7	0.05	0.60
F3	13.03	2067.33	1.9	0.0026	100	0.003	0.55	0.02	0.23
F4	27.58	2067.33	1.5	0.0026 / 0.0026	80 / 20	0.04 / 0.003	0.55 / 0.55	0.14 / 0.001	3.96 / 11.15
F5	23.47	2067.33	10.9	0.0026 / 0.0020	50 / 50	0.14 / 0	0.17 / 0.17	0.53 / 0.00	10.24 / 0.00

USLE = Universal Soil Loss Equation, R = rainfall and runoff factor, K = soil erodibility factor, LS = slope length-gradient factor,
C = crop/vegetation and management factor, P = support practice factor.
Note: To convert millimeters to inches, multiply by 0.03937; hectares to acres, multiply by 2.471; megajoules (MJ) to foot pounds,
multiply by 737,562.18; metric tons to tons, multiply by 1.1023.

Sedimentology by Distributed Model Treatment (SEDIMOT II)

The quantity of sheet and rill erosion during major storm events was estimated using the SEDIMOT II surface erosion model (WVNS 1993a), which simulates rainfall intensity and depth over a given time period, the resulting surface water runoff volume, and the soil volume washed from the ground surface.

For the West Valley Project, four 24-hour design storms were modeled: 2-, 10-, and 100-year, and the probable maximum precipitation event, which is the maximum rainfall that could conceivably occur. The hillslopes were modeled within the entire Franks Creek watershed. The watershed was divided into the same 22 subwatershed areas defined in the USLE and hydrologic modeling studies to provide consistency in the analyses. The rainfall amount expected from each of the design storm events was taken from standardized

maps developed by the Soil Conservation Service (USDA 1986) using a Type II Soil Conservation Service storm designation and rainfall depths of 6.35 centimeters (2.5 inches) for the 2-year storm, 9.4 centimeters (3.7 inches) for the 10-year storm, 13.2 centimeters (5.2 inches) for the 100-year storm, and 63.2 centimeters (24.9 inches) for the probable maximum precipitation event. Hydrologic parameters for each of the subwatershed areas were taken from the TR-20 simulations as shown in **Table F–8** (WVNS 1993c). Soil properties for each of the subwatershed areas were based on the geotechnical evaluation of samples from the Lavery till, Kent till, and North Plateau surficial sand and gravel unit. The particle-size distribution used for each of these soil units is also shown in Table F–8 (WVNS 1993e). The soil's cover condition within each subwatershed area was specified by a general land-use condition designation of either forest, agricultural, or disturbed.

Table F–8 SEDIMOT II Hydrologic and Soil Input Parameters

Soil Parameters – Particle-Size Distributions							
Particle Size (mm)	*Kent Till (%)*	*Surficial Sand and Gravel (%)*	*Lavery Till (%)*	*Particle Size (mm)*	*Kent Till (%)*	*Surficial Sand and Gravel (%)*	*Lavery Till (%)*
19	98	88	82	0.075	83	42	51
6.4	94	73	69	0.03	52	32	46
4.8	93	67	67	0.02	36	27	43
1.9	92	54	62	0.011	28	21	37
0.82	91	50	58	0.006	18	14	32
0.42	89	47	56	0.003	11	9	24
0.15	87	43	53	0.001	1	5	14

Hydrologic Parameters				Sediment Yield Results			
Sub-area	*Area (hectares)*	*SCS Runoff Curve Number*	*Time of Concentration (hours)*	*2-Year Storm Event (metric tons per hectare)*	*10-Year Storm Event (metric tons per hectare)*	*100-Year Storm Event (metric tons per hectare)*	*PMP Storm Event (metric tons per hectare)*
Q1	10.24	76	0.41	0.29	0.83	1.79	31.55
Q2	20.96	76	0.59	0.07	0.21	0.47	8.96
Q3	10.20	74	0.21	0.06	0.17	0.37	7.14
Q4	25.70	73	0.41	0.13	0.38	0.86	16.80
Q5	23.15	74	0.56	0.08	0.22	0.50	9.70
Q6	21.25	73	0.41	0.13	0.39	0.89	17.66
Q7	17.64	71	0.58	0.03	0.10	0.24	5.04
Q8	25.01	71	0.51	0.17	0.56	1.32	27.21
Q9	33.63	70	0.54	0.11	0.35	0.82	18.09
Q10	46.70	68	0.50	0.12	0.41	1.02	23.25
Q11	27.15	72	0.52	0.13	0.41	0.95	19.04
Q12	33.75	77	0.49	0.12	0.33	0.70	11.48
E1	20.88	72	0.40	0.08	0.25	0.58	11.89
E2	12.10	95	0.35	0.09	0.17	0.30	3.46
E3	2.79	80	0.34	0.13	0.34	0.71	12.66
E4	6.39	81	0.20	0.09	0.21	0.43	7.07
E5	11.90	81	0.42	0.17	0.38	0.72	9.79
F1	43.83	67	0.37	0.07	0.24	0.60	14.24
F2	12.18	77	0.48	0.03	0.09	0.20	3.85
F3	13.23	79	0.26	0.03	0.07	0.14	2.80
F4	27.96	70	0.76	1.84	3.77	6.60	92.06
F5	23.43	67	0.52	0.07	0.19	0.41	7.67

SEDIMOT = Sedimentology by Distributed Model Treatment, SCS = Soil Conservation Service, mm = millimeter, PMP = probable maximum precipitation.

Note: To convert hectares to acres, multiply by 2.471; metric tons to tons, multiply by 1.1023; millimeters to inches, multiply by 0.03937.

To predict the average annual soil loss rate, it was assumed that 500 2-year storms, 100 10-year storms, 10 100-year storms, and one probable maximum precipitation event occurred over a 1,000-year period. Thus, the average soil loss for the watershed was estimated to be 0.16 metric tons per hectare (0.07 tons per acre) per year. This soil loss rate is equivalent to an average decrease in elevation of 11 millimeters (0.04 feet) per 1,000 years. The SEDIMOT II simulation results are consistent with the USLE analysis results. As in the USLE calculations, the predicted soil erosion rate was greatest in an area of the Franks Creek-Erdman Brook Basin with disturbed or insufficient ground cover. The major determinant of the erosion rate was the large number of high-frequency storms (i.e., 2- and 10-year events), not the few low-frequency storms (i.e., 100-year and probable maximum precipitation events). This conclusion is consistent with other research findings reported in the literature (e.g., Wolman and Miller 1960).

Chemicals, Runoff, and Erosion from Agricultural Management Systems (CREAMS)

The CREAMS model was used to estimate erosion rates for a portion of the South Plateau over a 1-year period (Dames and Moore 1987). The purpose of the study was to evaluate the utility of the CREAMS model in predicting surface soil-water balances and erosion rates; therefore, only a small 2-hectare (5-acre) test area was used for the simulations instead of the entire Franks Creek watershed, as shown in **Figure F–8**. Unlike USLE and SEDIMOT II, CREAMS is a physically based, distributed-parameter, continuous-simulation erosion model capable of predicting sediment yield on a field-size area. The South Plateau portion selected for the study was a gently sloping open field covered with low-to-medium grasses.

Major input parameters used in the model are shown in **Table F–9**. The simulations involved the use of daily rainfall data for a single year as recorded at the West Valley Nuclear Services (WVNS) weather station in 1984. Soil properties for the weathered till were obtained from a New York State Geological Survey study conducted at WNYNSC (Hoffman 1980). When site-specific data were not available, input parameter values were estimated from the data provided in the appendices of the Soil Conservation Service model manual (USDA 1984) for conditions similar to those at the West Valley Site.

The CREAMS simulations produce an estimate of sediment yield for the study area that is greater than the soil loss estimates predicted by the USLE and SEDIMOT II models. According to those simulations, the average sediment yield for the watershed is 10.3 metric tons per hectare (4.6 tons per acre) per year. This rate is equivalent to an average decrease in elevation of 690 millimeters (2.3 feet) per 1,000 years. It should be noted that the CREAMS study is extremely limited in terms of areal extent and range of precipitation conditions. The small area used in the simulations has less protective ground cover and a more-limited range of slope conditions than the balance of WNYNSC, and thus is not considered representative of the watershed as a whole. Also, the 1-year simulation period is too short a time to account for long-term fluctuations in precipitation and thus cannot be used reliably for long-term projections.

Water Erosion Prediction Project

The WEPP model was used to predict sediment yield based on consideration of the physical processes affecting the watershed for a set of seven storms with return periods ranging from 1 to 100 years. Like CREAMS, WEPP is a physically based, distributed-parameter, continuous-simulation erosion model capable of predicting sediment yield. Unlike CREAMS, WEPP can predict sediment yield on a small-watershed scale; it is not restricted to a field-size area.
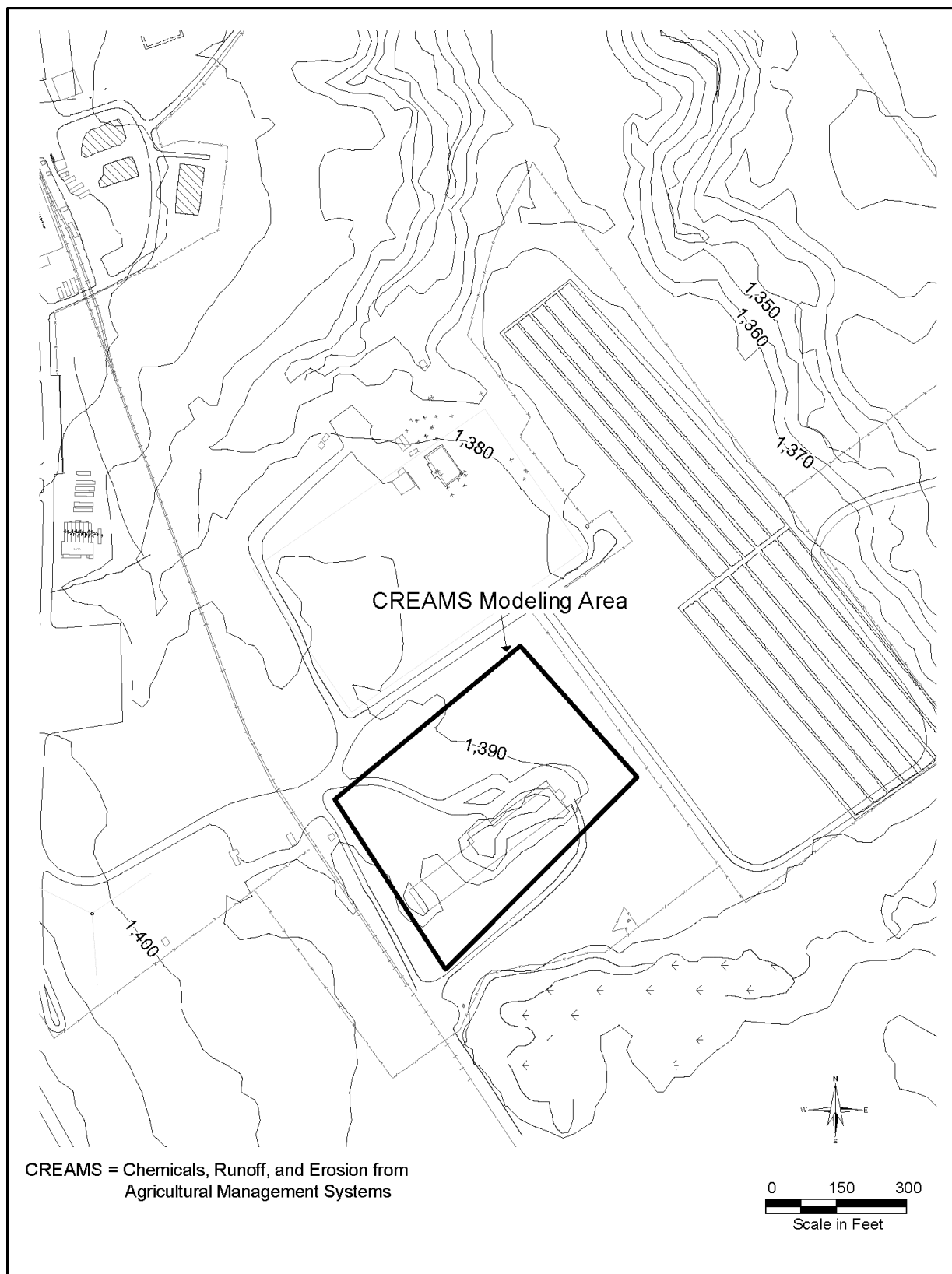
CREAMS Modeling Area

CREAMS = Chemicals, Runoff, and Erosion from
Agricultural Management Systems

Figure F–8 Location of CREAMS Study Area

Table F–9 CREAMS Model Input Parameters and Results

Input Parameter Names	Input Parameter Values
Field Area Acreage	2.2 hectares
Slope of Field	0.02
Length of Field	152 meters
Annual Precipitation (1984)	113.8 centimeters
Soil Type/Hydrologic Soil Group	Silty clay/Hydrologic Soil Group D
Effective Hydraulic Conductivity	0.01 centimeters per year
Soil Conservation Service Curve Number	84
Soil Erodibility Factor	6.0
Soil Loss Ratio	0.26
Mannings 'n' value for overland flow	0.046
Output Parameter Names	*Output Parameter Values*
Total Evapotranspiration	36.60 centimeters
Percolation	11.49 centimeters
Predicted Runoff	65.81 centimeters
Annual Soil Loss for Area	10.3 metric tons per hectare

CREAMS = Chemicals, Runoff, and Erosion from Agricultural Management Systems, Soil Conservation Service Curve Number = a value that describes a catchment's runoff production behavior, Mannings 'n' value = roughness coefficient which indicates the resistance to flow of the land surface.

Note: To convert centimeters to inches, multiply by 0.3937; hectares to acres, multiply by 2.471; metric tons to tons, multiply by 1.1023.

In this study, the Quarry Creek and Franks Creek watersheds were modeled separately. As shown in **Figure F–9**, a network of 11 channel sections and 28 hillslope areas within the Quarry Creek watershed and 3 channels and 8 hillslope areas within the Franks Creek watershed were used to characterize the same study area as that for the USLE and SEDIMOT II simulations. However, the subdrainage areas were defined in a slightly different manner than in those two simulations, because their size was dependent on the geometry of the branched-stream network in accordance with WEPP program constraints (USDA 1995). The subdrainage basin boundaries were delineated using the GeoWEPP ArcX 2004.3 version of the software package. Unlike the USLE and SEDIMOT II simulations, which modeled soil loss from individual hillslopes within the watershed, this study modeled sediment leaving the hillslopes and migrating downgradient through the stream network to the watershed outlet. This more comprehensive modeling approach simulates both erosion and depositional processes within the channels as well as on the hillslopes.

Data were entered into the model to describe the climate, topography, soil properties, and cover conditions within the watersheds. WEPP used 24-hour design storms with 1-, 2-, 5-, 10-, 50-, and 100-year return intervals to determine single-storm event sediment yield rates. The rainfall amount expected from each of the design storms events was taken from standardized maps developed by the Soil Conservation Service (USDA 1986) using a Type II Soil Conservation Service storm designation and rainfall depths of 5.3 centimeters (2.1 inches) for the 1-year storm, 6.4 centimeters (2.5 inches) for the 2-year storm, 8.1 centimeters (3.2 inches) for the 5-year storm, 9.4 centimeters (3.7 inches) for the 10-year storm, 11.2 centimeters (4.4 inches) for the 25-year storm, 11.9 centimeters (4.7 inches) for the 50-year storm, and 13.2 centimeters (5.2 inches) for the 100-year storm. To determine average annual sediment yield rates, WEPP's climate simulator (CLIGEN) was used to stochastically project changes in the climatic conditions daily over a 100-year period based on records supplied from the Little Valley, New York, weather station (Nicks and Gander 1997). Topographic profiles were entered for each hillslope area based on a high-resolution topographic map of the Project Premises as compiled by Erdman Anthony Consultants and
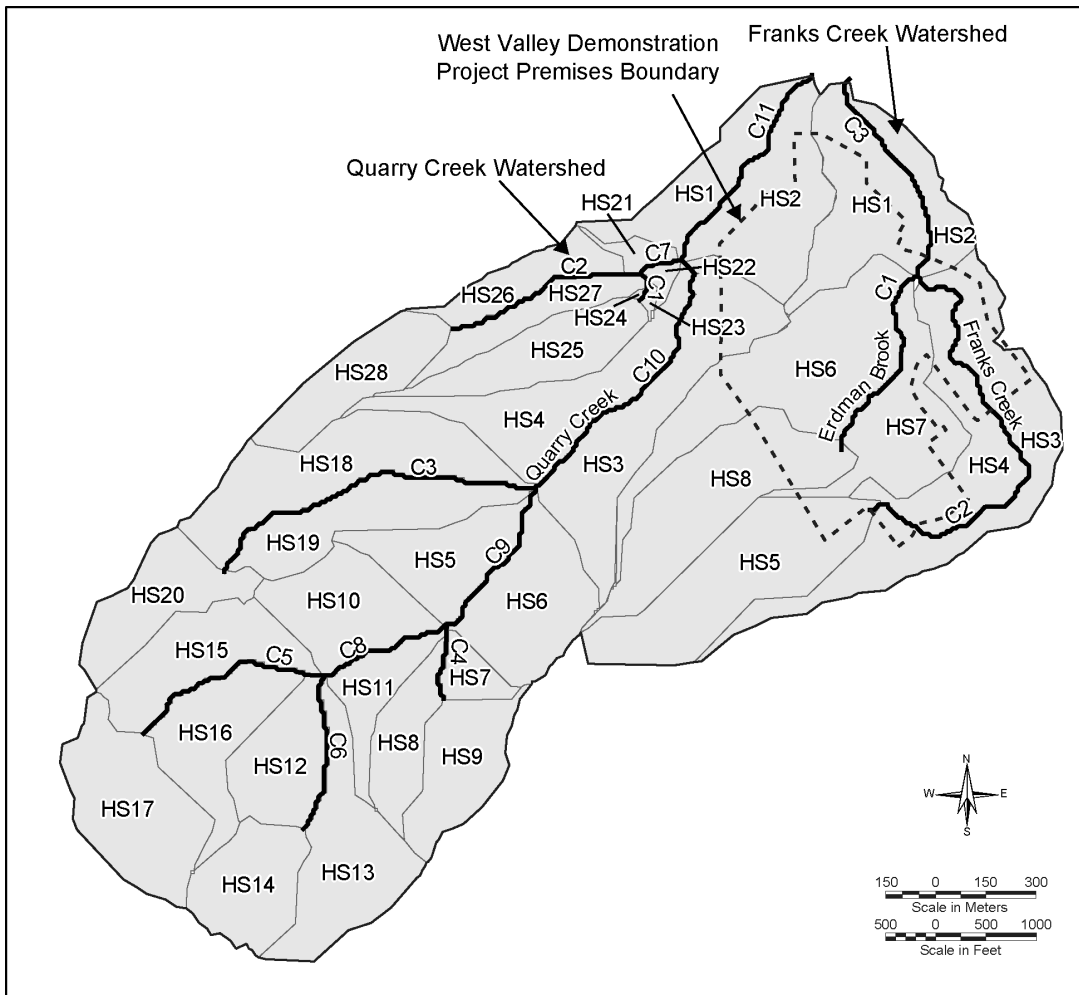
Figure F–9 Water Erosion Prediction Project Modeling Study Channel Network and Hillslope Areas

the 1:24,000 Ashford Hollow Quadrangle map compiled by the USGS. The soil unit distribution within the watershed area was determined from the Soil Conservation Service soil survey for Cattaraugus County (USDA 2004). Other soil parameters were established through review of site conditions and published values for similar conditions (Meyer and Gee 1999), as shown in **Table F–10**. Two cover conditions, 50-year-old forest and Old Field Recessional, were specified within the watershed area based on the site-specific vegetation survey (WVNS 1993f).

The WEPP simulation results are shown in **Tables F–11** and **F–12**. The best-estimate value for the average annual sediment yield of the hillslope areas was determined to be 6.1 metric tons per hectare (2.7 tons per acre) per year from regression analysis of the single-storm events. This yield is equivalent to an average decrease in elevation of 408 millimeters (1.3 feet) per 1,000 years. During the 100-year storm event, the sediment yields of individual subwatershed areas vary from 0.0 to 4.9 metric tons per hectare (0.0 to 2.2 tons per acre), with an average value of 1.3 metric tons per hectare (0.60 tons per acre). This is equivalent to an average decrease in elevation of 91 millimeters (0.3 feet) per 1,000 years, indicating that, over a long-term period, the high frequency of smaller-storm events has greater impact on erosion rate. Also, WEPP predicts that the average annual sediment yield of the watershed through creek channels is approximately 22,317 metric tons (24,600 tons) per year, equivalent to an average downcutting rate of 98,000 millimeters (320 feet) per 1,000 years.

Table F–10 Water Erosion Prediction Project Model Soil Units and Properties

Site Location	NRCS Soil Unit Number	NRCS Soil Unit Name	Soil Texture	Interrill Erodibility Kg × s/m4	Rill Erodibility (seconds per meter)	Critical Shear (newtons per square meter)	Hydraulic Conductivity (millimeter per hour)
North Plateau	81	Varysburg	Loamy Sand	263762	0.00068	0.24	57.600
	135	Hudson	Clay	1083060	0.00206	3.292	0.154
	29	Chenango	Loamy Sand	263762	0.00068	0.24	57.600
	32	Churchville	Clay	1083060	0.00206	3.292	0.154
	35	Rhinebeck	Clay	1083060	0.00206	3.292	0.154
South Plateau	32	Churchville	Clay	1083060	0.00206	3.292	0.154
	36	Canadice	Clay	1083060	0.00206	3.292	0.154
	75	Alden	Loam	945944	0.000788	2.508	3.427
	55	Darien	Clay Loam	951524	0.001184	2.76	0.446
West Hillslopes	51	Chadakoin	Loam	945944	0.000788	2.508	3.427
	55	Darien	Clay Loam	951524	0.001184	2.76	0.446
	61	Schuyler	Loam	945944	0.000788	2.508	3.427
	80	Fremont	Loam	945944	0.000788	2.508	3.427
	56	Chautauqua	Loam	945944	0.000788	2.508	3.427
	63	Langford	Silt Loam	928308	0.000704	2.62	1.094
	69	Erie	Loam	945944	0.000788	2.508	3.427
	72	Towerville	Loam	945944	0.000788	2.508	3.427
	78	Hornell	Clay	1083060	0.00206	3.292	0.154
	74	Ashville	Loam	945944	0.000788	2.508	3.427
	52	Valois	Loam	945944	0.000788	2.508	3.427
	76	Orpark	Loam	945944	0.000788	2.508	3.427

Note: To convert millimeters to inches, multiply by 0.03937; kilograms to pounds, multiply by 2.2046; newtons to pound-force, multiply by 0.225.
Sources: Soil Conservation Service Soil Survey for Cattaraugus County (USDA 2004) for soil unit and texture data and NUREG CR-6656 (Meyer and Gee 1999) for all other data.

Table F–11 Water Erosion Prediction Project Modeling Channels Sediment Yield Results

Watersheds	Channels	Length (meters)	Storm Event (metric tons)						
			1-Year	2-Year	5-Year	10-Year	25-Year	50-Year	100-Year
Franks Creek Channels	C1	642.47	21.77	31.03	49.80	67.68	90.54	110.13	155.13
	C2	1,425.68	48.63	64.86	101.06	128.73	160.57	187.52	236.96
	C3	731.96	127.28	166.83	249.57	314.79	390.09	452.78	576.97
Quarry Creek Channels	C1	646.12	2.09	4.72	10.98	15.42	23.31	30.48	45.90
	C2	107.31	2.27	3.18	4.99	4.63	9.43	16.60	26.76
	C3	140.15	6.71	11.61	22.04	27.94	43.09	59.24	87.54
	C4	1,135.66	11.97	20.50	35.47	46.90	59.87	71.67	94.08
	C5	681.53	7.08	12.52	23.22	31.39	41.00	49.17	63.68
	C6	518.98	4.99	9.43	18.33	26.31	36.92	46.18	63.23
	C7	425.85	16.51	32.39	66.32	93.53	126.46	154.04	208.02
	C8	246.88	0.82	1.72	4.08	5.99	8.98	12.52	22.32
	C9	558.38	34.20	65.32	127.46	176.27	233.78	282.32	384.10
	C10	960.77	74.39	137.08	256.82	346.27	455.86	548.76	745.71
	C11	750.37	207.20	324.86	536.78	688.73	873.62	1,028.66	1,343.36

Note: To convert meters to feet, multiply by 3.281; metric tons to tons, multiply by 1.1023.

Table F–12 Water Erosion Prediction Project Modeling Hillslope Sediment Yield Results

Watersheds	Hillslopes	Area (hectares)	Storm Event (metric tons per hectare)						
			1-Year	*2-Year*	*5-Year*	*10-Year*	*25-Year*	*50-Year*	*100-Year*
Franks Creek Hillslopes	HS1	14.27	0.00	0.00	0.00	0.00	0.00	0.00	0.00
	HS2	5.54	0.00	0.00	0.00	0.00	0.00	0.00	0.00
	HS3	20.70	0.11	0.18	0.09	0.16	0.20	0.27	0.15
	HS4	11.80	0.04	0.09	0.16	0.20	0.27	0.34	0.19
	HS5	20.62	0.20	0.47	1.26	1.93	2.76	3.50	2.19
	HS6	23.12	0.07	0.11	0.22	0.31	0.43	0.54	0.28
	HS7	12.40	0.00	0.00	0.00	0.00	0.00	0.00	0.00
	HS8	19.44	0.07	0.20	0.61	1.10	1.68	2.29	1.73
Quarry Creek Hillslopes	HS1	9.07	0.00	0.00	0.00	0.00	0.00	0.00	0.00
	HS2	14.49	0.04	0.09	0.13	0.20	0.25	0.31	0.36
	HS3	19.24	0.00	0.00	0.09	0.20	0.63	0.99	1.28
	HS4	14.96	0.09	0.11	0.20	0.04	0.02	0.04	0.09
	HS5	9.99	0.04	0.04	0.09	0.18	0.40	0.61	0.96
	HS6	13.67	0.81	1.32	2.17	2.82	3.43	3.90	4.91
	HS7	2.89	0.00	0.00	0.00	0.02	0.09	0.18	0.31
	HS8	7.07	0.00	0.00	0.00	0.00	0.00	0.00	0.07
	HS9	10.14	0.07	0.09	0.18	0.25	0.38	0.61	1.23
	HS10	11.79	0.09	0.29	0.85	1.32	1.91	2.31	3.18
	HS11	5.69	0.00	0.00	0.00	0.00	0.00	0.00	0.18
	HS12	9.52	0.04	0.04	0.11	0.27	0.56	0.83	1.30
	HS13	15.32	0.09	0.13	0.25	0.36	0.47	0.58	0.69
	HS14	10.40	0.04	0.11	0.27	0.40	0.58	0.74	1.08
	HS15	12.24	0.02	0.04	0.07	0.11	0.16	0.20	0.27
	HS16	11.58	0.07	0.11	0.20	0.29	0.38	0.47	0.58
	HS17	16.10	0.07	0.13	0.25	0.34	0.45	0.58	0.69
	HS18	18.78	0.07	0.11	0.18	0.25	0.34	0.45	0.54
	HS19	11.97	0.11	0.16	0.29	0.43	0.58	0.74	0.96
	HS20	10.44	0.04	0.07	0.13	0.20	0.25	0.31	0.43
	HS21	1.48	0.16	0.22	0.02	0.02	0.02	0.02	0.04
	HS22	0.83	0.00	0.00	0.02	0.04	0.11	0.13	0.18
	HS23	0.30	0.02	0.04	0.07	0.11	0.13	0.18	0.20
	HS24	0.09	0.00	0.00	0.00	0.00	0.00	0.00	0.00
	HS25	10.38	0.09	0.13	0.25	0.13	0.52	1.12	2.04
	HS26	6.07	0.04	0.07	0.13	0.18	0.25	0.29	0.34
	HS27	5.90	0.04	0.07	0.11	0.02	0.00	0.00	0.02
	HS28	10.08	0.04	0.04	0.09	0.16	0.45	0.76	1.59

Note: To convert metric tons to tons, multiply by 1.1023; hectares to acres, multiply by 2.471.

Summary

A comparison of the USLE, SEDIMOT II, CREAMS, and WEPP short-term predictions is presented as **Table F–13**. The USLE and SEDIMOT II methods predict the lowest average annual soil loss rate, followed by WEPP and, lastly, CREAMS. Of these results, the WEPP predictions are considered the most reliable. The USLE predictions are considered less reliable than those of WEPP because they predict only soil loss (not deposition) from individual hillslopes; the method does not provide a basis for examining erosion effects on a watershed scale; and the results are based on only 1 year of precipitation data, which is too short a timespan to be reliable for long-term projections. Likewise, the CREAMS modeling results are based on only 1 year of

precipitation data; and because only a small portion of the watershed is simulated (restricting the model to a field scale), the model does not provide a basis for examining erosion effects on a watershed scale. Finally, the SEDIMOT II predictions are considered less reliable because the model simulates only individual storm events, predicts only soil loss (not deposition) from individual slopes, and does not provide a basis for examining erosion effects on a watershed scale.

Table F–13 Short-Term Modeling Results Comparison

Model Name	Average Annual Soil Loss/Sediment Yield (metric tons per hectare per year)	Soil Loss/Sediment Yield During 100-Year Storm (metric tons per hectare)	Average Elevation Change (millimeters per 1,000 years)
USLE	0.19	N/A	12.8
SEDIMOT II	0.16	1.1	11
CREAMS	10.3	N/A	690
WEPP	6.1	1.3	408

USLE = Universal Soil Loss Equation, SEDIMOT = Sedimentology by Distributed Model Treatment, CREAMS = Chemicals, Runoff, and Erosion from Agricultural Management Systems, WEPP = Water Erosion Prediction Project.
Note: To convert metric tons to tons, multiply by 1.1023; hectares to acres, multiply by 2.471; millimeters to inches, multiply by 0.03937.

The larger-scale WEPP results are considered the better estimate of sheet and rill erosion from the Franks Creek watershed. The WEPP code, a physically based model, exploited available site-specific data, weather data from a nearby weather station, and a climate simulator to achieve more reliable long-term predictions. The WEPP method is also more encompassing in nature, predicting sediment yield on a watershed scale.

F.3.1.2   Short-Term Channel Downcutting and Valley Rim-Widening Prediction

Another estimate of valley rim-widening was developed by modeling channel downcutting rates for individual storm events. The downcutting rates in both Franks Creek and Erdman Brook were estimated for six different storm events with return intervals of 2, 5, 10, 20, 100, and 500 years. The individual storm downcutting rates were predicted using the Hydrologic Engineering Center (HEC) HEC-6 code, a one-dimensional open-channel-flow numerical model designed to predict scour and/or deposition resulting from gradually changing sediment and hydraulic conditions over moderate time periods. Owing to its one-dimensional nature, HEC-6 is not capable of simulating the bank erosion or lateral-channel migration processes that are actively causing Franks Creek and Erdman Brook to widen and adjust their course. These processes slow the downcutting rate by adding large quantities of sediment that must also be removed from the streambed. Thus, by assuming that the current channel width will remain constant over time, the model will overpredict the downcutting rate, which, in turn, will provide a conservative estimate of valley rim-widening.

The model requires measurements of the stream cross-sectional geometry, flow rates, and elevation, as well as the selection of a sediment transport function. The stream cross-sections, flow rates, and elevations for the current drainage system were taken from HEC-2 modeling runs performed by Dames and Moore (WVNS 1993c). Closely spaced cross-sections (generally 30.5 to 46 meters [100 to 150 feet]) were used to approximate a steady, gradually varied flow condition despite stream irregularities. The *Hydraulic Design Package for Channels (SAM)*, developed by the Waterways Experiment Station (ACE 1993), identified the Laursen (Madden) function as an appropriate sediment transport function based on site-specific measurements of the flow, sediment load, and geometry characteristics of Erdman Brook and Franks Creek (WVNS 1993c).

The calculated downcutting rate for the six reference storms is presented in **Table F–14**. These values represent the average downcutting that occurs along the stream profiles during the reference storms. The results show minimal change in downcutting for the storms with the higher frequency of occurrence, and there is little difference in the downcutting rates between Erdman Brook and Franks Creek. Table F–14 also shows the corresponding rim-widening, which results from dividing the downcutting by the tangent of the 21-degree stable slope angle. In other words, these rim-widening estimates assume that following channel downcutting, the adjacent slope fails at a constant 21-degree angle, resulting in rim-widening. This rim-widening rate is the rate at which each of the streambanks moves in a horizontal direction. The rim-widening estimate is considered conservative because it assumes the slope will fail everywhere along the channel profile instead of being restricted to the most susceptible areas, such as the outside of meander loops.

Table F–14 Estimates of Channel Downcutting on Erdman Brook and Franks Creek from Single-Storm Events

Storm Event	Frequency of Occurrence (1 per year)	Average Downcutting Distance from the Single Storm (meters) [a]		Average Rim-Widening Distance from the Single Storm (meters)	
		Erdman Brook	Franks Creek	Erdman Brook	Franks Creek
2-year storm	0.50	0.20	0.14	0.52	0.36
5-year storm	0.20	0.21	0.19	0.55	0.49
10-year storm	0.10	0.22	0.20	0.57	0.52
20-year storm	0.05	0.30	0.23	0.78	0.60
100-year storm	0.01	0.32	0.23	0.83	0.60
500-year storm	0.002	4.10	3.50	10.68	9.12

[a] Positive numbers means degradation and the area is being scoured.
Note: To convert meters to feet, multiply by 3.2808.

The storm frequency (return interval) estimates and rim-widening estimates were combined to develop probabilistic estimates for the long-term rim-widening rate from erosion. The probabilistic method estimated the probability of a specific storm combination (e.g., 20 2-year storms and 5 100-year storms) and combined it with the estimate for the total rim-widening for all storms in the specific combination (e.g., 20 times the 2-year storm rim-widening plus 5 times the 100-year storm rim-widening). The summation of combinations considered storms of all magnitudes, equivalent to averaging over an indefinite period of time. Nearly all (99.94 percent) possible storm combinations were considered. The sets of estimates for storm combination probability and total rim-widening were arranged in order of increasing total rim-widening. The ordered listing was used to estimate the likelihood of a specific rim-widening rate. Selecting a rim-widening rate and summing probabilities for all rim-widening rates lower than the selected rate gives an estimated likelihood of the rate being the same as, or less than, the selected rate. The probability of a specific number of storms having the same recurrence interval over a given time was estimated using the Poisson distribution.

This method was used to estimate the long-term rim-widening rate on Erdman Brook and Franks Creek for the current drainage condition. **Table F–15** presents the probabilistic rim-widening rates. Results show that the 90 percent quantile for Erdman Brook is 0.158 meters (0.518 feet) per year, while the 90 percent quantile for Franks Creek is 0.153 meters (0.502 feet) per year, meaning that 90 percent of the erosion rates for the two streams are expected to be equal to or less than their 90 percent quantiles. A narrow distribution for the rim-widening rate is shown because the major determinant in the probabilistic rim-widening rate is the large number of high-frequency storms. This observation is consistent with the results presented in Table F–14.

Table F–15 Estimate of Long-Term Rim-Widening for Erdman Brook and Franks Creek

Quantile (percent)	*Erdman Brook Average Rim Widening Rate (meters per year)*	*Franks Creek Average Rim Widening Rate (meters per year)*
10	0.138	0.134
20	0.140	0.137
30	0.143	0.139
40	0.145	0.141
50	0.147	0.143
60	0.149	0.145
70	0.151	0.147
80	0.154	0.149
90	0.158	0.153

Note: To convert meters to feet, multiply by 3.2808.

F.3.2   Long-term Models

The models discussed in Section F.3.1 are considered valid for short-term projections and are not generally used for long-term projections. Long-term projection considering the interaction between, and integrating the effects of, the different erosion processes over long time periods is an area of ongoing research. The types and diversity of natural processes, their spatial and temporal variability, and the interaction of the processes at differing spatial scales combine to produce the complexities of the long-term erosion processes. In this study, long-term erosion models are used not as the direct basis for dosimetry calculations (see Section F.3.2.6.6) but rather as a means of developing insight into potential rates, patterns, and modes of erosion under different scenarios.

F.3.2.1   Review of Erosion Models

A survey of long-term erosion models was conducted to identify models that could be used for analysis of the West Valley Site. Several criteria were used to help identify and evaluate models. These models must have the following capabilities and characteristics:

* Analysis of long-term erosion (thousands of years);

* Modeling of the dominant erosive processes of the West Valley Site, including hillslope movement (soil creep and landsliding), stream channel downcutting, and gully formation;

* Calibration directly or indirectly using available models or measurements;

* Public availability; and

* Peer review and general verification.

Three specific models for predicting landscape evolution were identified. These models, SIBERIA, Geomorphic/Orogenic Landscape Evolution Model (GOLEM), and Channel-Hillslope Integrated Landscape Development (CHILD), are briefly described in the following paragraphs.

The SIBERIA model was initially developed in the late 1980s to predict landform changes over long periods of time (hundreds to millions of years). It is a physically based model that uses average precipitation over a specified timeframe and accounts for both fluvial and diffusional processes that move sediment through a

drainage system. The fluvial processes include soil detachment and water transport (e.g., sheet and rill erosion, stream downcutting, gully advance), while the diffusional process represents soil creep and landsliding (e.g., slope movement). The central feature of SIBERIA is a sediment balance that is conducted over each rectangular grid element that makes up the total grid representing the site. The change in sediment thickness within a grid is the basis for prediction of erosion or sedimentation within that grid. The model is one of the earliest and most developed of the current generation of landform evolution models. A continuing research program has been under way during the past 10 years to validate SIBERIA predictions against small-scale laboratory experimental and large-scale natural landscapes over a range of different landforms, geologies, and climates. Studies in this program include: (1) Willgoose (1994), who demonstrated that SIBERIA is able to simulate the statistical form of the Pokolbin catchment in the Hunter Valley in Australia; (2) Hancock and Willgoose (2001a), who demonstrated that SIBERIA is able to simulate development of experimental model landscapes; (3) Ibbit, Willgoose, and Duncan (1999), who demonstrated that SIBERIA can simulate natural landforms in a tectonically active region of New Zealand; (4) Hancock and Willgoose (2001b), who demonstrated that, using parameters derived from a short-term analogue site (i.e., an abandoned uranium mine at Scinto 6 in the South Alligator River Valley, Kakadu National Park, Australia), SIBERIA can accurately model gully development on a manmade postmining landscape over timespans of around 50 years; and (5) Hancock, Willgoose, and Evans (2002), who demonstrated that, using parameters derived from a long-term analogue site (i.e., a natural, undisturbed site at Tin Camp Creek within the Myra Falls Inlier, Northern Territory, Australia), SIBERIA can accurately model the geomorphology and hydrology of a natural catchment over the long term.

The second model that was identified was GOLEM. This model was developed in the early 1990s to simulate evolution of topography over geologic time scales. Like SIBERIA, it is a physically based model that uses average precipitation over a specified timeframe; accounts for both fluvial and diffusional processes; and conducts sediment balances over the grid elements that represent the site. Its structure is also similar to SIBERIA in that it uses a rectangular, finite-difference grid. It uses a somewhat different method for computing erosion and sedimentation by running water.

The CHILD model was developed in the later 1990s and is a descendant of the GOLEM and SIBERIA models. Like SIBERIA and GOLEM, it simulates the interaction of fluvial processes (slope wash and channel and rill erosion) and diffusional processes (weathering, soil creep, and other slope transport processes). However, this basic capability has been expanded with the addition of several features. It uses an irregular gridding method that makes it possible to represent different parts of the landscape at different spatial resolutions and allows incorporation of lateral stream erosion. It is the first landscape evolution model in which the processes of vertical stream erosion and lateral channel migration (meandering) are coupled. Also, instead of using a single effective rainfall or runoff rate that represents a geomorphic average, it provides the option of stochastic rainfall input. In addition, it models floodplain (overbank) deposition, eolian (loess) deposition, multiple sediment sizes and layers, and chronostratigraphic deposition. Like the GOLEM model (and the related DELIM by Howard et al. 1994) it allows for detachment-limited, transport-limited, or mixed behavior in calculating runoff erosion.

On the basis of a review of existing models and their capabilities, the SIBERIA and CHILD models were selected to perform the long-term erosion analysis at the West Valley Site. The use of two models broadens the assessment through the development of two independent estimates of site erosion. GOLEM was not selected because its capabilities have been largely superceded by those of CHILD.

F.3.2.2   Approach to Erosion Modeling Using SIBERIA and CHILD

Erosion modeling objectives at WNYNSC are to develop an understanding of local erosion processes and the manner in which those processes may develop over a long period of time and to provide a basis for estimating potential health impacts related to erosion. Major analysis products include the estimation of local erosion

rates at facilities on the North and South Plateaus, evaluation of gully and stream channel development, and assessment of the potential for major-stream configuration alteration.

Application of the CHILD and SIBERIA models to the Buttermilk Creek drainage basin is designed to shed light on the nature and magnitude of potential long-term (10,000-year) geomorphic evolution of the area. Modeling over such long periods is based on a simple premise: If a model, when given a plausible set of parameters and boundary conditions, can adequately reproduce the observed pattern of landscape evolution over the last 10,000 to 20,000 years, then there is increased confidence in the ability of that model to indicate potential erosion trends over a similar timeframe under similar environmental conditions. This approach takes advantage of the rather simple and well-constrained postglacial geomorphic history of Buttermilk Creek, which, as noted above, is interpreted to involve post-glacial (circa 18ka) drainage network incision into glacial deposits due to baselevel lowering along Cattaraugus Creek.

In evaluating the output of landscape evolution models like SIBERIA and CHILD, it is important to bear in mind that the details of computed drainage network patterns are known to be sensitive to initial conditions. For example, Ijjasz-Vasquez et al. (1992) showed that small perturbations of initial conditions led to notable differences in simulated drainage pathways, though the topography and network geometry were robust in a statistical sense. This instance of the "butterfly effect" means that these models are more useful for indicating general trends, patterns, and parameter sensitivities than for predicting the detailed erosional history at a particular spot in the landscape. The particular geometry of any simulated drainage network should be considered merely one of many possible realizations. To some extent, the modeling strategy employed in this project reduces the butterfly effect but cannot entirely eliminate it. A second consideration concerns the nature of the physical laws ("geomorphic transport laws"; Dietrich et al. [2003]) that go into landscape evolution models like SIBERIA and CHILD. For the most part, these are semi-empirical statements about the relationship between sediment transport rates in accordance with a particular type of process (e.g., soil creep, channelized flow) and controlling variables such as gradient or fluid friction. For example, the linear and nonlinear soil creep laws rely on empirical rate coefficients that, at present, cannot be determined *a priori* from knowledge of soil type, biota, and climate alone. This means that, like most environmental models, landscape evolution models are provisional; they represent the current state of the science but are subject to continual improvement as the science evolves. In the context of evaluating erosion at the WNYNSC, the best available test of these models' reliability is their ability to reproduce past landscape evolution. This is the basis for the testing and calibration strategy.

Determination of erosion processes and processes influencing erosion requires vastly different scales of space and time. Representative scales for the detachment of soil particles in rills are on the order of millimeters and seconds; those for river meandering or tectonic uplift, from one to thousands of kilometers and from centuries to thousands of years. Within this range of scales, differing modeling approaches may be applicable. From the reductionist view, detailed specification of many processes is needed to understand all features of landscape evolution (Rodriguez-Iturbe and Rinaldo 1999). An opposing view holds that, for complex landform systems, a reductionist approach does not provide a self-consistent method (Werner 1999) and that large-scale structure is independent of detailed description of motion at small scales (Goldenfeld and Kadanoff 1999). The SIBERIA/CHILD modeling approach is designed to use macroscopic-scale correlation of measured conditions projected over differing space and time scales. The following sections provide the rationale for the selection of the initial postglacial topography, the model boundary conditions, and the SIBERIA and CHILD input parameters.

F.3.2.3   Model Calibration Strategy and Parameter Selection

Every conceptual model has parameters that are the coefficients and exponents in the model equations. These parameters must be estimated for a given watershed and for each computational segment of the model. This requires determining the parameters' inherent relationships with physical characteristics or tuning the parameters so that model response approximates observed response, a process known as calibration. In the calibration process, the modeling results are checked to determine whether they are reasonable for the area and time that was modeled, and for the conditions modeled. The calibration process can be quite complex and time consuming because of the limitations of the input and output data, imperfect knowledge of basin characteristics, the mathematical structure of the models, and limitations in the ability to quantitatively express preferences for how best to fit the models to the data.

Calibration of the SIBERIA and CHILD models was accomplished through a forward modeling exercise, which starts with a postglacial (pre-incision) valley topography and attempts to reconstruct the modern topography. Within this framework, a number of different potential strategies, with varying degrees of complexity could be used. These range from Monte Carlo-based, multi-parameter optimization schemes to simple single-parameter tuning exercises. The advantage of complex, multi-parameter schemes such as Monte Carlo methods is that they can achieve the closest possible match to data and can also reveal the potential for model equifinality (multiple solutions provide equivalent matches to the data). They can also be used to place uncertainty bounds on the calibrated parameters. Their main disadvantage is the high cost and long times of computation. Simpler parameter-tuning methods have the advantage of computational efficiency, and are most effective where the majority of parameters can be estimated *a priori* using site-specific data.

This analysis used a two-parameter "tuning-based" approach to calibrate each model on the basis of the postglacial landscape history. The approach involved estimating values for as many parameters as could be justified by some relationship with the watershed physical characteristics (i.e., site measurements or literature values), leaving only two parameters to be adjusted so that the model response approximated the observed response. For the CHILD model, a 5×5 matrix of runs was conducted in which the parameters governing bedrock detachment capacity, K_b, and fluvial transport efficiency, K_f, were varied. The K_b-K_f combination yielding the smallest misfit statistic (discussed below) was identified. For the SIBERIA model, a 6×7 matrix of runs was conducted in which the fluvial transport efficiency factor $\beta 1$ (comparable to CHILD's K_f) and the transport threshold QsHold were varied; the range of values tested is discussed below.

The two-parameter tuning approach is considered to yield a trial calibration and reveal whether either model is able to reproduce some of the key features of the postglacial landscape. A more thorough calibration would require a larger suite of test metrics (as discussed below) and exploration of a wider area of parameter space.

F.3.2.3.1   Reconstructed Postglacial Topography of Buttermilk Creek

The starting condition for the models was a Digital Elevation Model (DEM), which represented the topography of Buttermilk Creek as it would have existed following the initial retreat of the ice sheet. The last glacial retreat from the area left behind thick accumulations of glacial deposits within the main valleys, including the valleys of the modern Cattaraugus Creek and its tributaries. In the Buttermilk Creek watershed, these glacial deposits, together with a thin mantle created by postglacial fan deposits, formed a low-relief surface sloping gently downward to the north-northwest. Since deglaciation, Cattaraugus Creek and its tributaries have incised these glacial deposits (Fakundiny 1985). Extensive remnants of the incised postglacial valley surface remain throughout the Buttermilk Creek basin, forming a dissected, semicontinuous, low-relief surface with an altitude that ranges roughly from 400 to 430 meters (1,300 to 1,400 feet) within the Buttermilk Creek basin. These remnants appear to be only thinly mantled by postglacial deposits (see, for example, Quaternary geologic map

and generalized cross-section in LaFleur [1979]), so it is logical to assume that they provide a reasonably accurate representation of the valley topography shortly before stream incision began.

The pre-incision valley topography was reconstructed using the valley slope projection method. This method uses the slope of the existing topographic remnant features within the Cattaraugus valley. The slope of the initial, pre-incision valley was estimated by projecting the modern day slopes of the remnant surfaces down valley toward the outlet of Buttermilk Creek. The resulting pre-incision valley gradient lies between 0.003 and 0.004. Total postglacial incision depth at the Buttermilk Creek outlet was obtained from the difference between the modern creek elevation and the elevation of the surrounding terrace remnants, ranging between 60 and 80 meters (200 and 260 feet) of incision depending on which nearby plateau fragment is selected. The plateau heights in the confluence area appear to reflect the presence of a fill or strath terrace about 20 meters (60 feet) below the original valley surface; this feature is suggested by a gentle east-west trending scarp that separates two low-relief surfaces above the left bank of lower Buttermilk Creek, in the vicinity of Edies Siding. For purposes of model calibration, we have adopted intermediate values of 0.0035 for the paleo-valley gradient and 405 meters (1,329 feet) for the initial outlet elevation, which implies a total postglacial incision depth of 69 meters (226 feet). The topography of the pre-incision valley was reconstructed by combining two DEMs: one representing the modern topography of the catchment and one representing the postglacial valley-surface topography. The postglacial valley-surface DEM was built using the following algorithm:

- Assignment of a pre-incision elevation (in this case 405 meters [1,329 feet]) to the outlet point.

- Setting the elevation of each remaining DEM cell in the DEM to $z(x,y) = z_0 + L\,S_v$, where z_0 is the outlet elevation, L is the Euclidian distance from the outlet ($= \sqrt{x^2 + y^2}$), S_v is the projected valley slope (in this case 0.0035), and x and y are the east-west and north-south distances, respectively, from the outlet point.

The initial topography DEM was then constructed by assigning to each cell the value of the corresponding cell in either the modern topography DEM or the valley-surface DEM, whichever was higher. This method yielded a smooth, gently sloping central valley whose height corresponds approximately to the present-day height of the plateau remnants, as shown in **Figure F–10**. No attempt was made to reconstruct subtle variations in the initial valley topography that may reflect features such as recessional moraines or proglacial lake shorelines. Such features demonstrably exist, but for the most part they are below the resolution of the best available topographic maps, and are therefore subject to considerable uncertainty. Likewise, no attempt was made to correct for postglacial erosion or aggradation within the small tributaries above the valley remnants (in the bedrock region), such as upper Quarry Creek, because there appears to be no data set available at present on which to base such corrections. In the future, acquisition of high-resolution, vegetation-corrected airborne laser-swath maps could allow for greater precision in reconstructions of pre-incision topography because such data would allow for improved Quaternary geologic mapping and feature identification, mapping of smaller terrace features, and quantification of historic rates of land surface change. The final step in the construction of the initial topography was the addition of the modern stream channel pattern, which was etched into the valley-surface DEM at a depth of 1 meter.

Boundary Conditions: Base-Level History

Glacial recession from the Lake Erie basin appears to be the ultimate cause of stream incision within the Cattaraugus valley and its tributaries. For purposes of erosion evaluation, however, the key boundary condition is the elevation history in the reach of Cattaraugus Creek, for it provides the base level for the Buttermilk Creek catchment. To estimate this base-level history, it was necessary to answer the following questions: When did incision begin here? How fast did Cattaraugus Creek incise here? Has this rate varied through time, and if so, how?
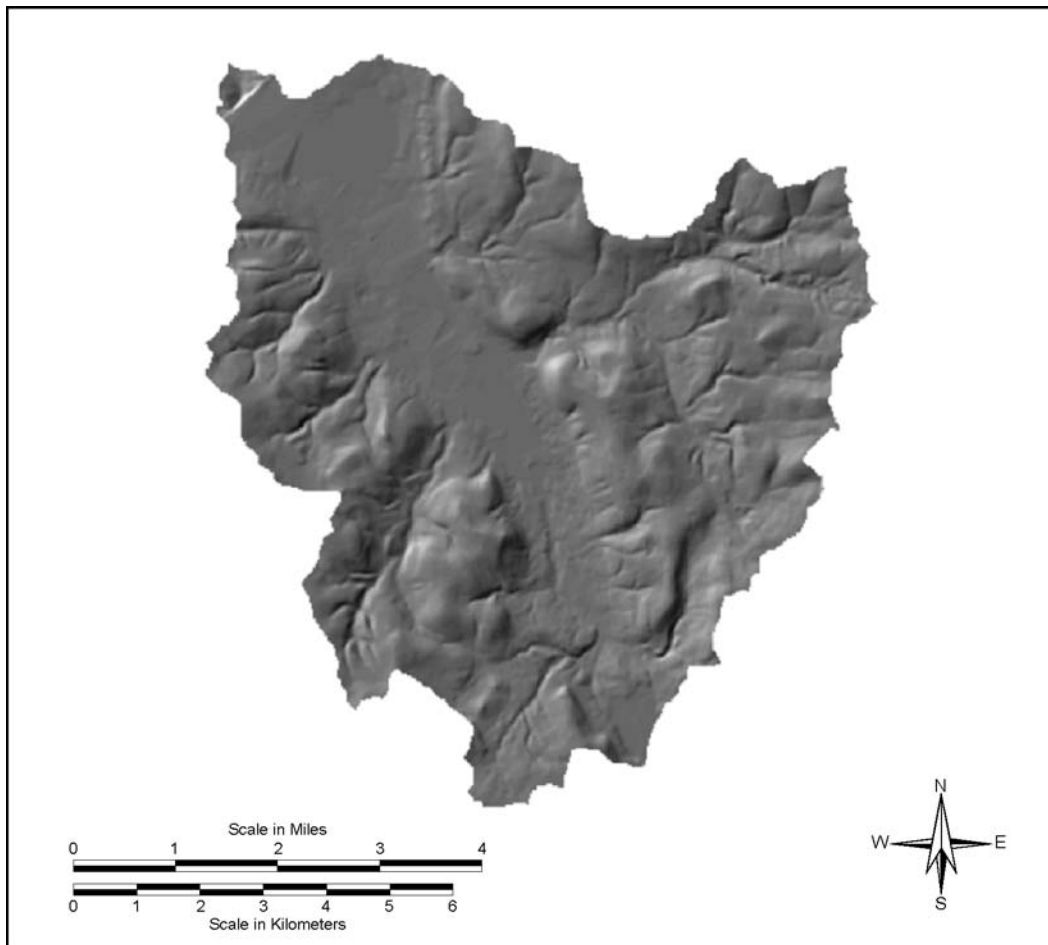
Figure F–10 Topography of the Pre-Incision Buttermilk Creek Valley that was used to Calibrate the Landscape Evolution Models

To constrain the timing of base level lowering, and also provide information on the history of incision within the Buttermilk valley itself, ten samples for OSL dating were collected from various points in and around the Buttermilk Creek catchment, as described in Section F.2.2 above. The samples were analyzed in the USGS Luminescence Dating Laboratory (Mahan 2007). A well-bleached sample obtained in fluvial sediments near the top of the plateau implies that Buttermilk Creek began incision about 17,000 years ago (i.e., 16,800 ±1,530 (one sigma) years from OSL sample 8A (see Table F–3). This timing agrees, within uncertainty, with the timing of glacial retreat from the Finger Lakes to the east (e.g., at Seneca Lake, final retreat is estimated to have occurred approximately 16,600 years before present; Anderson et al. 1997; Ellis et al. 2004). Note that the common practice in the literature of reporting uncalibrated carbon-14 ages can sometimes cause confusion; for example, 14,000 uncalibrated carbon-14 years corresponds to approximately 16,600 calendar years according to current calibration curves.

As noted earlier, OSL ages of ~15,000 years obtained from mid-level fluvial terrace deposits below the plateau suggest that incision was more rapid during the first approximately 2000 years than in the succeeding approximately 15,000 years. To quantify this change in incision rate near the outlet of Buttermilk Creek, an OSL sample was used from a fluvial terrace in the Cattaraugus valley near the confluence (sample 7A, with a central age model date of 15.2 ± 1.82 thousand years ago). The early incision rate of 22 millimeters (0.87 inches) per year is obtained by dividing the incision depth at the sample point (40 meters [130 feet]) by the duration of this phase of incision (17,000 – 15,200 = 1,800 years). The later incision rate of

1.6 millimeters (0.063 inches) per year is obtained by dividing the terrace's height above the modern stream (25 meters [82 feet]) by 15,200 years. In deriving incision rates from this mid-level terrace, it is assumed that the terrace is a strath (bedrock-cut platform mantled by alluvial) rather than a thick fill terrace. Without deeper (backhoe) sampling at this site, this assumption cannot be confirmed, but it is supported by similar ages from two confirmed strath terraces at similar levels in the Buttermilk Valley (samples 1A and 6A).

Uncertainty in the derived base level history reflects uncertainty in the dating. Reducing this uncertainty would require additional identification and dating of strath terraces in the vicinity of the Buttermilk-Cattaraugus confluence. This would produce a larger sample size, yield a greater likelihood of identifying well-bleached (and therefore more reliable) samples, and (if additional terrace levels could be identified) increase the time resolution in the base-level reconstruction.

F.3.2.3.2   Boundary Conditions: Glacio-Isostatic Uplift

Removal of the load of the ice sheets leads to isostatic rebound of the lithosphere. From the point of view of a drainage basin subjected to such glacio-isostatic uplift, there are three potential effects. First, if a catchment drains to a body of water such as a lake or ocean that has a fixed altitude, glacio-isostatic uplift (or subsidence) will change the elevation difference between the catchment and its base level. It may also alter the length of the catchment by, for example, exposing part of a coastal shelf (or drowning the lower part of a catchment, in the case of subsidence). Isostatic uplift along a shoreline can lead to either increased or decreased erosion and transport rates, depending on the slope of the uplifted shelf relative to the stream slope near the coastline (e.g., Summerfield 1986, Snyder et al. 2002). Regional postglacial isostatic uplift in the Lake Erie basin has been well documented, as have fluctuations in lake levels through time (Holcombe et al. 2003). From the point of view of Buttermilk Creek, the net effect of these processes has been to change the base level at its junction with Cattaraugus Creek, as discussed above. In other words, the influence of postglacial isostatic uplift on local base level is incorporated in the model by specifying the base-level history at the Buttermilk-Cattaraugus confluence.

A second potential effect of postglacial isostatic uplift relates to climatology. A substantial increase in the absolute elevation of a catchment can indirectly influence rates of weathering and erosion by altering the catchment's mean temperature (due to the environmental lapse rate) and precipitation (due to orographic effects). However, in this case the magnitude of absolute uplift is sufficiently small (likely less than a few hundred meters [several hundred feet]) that any associated changes in temperature or precipitation fall well within the existing uncertainties regarding postglacial climate variation.

The third potential effect of isostatic adjustment is tilting of the surface due to spatial variations in uplift rate. Spatial variations in glacio-isostatic uplift rates are well documented in eastern North America. For the Lake Erie basin, Holcombe et al. (2003) used bathymetry data to map submerged paleo-shorelines. Based on a tilted 13.4 thousand year old shoreline, their data suggest about 52 meters (170 feet) of differential uplift over a distance of approximately 130 kilometers (80 miles), which implies a down-to-the-west tilt of about 4×10^{-4}. By comparison, the gradient of the modern Buttermilk valley in its lower-middle reaches is about 8×10^{-3}, while the gradient of the plateau is approximately 3.5×10^{-3}, as discussed above (see also the generalized Buttermilk valley profile of LaFleur [1979]; i.e., Figure 3, which shows an average creek gradient from Riceville Station to the outlet of approximately 0.0085, and a plateau gradient of approximately 0.003). Thus, assuming that Buttermilk Creek experienced postglacial tilting of a similar magnitude to that observed in Lake Erie, even if that tilt were aligned directly along the valley axis, it would alter the initial valley gradient by only about 10 percent. Therefore the postglacial tilting likely had only a second-order effect on stream gradients. Because the likely magnitude of tilt is comparable to the uncertainty in the estimates of paleo-valley gradient, it is not incorporated in the model calibration.

F.3.2.3.3   Description of the SIBERIA Model Input Parameters

This section discusses the selection of default parameter values for SIBERIA, as shown in **Table F–16**. A detailed description of the model can be found in Willgoose (1989) and Willgoose et al. (1991). Validation and applications of the model can be found in a number of publications (Hancock and Willgoose 2001b; Hancock et al. 2002; Hancock 2003a, 2003b, 2004; Hancock et al. 2000, 2002; Willgoose 2005).

Table F–16 Values of SIBERIA Input Parameters Selected for Forward Modeling Runs

Parameters	*Symbols*	*Values*
Fluvial Transport Parameters		
Runoff rate constant	β_3	48 [a]
Runoff rate exponent of area	m_3	0.842
Sediment transport constant	β_1	Determined
Sediment transport exponent of discharge	m_1	1.5
Sediment transport exponent of slope	n_1	1.5
Sediment transport constant	O_t	1.0
Sediment transport threshold	QsHold	Determined
Channel Initiation Parameters		
Channel initiation constant	β_5	3.00×10^{-4} [a]
Channel initiation exponent of discharge	m_5	0.67
Channel initiation exponent of slope	n_5	0.67
Hillslope Diffusivity Parameters		
Hillslope diffusive transport coefficient	Dz	0.01 square meters per year
Maximum stable slope in hillslope transport equation	S_{0max}	20 degrees

Determined = determined as part of the forward modeling calibration exercise; see text.
[a] See text for units.

Selection of Fluvial Transport Parameters for the SIBERIA model

Use of the SIBERIA model requires specification of empirical parameters that determine the discharge (water flow rate) and fluvial sediment transport rate at each node. The SIBERIA model represents discharge as a function of area contributing to the flow and a runoff coefficient:

$$Q = \beta_3 A^{m_3}$$

where:
  Q =   discharge at a grid block (cubic meters per year)
  β_3 =   runoff rate constant (cubic meters per year / square meters raised to the exponent m_3)
  A =   area contributing to flow (square meters)
  m_3 =   exponent of area, unitless

SIBERIA uses a steady-state discharge to represent the effects of long-term sediment transport. This dominant discharge is defined as that which, if it were maintained indefinitely, would produce the same long-term average erosion or deposition rate as the natural sequence of flows. This use of a single characteristic discharge to represent a natural frequency-magnitude of flows (the "dominant-discharge approximation") is based on the observation that much of the work performed by fluvial systems can be associated with a specific discharge. It is a common assumption in fluvial geomorphic analysis, and one that is widely used in models of landscape and sedimentary basin evolution (for discussion and derivations, see Willgoose [1989], Willgoose et al. [1991], Tucker and Bras [2000], Willgoose [2005], and references therein).

The dominant discharge can be variously identified with channel-forming discharge, bankfull discharge, effective discharge, and discharge having a particular recurrence interval. The channel-forming discharge is defined as a theoretical discharge that if maintained indefinitely would produce the same channel geometry as the natural long-term hydrograph (Copeland et al. 2000). The bankfull discharge is the maximum discharge that the channel can convey without flowing onto its floodplain. The effective discharge is that which transports the largest fraction of the average annual bed-material load. If dominant discharge is based on a specified recurrence interval, that interval is typically defined between the mean annual and 5-year peak.

The selection of the appropriate method is based on data availability and site physical characteristics. Agreement among the methods is considered to be the best for snowmelt-hydrology, nonincised channels with coarse substrate (Doyle et al. 2007). Classic work in fluvial geomorphology has also shown that in many alluvial rivers, the most effective discharge in terms of downstream sediment transport is close to the bankfull discharge, which commonly has a return interval between 1 and 2 years (e.g., Wolman and Miller 1960).

Of the two hydrologic parameters, β_3 and m_3, the most critical for this study is the scaling factor m_3 because it strongly influences the rate at which sediment-transport capacity changes downstream. This parameter was chosen using the bankfull-discharge method, while the runoff coefficient β_3 was based on the mean annual runoff. Choice of this method is based on the close agreement between the bankfull and effective discharges in alluvial rivers, and the fact that USGS hydrologic investigations provide data on bankfull discharge and its scaling with basin size in New York's Hydrologic Region 6, which includes the study area. The USGS study used regression analysis of stream survey data and discharge records from 11 active and 3 inactive sites within Hydrologic Region 6 to relate bankfull discharge to the size of the drainage area (Mulvihill et al. 2005). The resulting equation is:

$$\text{Bankfull discharge (cfs)} = 48.0 \text{ (drainage area, in square miles)}^{0.842}$$

This equation was used to establish the exponent of area (m_3) in the SIBERIA discharge equation. To check the applicability of the USGS regional bankfull discharge equation to Buttermilk Creek, the annual peak discharge values were obtained from the USGS Buttermilk Creek gauging station (Station 04213450) at Bond Road near Springville, New York. Peak flows were recorded at this station for 7 years (1962 through 1968). The 1.2-year return interval was calculated to be 30 cubic meters per second using the procedure in Chow et al. (1988) for the 77.7 square-kilometer (30.0 square-mile) drainage area. This bankfull discharge is consistent with the bankfull stage height and stage-rating curve data reported in Boothroyd et al. (1979). **Figure F–11** shows the 1.2-year return interval discharge data from the Buttermilk Creek drainage area plotted on a graph with the regional bankfull discharge values as a function of drainage area size, as collected in the USGS regional curve study. The 1.2-year return interval discharge data from the Buttermilk Creek drainage area is shown to be consistent with the USGS study results.
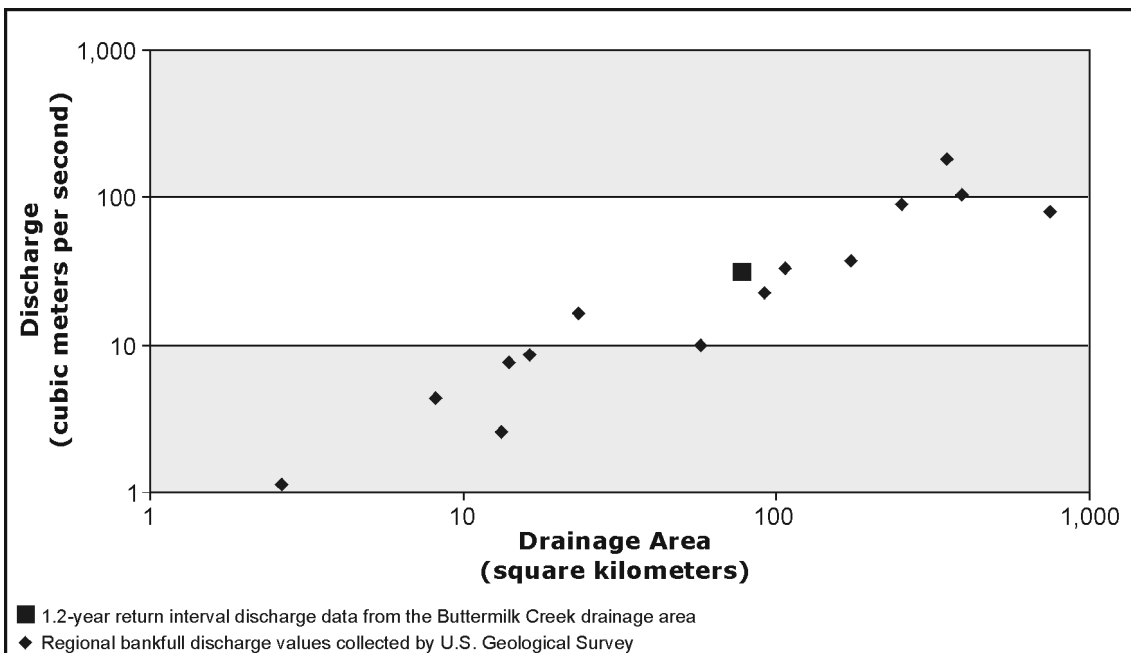
Figure F–11 Bankfull Discharge Values for Buttermilk Creek and New York Region 6

The SIBERIA fluvial transport relation represents the rate of transport of sediment per unit width of flow as a power law function of discharge per unit width of flow and slope along the flow path, contingent on exceeding a threshold shear stress. The power law functional form has a mass-momentum balance theoretical basis in analysis of flow down inclined planes and an empirical basis in force balance-derived relations for gravity-driven flow in channels and for flow around submerged objects. More precisely, the first term on the left-hand side can, depending on the choice of m_1 and n_1, be configured such that transport rate depends on either tractive force per unit bed area or on the rate of energy dissipation (stream power) per unit bed area (for derivations, see, for example, Willgoose et al. [1991], Howard et al. [1994], Tucker and Slingerland [1997]). The functional form of the SIBERIA fluvial sediment relation is:

$$q_s = \beta_1 \ O_t \ q^{m}_1 \ S^{n}_1 - QsHold$$

where:

q_s = sediment transport rate per unit width, kg/m-s
β_1 = correlation coefficient for flow in channels and hillslopes, kilograms per meter-second / cubic meters per meter-second raised to the exponent m_1
O_t = coefficient for sediment transport on hillslopes, dimensionless
q = discharge per unit width, m^3/m-s
S = slope, dimensionless
$QsHold$ = threshold for sediment transport
m_1 = exponent of discharge
n_1 = exponent of slope

The parameter O_t has a value of unity in channels and a value less than unity for hillslopes (reflecting the attenuating effects of factors such as vegetation cover and surface roughness). The threshold for sediment transport may also be represented as a power law function of discharge per unit width and slope. With discharge per unit width and slope as independent variables of the landscape evolution model, the relation has five adjustable parameters whose values must be specified to allow use of the relation in simulation of landscape evolution. As described for the overall calibration procedure, the approach is to provide a basis for specification of a subset of the parameters, leaving the remaining parameters to be adjusted in order to calibrate

the model to current conditions. The approach adopted for the Buttermilk Creek scale calibration is selection of values of the exponents m_1 and n_1 as constant during a simulation. The values of the parameters β_1, QsHold, and O_t are then adjusted during calibration to match the elevation of channels and hillslopes (plateaus) of the Buttermilk Creek watershed. The following paragraphs describe the technical basis for identification of parameter ranges and identify values selected for use in the current calibration.

The range of reasonable values for the power law exponents, m_1 and n_1, may be established through considerations of theory, geomorphology modeling practice, and measurement. A relation between sediment transport rate, discharge, slope, and hydraulic radius is provided assuming sediment transport rate is a power law function of shear stress and using Manning's equation for dependence of discharge on slope and hydraulic radius (Willgoose 1989). Values of hydraulic radius consistent with differing channel geometries may then be applied to derive estimates of m_1 and n_1. Using a value of three for the exponent in the power law relation between sediment transport rate and shear stress (as in the Einstein-Brown equation) leads to values of 1.1 and 1.8 for m_1 and values of n_1 of 2.4 and 2.1 for triangular and wide channels, respectively.

Another commonly used form states that rate of sediment transport is a power law function of stream power per unit bed area, expressed as the product of discharge per unit width and slope. Evaluation of a correlation of this type, the Bagnold equation, with the power law exponent of 1.5, has been shown to provide a reasonable fit to experimental and field data (Gomez and Church 1989, Martin and Church 2000). Another evaluation of sediment transport relations (Prosser and Rustomji 2000) reports that experimental measurements of m_1 ranged from 1.0 to 1.8, that values of n_1 ranged from 0.9 to 1.8, and that values of m_1 and n_1 of 1.4 were the best single combination.

Estimates of m_1 and n_1 values have also been investigated based on measurement of Buttermilk Creek physical parameters. The SAM Hydraulic Design Package for Channels (ACE 2002) was used as an aid in selecting a sediment transport equation applicable to the Buttermilk Creek hydraulic conditions. SAM compares calculated screening parameters for a given river to the same screening parameters from a database of rivers (Brownlie 1981) that have sufficient sediment data to determine an appropriate sediment transport function. The screening parameters used in the SAM analysis were velocity, depth, slope, and width, as measured at bankfull conditions along Buttermilk Creek, and d_{50} values (i.e., median bed material gradations) (Boothroyd et al. 1979). SAM identifies a "match" when a parameter falls within the range of data for a database river and then recommends the three best sediment transport functions for the river. Buttermilk Creek's screening parameters matched four of the five screening parameters for a database stream (North Saskatchewan River) and recommended the Madden extension of the Laursen function as an appropriate sediment transport function. The Laursen equation has the form:

$$f\left\{ [\sqrt{\tau_0/\rho}]/W \right\} = c / \left\{ (d/D)^{7/6} \left[(\tau_0'/\tau_c) - 1 \right] \right\}$$

$$\tau_0 = \gamma\, D\, S$$
$$\tau_0' = (V^2/30d_m/D)^{1/3}$$
$$\tau_c = 4\, d$$

where:

W = channel width
γ = specific weight of water
D = channel depth
S = channel slope
c = correlation constant
d = particle diameter
d_m = median particle diameter
V = stream velocity

Values of the function f { $[\sqrt{\tau_0/\rho}]/W$ } are provided graphically as a log-log function of $[\sqrt{\tau_0/\rho}]/W$ (Madden 1993). The function is nonlinear on a log-log plot but does have a linear segment extending over a range of values of $[\sqrt{\tau_0/\rho}]/W$. The slope of this linear segment is approximately 2.6. Using this estimate and rearranging the Laursen equation provides values of m_1 and n_1 of 1.7 and 1.3, respectively. A literature review (Howard 1980) provides estimates of m_1 and n_1 of 1.5 and 1.7, respectively as appropriate for the Laursen correlation.

The above discussion identifies a range of 1 to 2 as reasonable for both m_1 and n_1. In addition, generic site and site-specific data suggest that the best estimates of values for both exponents are in the midpoint of the identified range. On the basis of these considerations, a value of 1.5 was selected for both m_1 and n_1 for the Buttermilk Creek calibration study.

Selection of the Channel Initiation Parameters for SIBERIA

The SIBERIA model provides the capability to represent nodes as belonging to hillslopes or channels, where the rate of hillslope sediment transport is a fraction of the fluvial transport rate controlled by the O_t parameter. In the calibration study, O_t was set to unity, and in this case the channel initiation parameters play no meaningful role. However, alternative values of O_t were used in initial exploratory simulations, and for these simulations the channel initiation parameters do matter. The method for calibrating the channel initiation parameters is described here.

The potential for transformation of a hillslope node into a channel node is predicted using an activation index that is a function of discharge and slope at the node, referred to as the Channel Initiation Function. The node activation equations at node j are:

$$a_j = \beta_5 \, Q^{m_5} \, S^{n_5}$$

where:
  a_j = channel initiation function equation
  β_5 = coefficient for channel initiation
  Q = discharge
  S = slope
  m_5, n_5 = exponents for channel initiation function (dimensionless)

Selection of the exponents for the channel initiation function (m_5 and n_5) was based on the premise that channels form where overland flow shear stress exceeds a threshold with shear stress, represented by $m_5 = n_5 = 2/3$. Calibration of the coefficient for channel initiation (β_5) was based on the configuration of the modern channel network, which is unlikely to have changed much over time in this fixed-basin scenario. A trial and error approach was used, whereby a range of β_5 values were input into SIBERIA simulations. From the SIBERIA output files, plots of nodes that were transformed from a hillslope to a channel were generated and compared with the modern channel network as shown on the USGS quadrangle map. The β_5 value that best fit the modern channel network configuration was selected for use in the forward modeling runs.

Selection of Hillslope Diffusivity Coefficients

In the SIBERIA model, sediment transport rate (Q_s) for creep-related processes (often referred to as "hillslope diffusion") is related to slope change rate using a relation of the form:

$$Q_s =(Dz\ S^{dzn}) / (1-| S/ So_{max}|) - D_t$$

where:

Dz = coefficient of diffusion, square meters per year
dzn = exponent of nonlinearilty (default = 1), unitless
D_t = threshold below which diffusive sediment transport does not occur (default = 0), g/m-yr
S = slope, unitless
So_{max} = maximum stable slope in the diffusive transport model, unitless

At low slope angles, SIBERIA's model for hillslope mass transport is equivalent to the well-known slope-linear soil creep law, in which the volumetric rate of downslope sediment transport per unit slope width is equal to the product of slope angle times a transport coefficient, Dz. Values of Dz have been estimated in many parts of the world, often for purposes of morphologic dating of landforms such as earthquake fault scarps. In general, the inferred creep coefficients range over two orders of magnitude, from approximately 10^{-4} to approximately 10^{-2} square meters per year (Hanks 1998). There is some evidence that creep rates vary according to climate, with colder and/or wetter environments generally experiencing higher rates of creep. For example, in the compilation by Hanks (1998), the highest creep coefficients come from Michigan and coastal California, while the lowest are found in desert regions in Israel and the arid U.S. Basin and Range province (Nevada and Utah). Oehm and Hallet (2005) compared modern creep rates across a broad range of climates, and found a strong increase in the effective creep coefficient with latitude north of 50 degrees north.

For purposes of this study, published estimates of Dz were compiled (**Table F–17**). Among these, those that match most closely in climate include studies in Michigan, Ohio, Northern Europe, northwestern Wyoming (Yellowstone), and Japan. In a study of fault-scarp degradation in the Rhine River Valley near Basel, Niviere et al. (1998) calibrated a creep coefficient using observed degradation of an approximately 100-year-old railway embankment, arriving at an estimate of 0.0015 square meters (0.016 square feet) per year. Farther north in the Rhine Valley, Camelbeek et al. (2001) obtained creep coefficients from forward modeling of dated fault scarps, with Dz estimates ranging between 0.002 and 0.008 square meters (0.021 to 0.086 square feet) per year in sand-gravel alluvium. A study by Nash (1984) of a single degraded terrace scarp in the subhumid climate of northwestern Montana yielded an estimate of 0.002 square meters (0.021 square feet) per year. In a compilation of modern creep rates and profiles by Oehm and Hallet (2005), data from Japan (latitude 35 degrees north) suggest creep coefficients ranging from 0.0036 to 0.014 square meters (0.039 to 0.151 square feet) per year. The degradation of an 1800-year-old embankment and trench in south-central Ohio provided O'Neal et al. (2005) an opportunity to estimate a creep coefficient of 0.0005 square meters (0.0054 square feet) per year through forward modeling. Nash (1980) analyzed modern and abandoned wave-cut cliffs cut in glacial till along the Lake Michigan shoreline, and derived a best-fit estimate of 0.012 square meters (0.129 square feet) per year.

Table F–17 Published Values of the Diffusivity Coefficient (Dz)

Location	Reference Dz (square meters per year)	Source
Lake Bonneville, UT, shoreline scarps	0.00052	Andrews DJ and RC Bucknam 1987 JGR 92(B12):12857–12867
San Andreas Fault system	0.0085	Arrowsmith 1995, PhD Thesis, Stanford U
Carrizo Plain, California	0.0086	Arrowsmith, JR et al. 1998 JGR-Solid Earth 103(B5):10141–10160
S. Xingiang, China/Hotan-Qira fault	0.0033	Avouac & Peltzer 1993, JGR 98:21773–21807
Longmu, western Tibet	0.0055	Avouac et al. 1996, Palaeogeog.,120:93–104
Northern Tien Shan	0.0055	Avouac 1993 JGR-Solid Earth 98(B4):6755–6804
Northwestern Negev, Israel	0.0001	Begin 1992, Israel J Earth Science 41:95–103
Northwestern Negev, Israel	0.0005	Begin 1992, Israel J Earth Science 41:95–103
Gulf of Elat, eastern Sinai	0.0004	Bowman 1986, Tectonophysics 128:97–119
Northern Arava	0.0004	Bowman 1989, Israel DoE in Martin 2000)
Bree, Belgium; Neer, Netherlands	0.006	Camelbeeck, 2001, Neth J GEOS 80(3–4):95–107
Arava, Israel	0.00025	Enzel et al. 1996, Tectonophysics 253: 305
Idaho	0.001	Hanks 1998, NUREG/CR 5562, 2-497-2-535
Bonneville (UT) & Lahontan (NV)	0.00052	Hanks & Andrews 1989, JGR 94(B1):565-573
Bonneville (UT) & Lahontan (NV)	0.0011	Hanks & Andrews 1989, JGR 94(B1):565-573
Bonneville (UT) & Lahontan (NV)	0.00069	Hanks & Andrews 1989, JGR 94(B1):565-573
Lake Lahontan, Pershing, Nevada	0.0011	Hanks & Wallace 1985, Bulletin SSA 75:835
Seacliff, Santa Cruz, CA	0.011	Hanks et al. 1984 JGR 89(NB7):5771–5790
Fault scarp, southern California	0.016	Hanks et al. 1984 JGR 89(NB7):5771–5790
Lake Bonneville (Utah) shoreline	0.0011	Hanks et al. 1984 JGR 89(NB7)5771–5790
West-central Nevada	0.0011	Hecker 1985, MSc thesis, Univ Arizona, Tucson
Basin and range	0.0001	L.W. Anderson (personal comm. NUREG 1989)
Various	0.0002	Martin 1997 22:273-279
East Bay Reg Park, San Fran, CA	0.036	McKean et al. 1993, Geology 21:343-346
Tennessee	0.0004	Mills, HH 2001 Geomorphology 38(3–4):317–336
Emmet County, Michigan	0.012	Nash 1980a ESPL 5:331–345
Western US	0.00044	Nash 1980b JoG 88:353–360
West Yellowstone, Montana	0.002	Nash 1984, GSA Bulletin 95(12):1413–1424
Upper Rhine graben	0.0014	Niviere B 2000 Geophysical JI 141(3):577
Near Basel	0.0015	Niviere B. 1998 Geophy Res Letters 25(13):2325
Chillicothe, OH	0.0005	O'Neal et al. 2005
Switzerland	0.0021	Oehm 2005 Zeithschrift fur Geomorph 49(3):353
Switzerland	0.0031	Oehm 2005 Zeithschrift fur Geomorph 49(3):353
Switzerland	0.0047	Oehm 2005 Zeithschrift fur Geomorph 49(3):353
Switzerland	0.0003	Oehm 2005 Zeithschrift fur Geomorph 49(3):353
Japan	0.0036	Oehm 2005 Zeithschrift fur Geomorph 49(3):353
Japan	0.0093	Oehm 2005 Zeithschrift fur Geomorph 49(3):353
Japan	0.0135	Oehm 2005 Zeithschrift fur Geomorph 49(3):353
Japan	0.0059	Oehm 2005 Zeithschrift fur Geomorph 49(3):353
Central California coastline	0.01	Rosenbloom 1994, JGR 99:14,013–14,029
N flank Qilian Shan, Gansu, China	0.0033	Tapponnier 1990, Earth Planet. Sci. 97:382

Note: To convert meters to feet, multiply by 3.2808.

In summary, estimates of Dz obtained in humid to subhumid climates range over more than an order of magnitude, from 5×10^{-4} square meters (0.0054 square feet) per year to a little over 10^{-2} square meters (0.108 square feet) per year. In terms of climate, soil texture, and time scale, the closest match to West Valley appears to be that presented in the study of Nash (1980). The regional climate is humid temperate with cold winters; temperatures drop below zero on 150 or more days per year on average, promoting transport by frost heave. Like West Valley, the environment is predominantly forest covered, and both sites are underlain by glacial sediments. Unlike some of the other studies, the time scale for Nash's (1980) estimate spans a large fraction of the postglacial period (10,500 and 4,000 years, respectively, for two different scarp populations), and the data come from a population of scarp profiles rather than a single profile (as used for example by Nash [1984], O'Neal et al. [2005], and Niviere et al. [2005]). Given these considerations and the fact that most field estimates are only precise to within a single digit, a Dz value of 0.01 square meters (0.108 square feet) per year is adopted. The exponent of nonlinearity (dzn) was calibrated by comparing the curvature of slopes along Buttermilk Creek to the curvature of slopes predicted by the diffusion equation in SIBERIA. Cross sections were cut along the Buttermilk Creek drainage using existing topographic maps of the area to determine the curvature of the slopes. A series of one-dimensional runs were completed using SIBERIA to determine the curvature of the slopes predicted by the diffusion equation. The diffusion equation's exponent of nonlinearity was varied in the runs, and the resulting slope evolution was plotted and compared with the existing Buttermilk Creek slope angles. The SIBERIA run that best matched the existing slope angles was determined (dzn value of 1) and used in the forward modeling exercise. Also, approximately 60 measurements of the valley side-slope angles from the digital elevation model of current topography were used to establish a range for the maximum stable slope angle (So_{max}) of 20 to 30 degrees.

F.3.2.3.4   Description of the CHILD Model Input Parameters

This section discusses the selection of default parameter values for CHILD, as shown in **Table F-18**. A detailed description of the model can be found in Tucker et al. (2001a), while some of the basic data structures and algorithms are presented in Tucker et al. (2001b). Applications of the model to various research problems can be found in a variety of publications (Tucker and Bras 2000, Lancaster et al. 2001, Bogaart et al. 2003, Lancaster et al. 2003, Colllins et al. 2004, Sólyom and Tucker 2004, Tucker 2004, Istanbulluoglu et al. 2005, Clevis et al. 2006, Flores-Cervantes et al. 2006, Crosby et al. 2007, Gasparini et al. 2007).

Parameters Related to Climate

CHILD uses a stochastic representation of rainfall and runoff in which a sequence of storm and interstorm events is drawn at random from exponential frequency distributions (Eagleson 1978; Tucker and Bras 2000). The rainfall model requires three parameters: the average storm intensity, P, the average storm duration, T_r, and the average time period between storms, T_b. Hawk (1992) derived sets of these three parameters from hourly rainfall data for each month of the year at several dozen meteorological stations around the United States. For this study, the default parameters were based on Hawk's data from the Buffalo, New York, station for the month of August (P = 2.131 millimeters (0.084 inches) per hour, T_r = 5 hours, T_b = 65 hours). The month of August, which has the highest precipitation intensity, was selected because the nonlinearity inherent in the water erosion and transport rate laws makes them sensitive to precipitation intensity (Tucker and Bras 2000); in effect, the assumption was made that rainfall in August contributes more to erosion and sediment transport than any other month (for future analyses, it would be feasible to develop an annualized rainfall distribution, which would circumvent the need to choose a particular month). The mean storm and interstorm durations were magnified by a factor of either 10^2 (initial calibration runs) or 10 (regridded calibration runs and forward runs). Magnifying the mean storm and interstorm duration preserves the frequency-magnitude distribution of rainfall intensity while allowing for greater computational efficiency. A comparison of simulations using different values of this magnification factor (using Buttermilk Creek's topography as an initial condition and running forward in time for 10,000 years) showed that the error introduced by a tenfold storm/interstorm magnification

is small (less than 3 percent difference in average elevation change) while yielding a ninefold speed improvement. No attempt was made to explore scenarios in which precipitation frequency and/or magnitude change through time.

Table F–18 Values of CHILD Input Parameters Selected for Forward Modeling Runs

Parameter	Symbol	Value
Mean rainfall intensity	$\bar{P}$	2.1 millimeters per hour
Mean storm duration	$\bar{T}_r$	0.0057 years
Mean inter-storm duration	$\bar{T}_b$	0.74 years
Infiltration capacity	I	1 millimeter per hour
Sediment transport efficiency factor	k_f	246.5 square meters per year per pascal [3/2]
Sediment transport capacity discharge exponent	m_f	0.667
Sediment transport capacity slope exponent	n_f	0.667
Excess shear stress exponent	p_f	1.5
Bedrock erodibility coefficient	k_b	18 meters per year per pascal
Regolith erodibility coefficient	k_r	10,000 meters per year per pascal
Shear stress coefficient (=ρ $g^{2/3}$ $C_f^{1/3}$; see text)	k_t	900 pascals per (square meter per second) [2/3]
Bedrock erodibility specific discharge exponent	m_b	0.667
Bedrock erodibility slope exponent	n_b	0.667
Exponent on excess erosion capacity	p_b	1
Critical shear stress for bedrock	τ_{cb}	3 kg/m/s^2
Critical shear stress for regolith	τ_{cr}	23 kg/m/s^2
Diffusivity coefficient	k_d or κ	0.01 square meters per year
Critical Slope	S_c	0.5774 m/m
Initial regolith thickness	H_{r0}	1.0 meter
Base level lowering rate and duration	U	0.0224 meters per year for 2,000 years 0.00164 meters per year for 15,000 years
At-a-station channel width-discharge exponent	ω_s	½
Downstream channel width exponent	ω_b	½
Channel width coefficient	k_w	10 meters per (cubic meters per second) [1/2]

Parameters Related to Hydrology

The current version of CHILD provides four alternative means of computing runoff. Of these, the simplest and most commonly used is a single-parameter infiltration capacity model in which any rainfall in excess of a specified infiltration rate contributes to runoff. In general, the use of such a model in a humid temperate setting would be questionable because rainfall intensity rarely exceeds soil infiltration capacity under normal circumstances. In such settings, most runoff tends to be generated in localized areas where soils readily become saturated due to topographic convergence and/or low gradient (Dunne and Black 1970). However, the study area is somewhat unusual in having a high proportion of soils derived from clay-rich and therefore fairly impermeable glacial sediments, and therefore widespread hillslope runoff generation during heavy rains will be more common than in many humid-temperate environments. This is supported by the results of hydrologic monitoring discussed in the Surface Water Environmental Information Document (WVNS 1993c). In the

South Plateau disposal area, nearly 80 percent of the gauged flow resulted from runoff, implying that the effective infiltration capacity of soils formed from the clay-rich glacial sediments is rather low (not surprisingly, the study also found a higher effective permeability in the alluvial fan-derived soils of the North Plateau). For purposes of this study, a simple one-parameter infiltration-capacity runoff model is adopted, with the recognition that future studies of hydrologic response may point toward a different choice. An infiltration capacity of 1 millimeter per hour, which lies toward the low end of commonly observed infiltration rates (see, for example, Table 7.1 in Dunne [1978]), is used as a default parameter. The combination of rainfall parameters with a 1 millimeter per year infiltration capacity yields an average annual flow at the former gauging station of about 2 cubic meters per second (70 cubic feet per second), which is within a factor of two of the annual flows of 1.1 to 1.47 cubic meters (38 to 52 cubic feet) per second recorded during the station's brief period of operation during the 1960s. By using a relatively low value of infiltration capacity, the model emphasizes areas underlain by clay-rich, till-derived soils such as the South Plateau and the Franks Creek and Erdman Brook valleys.

The channel width, W, at any given node is calculated using an empirical relationship between width and discharge,

$$W = W_b \left(\frac{Q}{Q_b} \right)^{\omega_s} = k_w Q^{\omega_s} Q_b^{\omega_b - \omega_s}$$

where the subscript b denotes quantities at bankfull stage and W_s, W_b, and k_w are parameters. There do not appear to be any data available on variations in channel width downstream and at a station in the Buttermilk Creek watershed. Based on traditional hydraulic geometry data (Leopold et al. 1964), the following parameters provide a reasonable depiction of a range of alluvial rivers: $k_w = 10$ (in meters and seconds) and $W_s = W_b = 0.5$. For these parameters, the Buttermilk Creek bankfull discharge of 23.85 cubic meters per second yields a width of 48.8 meters, which is compatible with measured width in the bar complex maps of Boothroyd et al. (1982).

Parameters Related to Water Erosion and Sediment Transport

The erosion and transport laws should be appropriate to the processes occurring at the site. Based on reports and field observations, fluvial processes in the Buttermilk Creek watershed include: (1) transport of gravel through the stream network (Boothroyd et al. 1979, 1982), and (2) stream incision into cohesive clay-rich till (as well as other units, e.g., fan gravels, proglacial lake sediments). The presence of coarse bed sediment in Buttermilk Creek suggests that the stream system cannot be realistically treated solely with a detachment-limited model (Howard et al. 1994). One method would be to use a transport-limited fluvial model, which effectively treats the channel bed as loose sediment. However, the active incision of till and bedrock by Franks Creek and other tributaries and the observation of till exposed in the bed of Franks Creek near the SDA, suggest that a transport-limited model may not correctly capture incision of Lavery Till. Therefore, it is reasonable to use a hybrid model that accounts both for bed-load transport of gravel and for detachment of the till (or other bedrock) substrate. CHILD's standard water erosion algorithm computes bed lowering as the lesser of: (1) bedrock detachment capacity, and (2) excess sediment transport capacity per unit surface area.

This approach requires a choice of transport-capacity law and a choice of detachment-capacity law. Because the substance being detached is mostly clay till, it is appropriate to choose a detachment-rate formula that is applicable to cohesive, clay-rich substrates. Howard and Kerby (1983) found that the detachment (lowering) rate of cohesive clay sediments in a badland area was roughly proportional to the cross-section average bed shear stress. Correlations between detachment rate and boundary shear stress have been also been found in field tests of soil erosion (Elliot et al. 1989) and in studies of hydrodynamic erosion of cohesive riverbanks (Julian and Torres 2006). This motivates the use of the following widely used du Boys formula for computing the detachment capacity of cohesive material:

$$D_c = K_b \left(\tau - \tau_{cb} \right)_+$$

where D_c is the detachment capacity (with dimensions of length per time [L/T]), τ is boundary shear stress, τ_{cb} is a threshold shear stress below which detachment is negligible, and K_b is a lumped dimensional coefficient that depends on bulk density, effective particle size, and the strength of cohesive bonds between particles. The subscript indicates that the relationship only applies when $\tau > \tau_{cb}$; otherwise, the detachment capacity is zero. The detachment coefficient Kb is used as one of two calibration parameters. A default value of 4.5 (in meters, kilometers, and years) is based on field experiments in soil detachment (Elliot et al. 1989). The detachment threshold τ_{cb} (b for bedrock) could, in principle, be estimated for the clay-rich till units in the study area using jet testing. For the present, it is set to 3 Pascals (Pa), a value that falls within the general range of values estimated from field experiments on soils (Elliot et al. 1989) and cohesive river banks (Julian and Torres 2006).

CHILD offers several alternative formulations for calculating the sediment transport capacity of channelized flow. The coarser fraction of sediment, which tends to move as bed load, is considered to be the limiting factor for erosion of detached sediment. Therefore, a transport formula designed for bed load is considered appropriate. For practical reasons of simplicity and computational efficiency, a single effective grain size, rather than multiple grain-size fractions, is used for this study. The general form is

$$Q_c = W K_f \left(\tau^p - \tau_c^{\,p} \right)_+$$

where Q_c is the volumetric sediment transport capacity, W is the width of the channel, and K_f is a transport efficiency factor that incorporates fluid and sediment density and gravitational acceleration. A number of laboratory and field studies show a strong correlation between transport rate and excess shear stress raised to the 3/2 power, which is consistent with the hypothesis that transport rate depends on unit stream power (which represents the rate of energy expenditure per unit bed area and is equal to the product of shear stress and flow velocity). This motivates a choice of $p = 3/2$. The default value of the motion threshold, τ_c, is based on the observed median grain size of bar sediment on the order of 32 millimeters (1.26 inches) in Buttermilk Creek (Boothroyd et al. 1982, Figure 5A), assuming a critical Shields stress of 0.045, water density of 1,000 kilograms (1.1 tons) per cubic meter, and sediment density of 2,650 kilograms (2.9 tons) per cubic meter. The transport capacity coefficient K_f is used as a calibration parameter. Its default value of ~1.56×10^{-5} (meters, kilograms, seconds) is derived from the Meyer-Peter and Mueller transport formula, which has the same scaling as the transport equation above.

Note that there is no single generally accepted transport formula for bed-load flux. Rather, there are a number of competing approaches that involve somewhat different scaling of the key variables (Howard 1980; Martin and Church 2003) and have varying degrees of explanatory power depending on what data sets are examined. The choice of the above equation is based on the fact that its scaling is common to a number of frequently used and reasonably successful transport formulas. One limitation is that CHILD presently has no way to address suspended or wash load; thus, for example, when a cubic meter of clay is eroded, it all turns into "sediment" of a specified size. SIBERIA has the same limitation. A more realistic approach would be to specify a percentage of fines for the eroded substrate, and have these directly removed (Kirkby and Bull 2000), but this would require additional model development and testing, and it is considered unlikely to have a significant effect on the behavior of the model in this setting.

The cross-section averaged bed shear stress exerted by running water is based on a force balance between gravity and friction for steady, uniform, fully turbulent flow in a wide channel:

$$\tau = \rho \, g^{2/3} C_f^{1/3} \left(\frac{Q}{W} \right)^{2/3} S^{2/3}$$

where Q is water discharge, S is channel gradient, ρ is water density (= 1,000 kilograms (1.1 tons) per cubic meter), g is gravitational acceleration at earth's surface, and C_f is a dimensionless friction factor that depends weakly on relative roughness (flow depth relative to roughness height); C_f is set here to 0.0076 (equivalent to a "Darcy-Weisbach f" of 0.06), which is consistent with a relative roughness of ~30 based on pipe-friction experiments (Middleton and Southard 1984).

Parameters Related to Sediment Transport by Soil Creep and Landsliding

For this application, CHILD uses a nonlinear soil creep transport law that was introduced by Howard et al. (1994) and tested in the field and laboratory by Roering et al. (1999, 2003):

$$q_{sc} = \frac{K_d \nabla z}{1 - \left(|\nabla z| / S_c\right)^2}$$

where z is land surface height, K_d is a transport coefficient [L2/T], and S_c is a threshold slope gradient. This formula is nearly identical to that used in SIBERIA, and the parameters K_d and S_c are equivalent to SIBERIA's Dz and Somax. They are set to 0.01 square meters (0.11 square feet) per year and 30 degrees, respectively, as discussed above.

F.3.2.3.5   Model-Data Comparison Metrics

There are a number of different metrics that could be used in comparing observed and modeled topography. Studies of stream and hillslope profile evolution using one-dimensional models that typically use metrics based on the differences between observed and modeled surface height at a series of points along the profile (Rosenbloom and Anderson 1994, Stock and Montgomery 1999, Whipple et al. 2000, van der Beek and Bishop 2003, Tomkin et al. 2003). Comparing two-dimensional models of drainage basin evolution with observed topography is less straightforward. Point-by-point comparison of observed and simulated topography suffers from the problem that small differences in drainage pathways can lead to large apparent errors, even though the modeled topography may be statistically very similar to the real landscape. Thus, most tests of drainage basin evolution models have been based on statistical measures of terrain such as the catchment-wide slope-area relationship, the hypsometric curve, and the drainage-area distribution function (Hancock et al. 2002). These methods essentially weight all portions of the landscape equally. For purposes of the present project, however, the primary interest lies in capturing the evolution of the incised plateaus, not only because this is where WNYNSC lies, but also because of the much better knowledge of topographic change in the glacial plateau areas than in the bedrock uplands. Thus, it is appropriate to use a goodness-of-fit metric that emphasizes the incised plateau landscape. For the CHILD simulations, the longitudinal profile of Buttermilk Creek within the main valley was chosen as a preliminary test metric. For the SIBERIA simulations, which were limited to the Franks Creek watershed, the longitudinal profile from Erdman Brook through lower Franks Creek was used as a test metric. The choice of longitudinal profiles as the basis for model-data comparison reflects the finding that in cases of transient response, different erosion laws predict distinctly different longitudinal profile shapes (Tucker and Whipple 2002, Whipple and Tucker 2002). The main drawback of using longitudinal profiles is that they contain little or no information about properties such as hillslope form, drainage density, or tributary shapes and positions. Ultimately, there is a need for multi-objective criteria that describe a range of terrain attributes and have a demonstrated ability to discriminate between alternative models and rule out poor ones, but development and testing of such criteria were considered beyond the scope of this study.

For the CHILD calibration runs, observed and modeled profiles were compared along a portion of the main stem extending from a tributary junction at the head of the main Buttermilk Creek valley to the confluence with Cattaraugus Creek (coordinates at the head of the profile: UTM Zone 17T, E693320 meters,

N4700742 meters, datum NAD27). For the SIBERIA calibration process, the corresponding long profile ran from the headwaters of Erdman Brook to the confluence of Franks and Quarry Creeks (coordinates at the head of the profile: UTM Zone 17T, E693022 meters, N4703031, datum NAD27). The observed longitudinal profiles were extracted from a 10-meter resolution USGS digital elevation model. Because the lengths of the observed and modeled long profiles tend to differ slightly, linear interpolation was used to divide the observed and modeled profiles into 101 equally spaced points. This approach allows for point-by-point comparison. The misfit between observed and modeled profiles was calculated as:

$$E_{lp} = \frac{1}{N} \frac{\sum_{i=1}^{N} \sqrt{(z_{im} - z_{iobs})^2}}{\langle z_{obs} \rangle}$$

where $N = 101$ is the number of profile points compared, z_{im} is the modeled height above the outlet at point i, z_{iobs} is the observed height above the outlet at point i, and $\langle z_{obs} \rangle$ is the observed mean profile height above the outlet. Parameter combinations with the lowest value of the mis-fit index, E_{lp} were identified. The resulting best-fit run was considered adequate if it met two other (qualitative) criteria: (1) extensive remnants of the initial plateau were preserved along the flanks of the main channel network, and (2) the modeled longitudinal profile of Franks Creek provided a reasonable match (comparable to that of the Buttermilk profile) to the observed profile. With the CHILD model, after the best-fit parameter pair was identified, the model was rerun with the same parameter set but with the node spacing reduced by a factor of four (from approximately 90 meters to approximately 22.5 meters [295 feet to 73.8 feet]) in the vicinity of WNYNSC, and with the mean storm and interstorm duration parameters reduced by a factor of 10. The variable-resolution mesh used in these model runs is shown in **Figure F–12**.
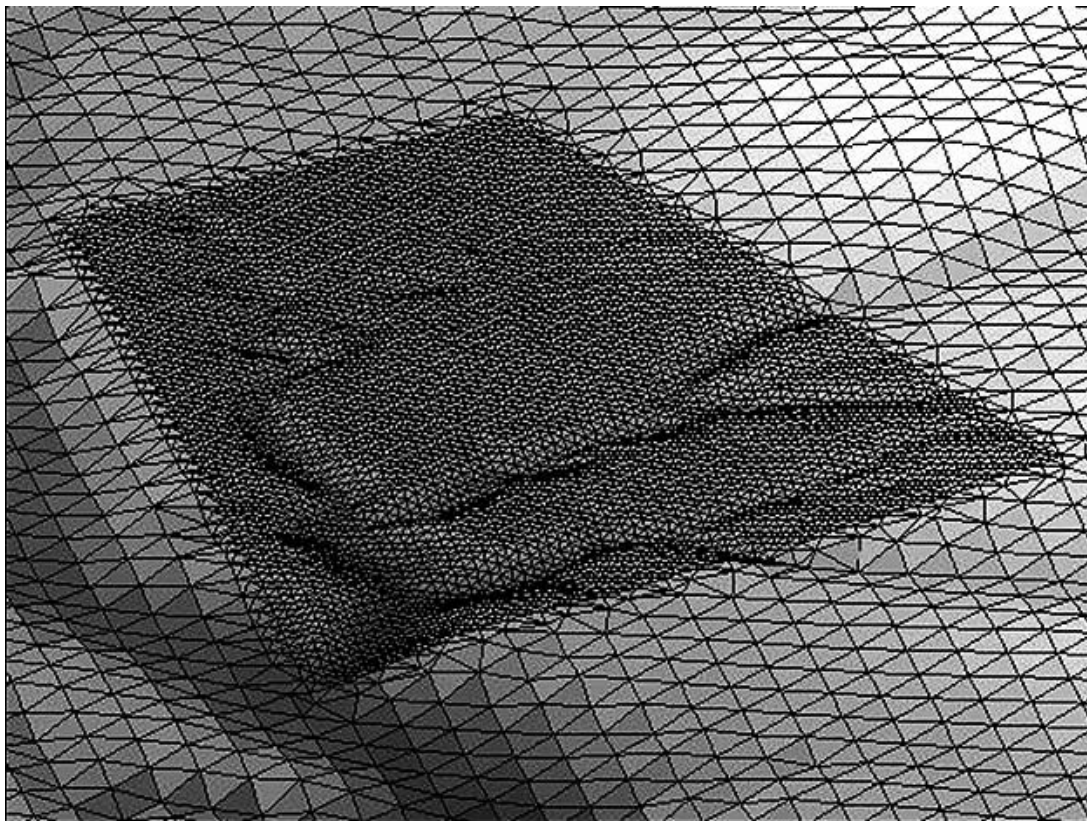

Figure F–12 Perspective Image Showing CHILD Simulation Mesh with Tighter Node Spacing in Vicinity of the Western New York Nuclear Service Center

F.3.2.4   Calibration Results

F.3.2.4.1   CHILD Calibration

The error estimates from 25 calibration runs are listed in **Table F–19**. Figure F–13 compares the observed and modeled longitudinal profile of Buttermilk Creek for the best-fit run. The model captures the weakly concave-upward shape of the profile. The profile is relatively insensitive to K_b, implying that transport capacity, rather than detachment capacity, is the primary limiting factor on profile development in these runs. The simulated present-day topography preserves remnants of the till plateau flanking the incised valley, and it predicts about the right depth of incision along the main trunk stream (**Figures F–13** and **F–14**). It significantly over predicts the degree of landscape dissection, particularly in the bedrock uplands. Part of this may be due to the difference in erosion resistance between glacial valley fills and Paleozoic bedrock, which was not accounted for in the trial calibration runs. A better fit to the drainage density could probably be achieved by incorporating such a difference (in the form of a second K_b parameter to represent Paleozoic bedrock) and/or by searching a broader range of parameter space using a multi-parameter optimization method such as a Monte Carlo approach.

Table F–19 Best-Fit Longitudinal-Profile Scores for 25 CHILD Calibration Runs

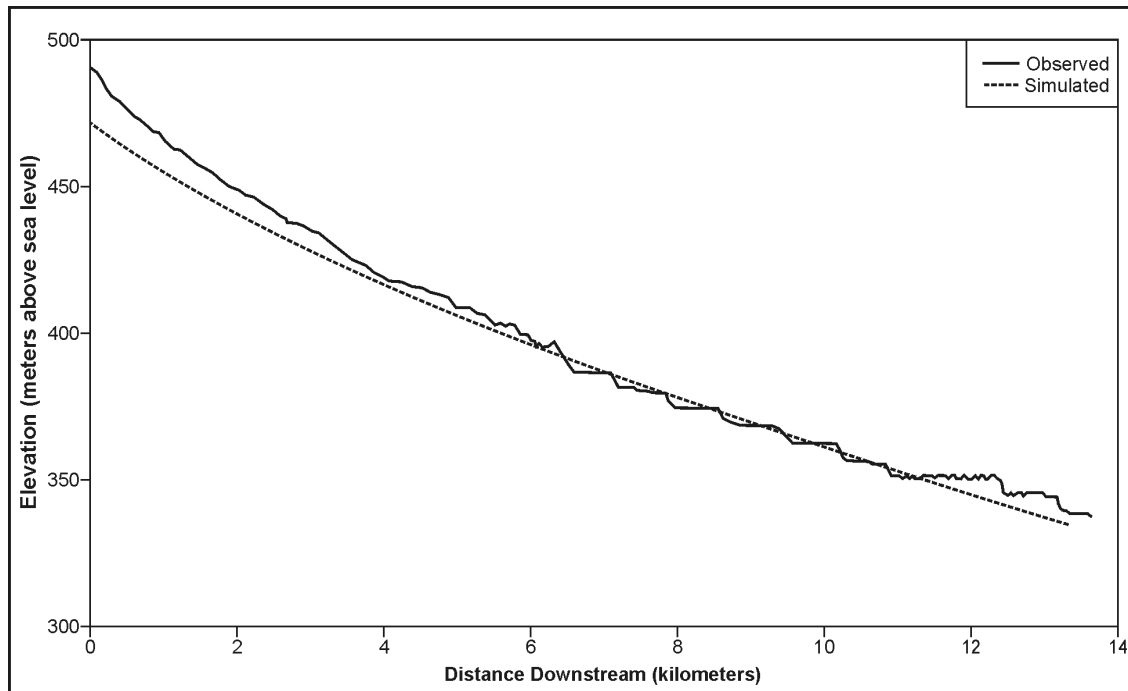|		K_f				
		123.25	246.5	493	986	1972
	1.125	0.0905	0.0727	0.0769	0.1136	0.2273
	2.25	0.0889	0.0716	0.0996	0.1363	0.2333
K_b	4.5	0.0904	0.0700	0.0846	0.1518	0.2504
	9.0	0.0837	0.0729	0.0805	0.1280	0.2351
	18.0	0.0870	**0.0694**	0.0723	0.1393	0.2477

Note: Best-fit value shown in **bold**.

Figure F–13 Comparison of Observed and Modeled Longitudinal Profile of Buttermilk Creek in Best-Fit CHILD Calibration
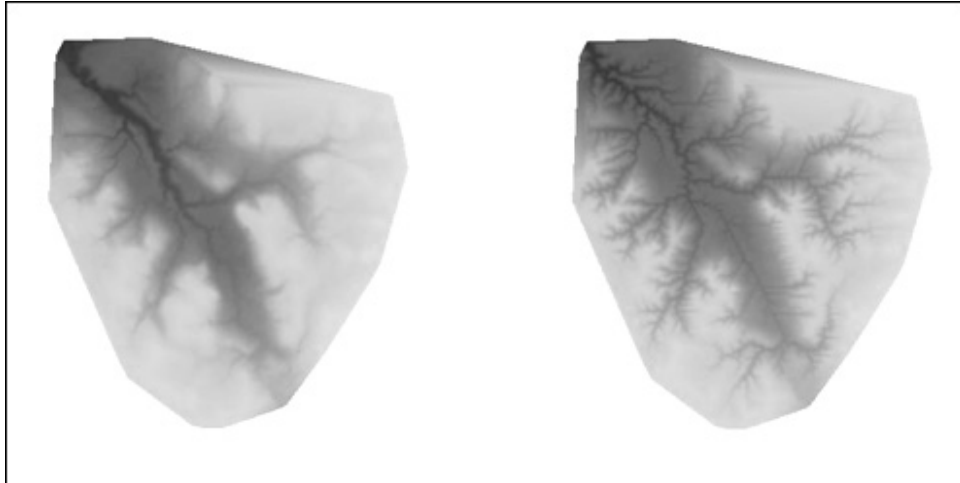
**Figure F–14 Plan-View Images of Buttermilk Creek (left) and
Best-Fit CHILD Calibration Run (right)**

The simulated drainage patterns in the Franks Creek area are similar, though not identical, to the observed patterns (**Figure F–15**). The disparity reflects the known sensitive dependence of drainage patterns on initial conditions, and also the nature of the topography itself: alluvial fans form in this area early in the simulation (presumably for the same reason that fans formed on the actual plateau during the postglacial period), and this naturally leads to frequent drainage switching. As a result, the model's versions of Quarry Creek and Outwash Creek (next major tributary northwest of Quarry Creek as shown on Figure F–1) have merged; below their confluence, the modeled streams roughly follow the path of the real Outwash Creek. The modeled valleys are generally narrower, which is to be expected because the model runs did not incorporate the lateral channel migration process (i.e., the lateral shifting in channel position due to natural instabilities in the flow that lead to bank erosion and gradual horizontal migration in the channel position).

One way to test the calibration is to compare the observed and simulated longitudinal profiles of streams that were not used to calibration the model. The best-fit calibration run does a reasonable job with the longitudinal profile of Franks Creek between its entry onto the till plateau and its confluence with Buttermilk Creek (**Figure F–16**).

F.3.2.4.2   SIBERIA Calibration

The SIBERIA calibration was completed on the Franks Creek watershed. Although calibration was also attempted on the Buttermilk Creek scale, there were numerical stability issues at practical time steps and so the analysis was not completed.

The error estimates from 46 calibration runs are listed in **Table F–20**. **Figure F–17** compares the observed and modeled longitudinal profile of Upper and Lower Franks Creek for the best-fit run. The model captures the concave-upward shape of both profiles rather well; however, it over predicts incision in the upper bedrock portion of the watershed and under predicts incision in the Upper Franks Creek portion. The models over prediction of incision in the upper portion of the watershed is likely due to the difference in erosion resistance between glacial valley fills and Paleozoic bedrock that was not accounted for in the trial calibration runs (i.e., variable material properties were not represented in the models to account for the differences in geologic units). As in the CHILD simulations, a better fit to the drainage density could probably be achieved by incorporating such a difference (in the form of a second β_1 parameter to represent Paleozoic bedrock) and/or by searching a broader range of parameter space using a multi-parameter optimization method such as a Monte Carlo approach.
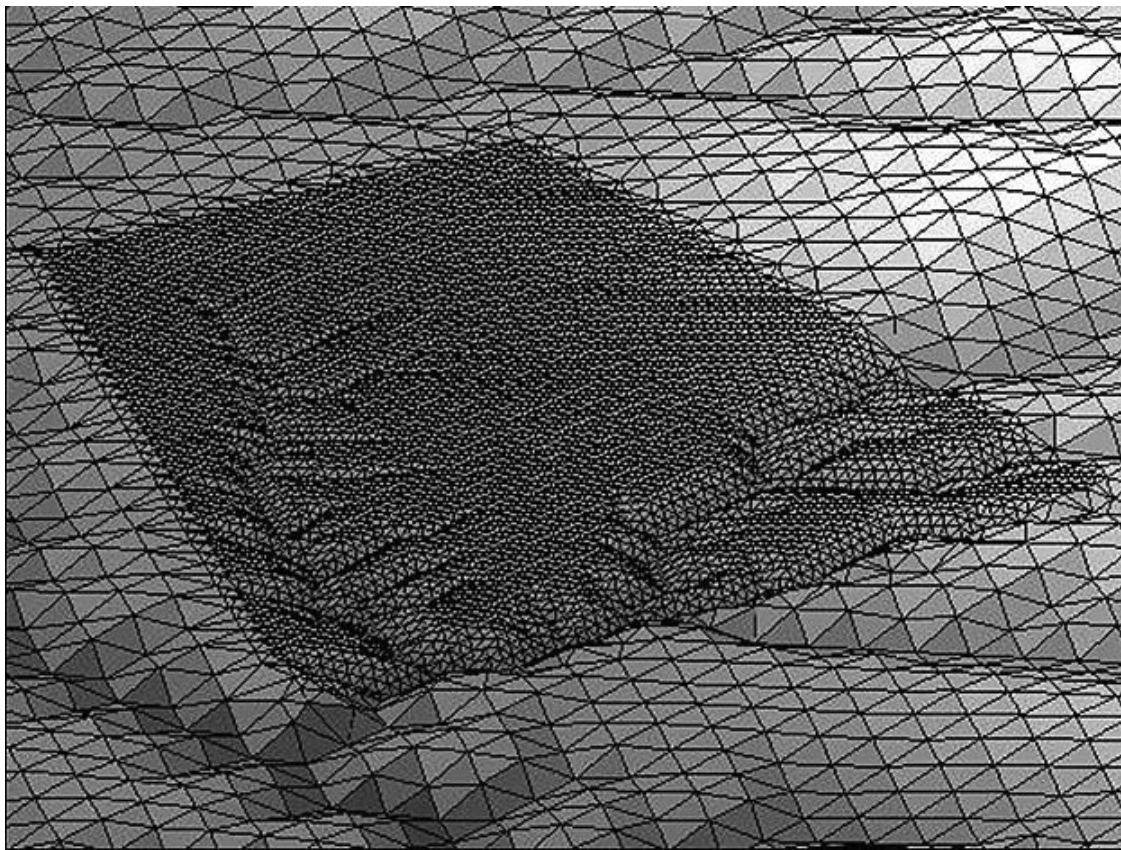
Figure F–15 Perspective View of Present-Day Topography and Drainage Patterns in the Franks Creek Area as simulated by the CHILD Model
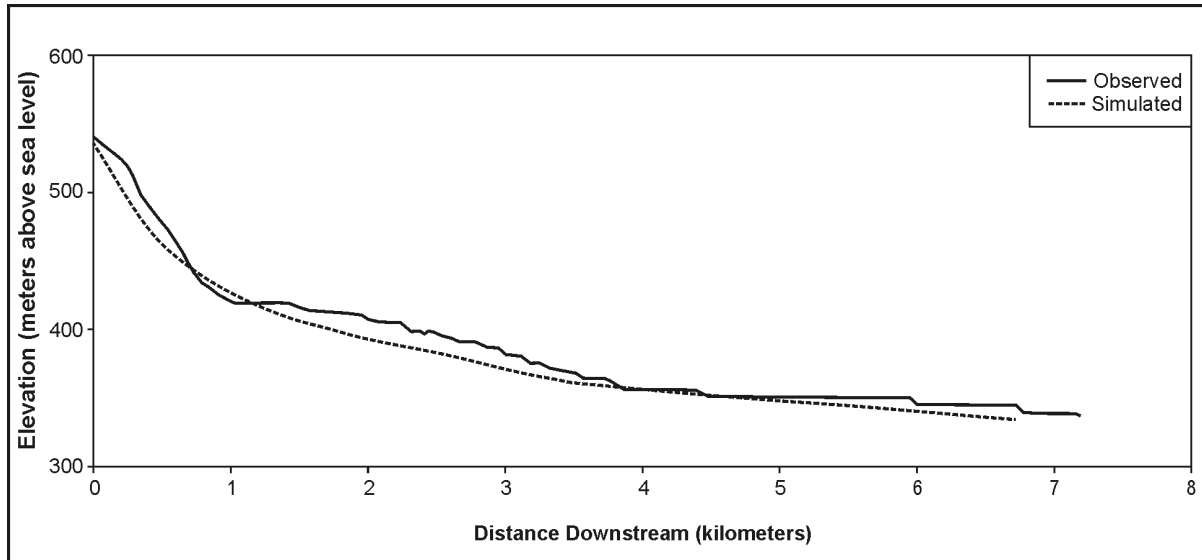

Figure F–16 Comparison of Observed and CHILD Simulated Longitudinal Profiles of Franks Creek and Lower Buttermilk Creek from the Point where Franks Creek Enters the Plateau Area to the Outlet of Buttermilk Creek (steps in the observed long profile are artifacts in the digital elevation model)

Table F–20 Best-Fit Longitudinal-Profile Scores for 46 SIBERIA Calibration Runs

		QsHold						
		0.01	*0.2512*	*0.631*	*1.5849*	*3.9811*	*10*	*20*
Beta1	4.64×10^{-7}						**0.1132**	0.1318
	1.00×10^{-6}	0.1422	0.1642	0.2662	0.2887	0.1413	0.1718	0.1624
	2.15×10^{-6}	0.1984	0.1862	0.1869	0.3109	0.2846	0.2600	0.2426
	4.64×10^{-6}	0.3172	0.2263	0.2218	0.2151	0.2981	0.2809	
	1.00×10^{-5}	0.2789	0.2909	0.2971	0.2850	0.3165	0.3219	
	2.15×10^{-5}	0.4795	0.4525	0.4080	0.3336	0.4923	0.5283	
	4.64×10^{-5}	0.5687	0.6997	0.5908	0.5496	0.7613	0.7531	
	1.00×10^{-4}	0.8360	0.7102	0.8089	0.6766	0.8938	0.5548	

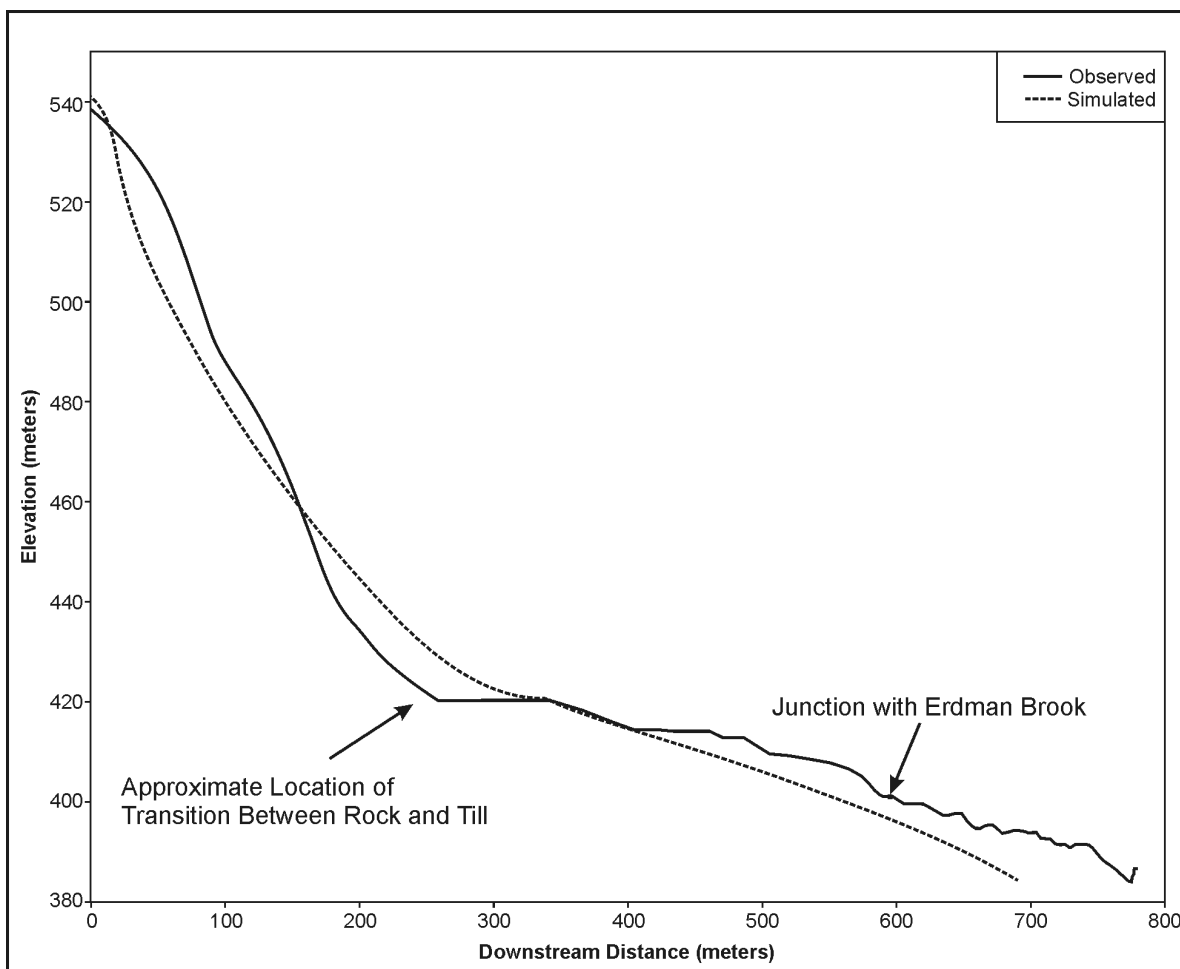Best-fit value shown in **bold**.

Figure F–17 Comparison of Observed and Modeled Longitudinal Profile of Franks Creek in Best-Fit SIBERIA Calibration Run

The simulated drainage patterns in the Franks Creek watershed are similar, though not identical, to the observed patterns (**Figures F–18** and **F–19**). Lower Franks Creek, Upper Franks Creek, and Erdman Brook all follow the paths of the real stream channels. One discrepancy is the formation of a new channel near the confluence of Franks Creek with Quarry Creek that is progressing along a path parallel to Lower Franks Creek. The length of the NDA Gully is also a bit longer and branched, although it is in the right location. The modeled valleys are narrower, which is to be expected because the model runs did not incorporate valley-widening processes such as lateral channel migration. Despite these differences in drainage pattern and width, the best-fit calibration run does a reasonable job of replicating the existing stream pattern.
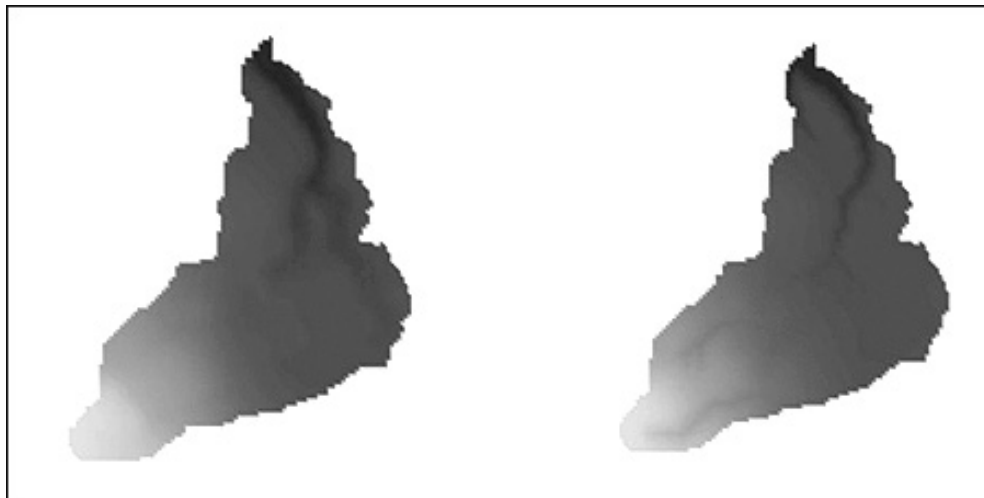

**Figure F–18 Shaded Relief Images of Franks Creek (left) and Best-Fit
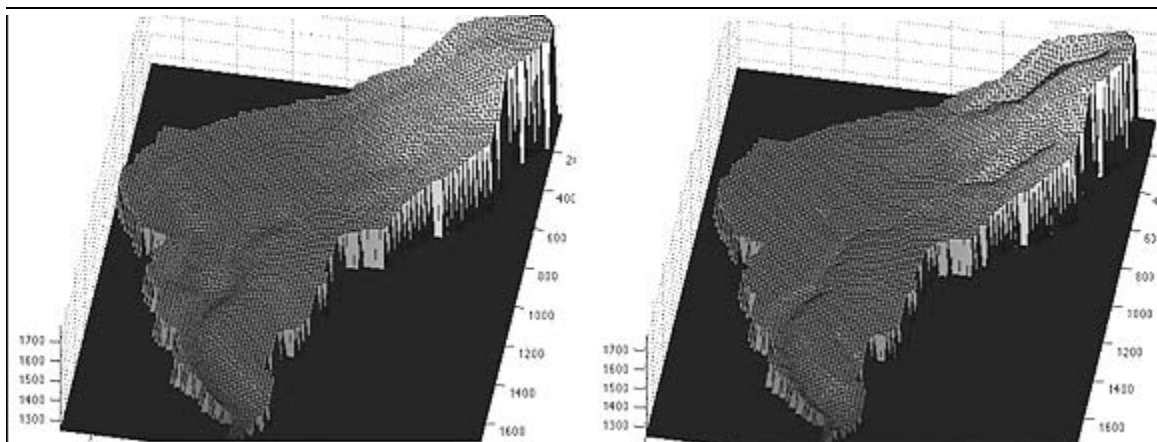SIBERIA Calibration Model (right)**

Figure F–19 Perspective Images of Franks Creek Basin as Observed (left) and Simulated (right)

F.3.2.5 Calibration: Discussion and Interpretation

Although there are obviously important differences between the observed and modeled landscapes, the degree to which the CHILD and SIBERIA models are able to reproduce key features of the topography is somewhat remarkable given the limited calibration strategy, the sensitive dependence of drainage pathways on initial conditions, and the intentional neglect of any spatial variation in material properties (chiefly, the contrast between glacial valley fill and Paleozoic bedrock). It is likely that the degree of fit could be improved with a more thorough calibration strategy. Such a strategy would involve multiple terrain metrics, rather than reliance on the main-stream longitudinal profile as the sole test criterion. It would also need to explore a broader range of parameter space, using some form of Monte Carlo approach in which parameter ranges were bounded by physical and/or empirical constraints. Nonetheless, some aspects of the observed terrain are unlikely to be matched in a deterministic sense. The details of the drainage pattern are sensitive to small perturbations, and are therefore unlikely to be matched by any model in a deterministic sense. This is particularly true in areas of sediment accumulation, such as the alluvial fans that flank the main valley, as such areas are naturally prone to rapid drainage switching.

One element that would likely be improved by a more through calibration approach is the degree of landscape dissection. The current best-fit CHILD run over predicts the degree of dissection (Figure F–14). The unrealistic extent of dissection in the bedrock uplands partly reflects the assumed uniformity of material properties: in essence, the bedrock uplands were modeled as if they were made of glacial till and, appropriately enough, the model predicts rather intense gullying in these areas. This issue could be addressed by allowing K_b to vary with lithology, although at the cost of introducing an additional parameter to be constrained. The degree of dissection within the plateau and canyon areas is also somewhat over predicted. In general, the degree of landscape dissection is controlled by (1) the intensity of diffusive (creep) processes relative to water erosion processes, and (2) the magnitude of erosion thresholds (Kirkby 1995, Tucker and Bras 1998). It is also likely that gully extension in this environment is limited by vegetation growth, which can effectively impose a large erosion threshold on the landscape in hollows and ephemeral channels. To test this premise, it would be necessary to determine whether a better overall fit to the modern topography is obtained when a dynamic vegetation layer is used (Collins et al. 2004).

With the SIBERIA calibration, a combination of β_1 and Q_sHold was identified that produces a reasonable match to the observed longitudinal profile along Erdman Brook and lower Franks Creek (Figures F–17). This parameter combination lies toward the edge of the zone of parameter space that was explored, so it is possible that with additional computation and analysis time, a better fit could be identified. However, the match is sufficiently close that it was considered adequate for the present study. Comparison between the observed and modeled longitudinal profile of the whole of Franks Creek shows modeled elevations on the plateau that are significantly higher than those observed (Figure F–18). This is thought to reflect, at least in part, the assumption of uniform materials in the landscape. Because the higher erosion resistance of the paleozoic bedrock areas in the headwaters is not accounted for, the upland areas undergo significant erosion in the calibration runs. This provides a large sediment source to the plateau surface, which inhibits channel incision. It is likely that this mis-match could be reduced or eliminated if it were possible to account for spatial variations in erodibility.

F.3.2.6 Forward Modeling of Erosion Patterns

F.3.2.6.1 General Approach

Using the calibrated parameters, both models were run forward in time for a period of 10,000 years. With CHILD, the runs included all of Buttermilk Creek, with the region around WNYNSC represented at a higher resolution than the rest of the basin (Figure F–12). With SIBERIA, the runs were computed for the

Franks Creek watershed only. The initial condition for these runs was the modern topography, both with and without the engineered structures proposed in the Sitewide Close-In-Place Alternative.

One potential disadvantage to starting from modern topography is the potential for "model shock" as the model adjusts to irregularities and errors in the data, as well as to certain topographic features that the model does not simulate (e.g., incised valleys wider than one cell). To test the degree to which this might obscure the overall erosion and sedimentation patterns, an additional run was performed with CHILD using the calibration topography as the starting condition. Note that the forward runs reported here are essentially deterministic in nature, and they involve uncertainties that are not easily quantified. Potential sources of error and uncertainty are discussed in Section F.3.2.6.5 below. Probabilistic erosion estimates with uncertainty bounds, based on ensembles of model runs, are feasible in principle but would require additional computation and analysis time; this was considered beyond the scope of the present study.

F.3.2.6.2   Forward Modeling: Mathematical Representation of Tumuli

The burial structures (tumuli) proposed for the Sitewide Close-In-Place Alternative (Appendix C) are designed to withstand direct water erosion, and to be geomechanically stable. However, few engineered structures without deep pilings can withstand being undermined by erosion of the ground that supports them. Thus, the greatest erosional threat to these structures is considered to be undermining by mass movement as valley rims widen in response to stream incision. It was assumed that, with regard to hillslope mass movement, the materials composing the tumuli would not differ substantially from the natural soils and sediments on which they are built. On the other hand, the coarse armor layer capping the tumuli has the potential to resist water erosion more effectively than the glacial sediments underlying the plateau area. With the CHILD model, simulations were conducted with two alternative representations of the tumulus materials: one (the "soft cap" model) assumes that the cap material is just as susceptible to water erosion as the natural soils; the other (the "hard cap" model) assumes that the cap material cannot be entrained by running water. Comparing these cases can shed light on the potential importance of a resistant cap. The version of SIBERIA used in these analyses lacks the capability to vary erosion properties in space, and so only the soft-cap scenario was run with SIBERIA. In all of these cases, the topography associated with the proposed tumuli was added to the initial conditions.

F.3.2.6.3   Forward-Modeling: Results from CHILD

In the No Action Alternative no cap scenario, erosion is concentrated along existing gullies (as shown in Figure F–5), which generally extend headward into the plateau (**Figure F–20** [b]). The NP-1 gully extends southward into the North Plateau, with maximum modeled erosion depths on the order of 10 to 12 meters (32.8 to 39.4 feet). Significant deepening and extension also occurs along the NP-2 and NP-3 gullies (up to 12- to 15-meter (39.4- to 49.2-feet) deep) and the EQ-1 gully (on the order of a 6- to 7-meter (19.7- to 23.0 foot) maximum lowering). In addition, gully erosion impacts the eastern rim of the North Plateau between NP-3 and EQ-1, as well as the western rim along the edge of Quarry Creek. In the area of the North Plateau Waste Management Areas 1 and 3, erosion depths are on the order of 0.1 to 0.3 meters (0.33 to 0.98 feet). The greatest threat to this area appears to come from expansion of the southeast valley wall on Quarry Creek, where the advancing valley rim advanced to within 150-meters (492-feet) of the process building and tanks. On the South Plateau, the model produces incision depths on the order of 1 to 4 meters (3.28 to 13.12 feet) along the "NDA Gully" that runs between the SDA and NDA. Similar erosion depths occur in the west-central portion of the NDA, where the headwaters of Erdman Brook are diverted around a low embankment. The southeast corner of the SDA shows locally high creep erosion, with a maximum erosion depth a little over a meter (3.28 feet).
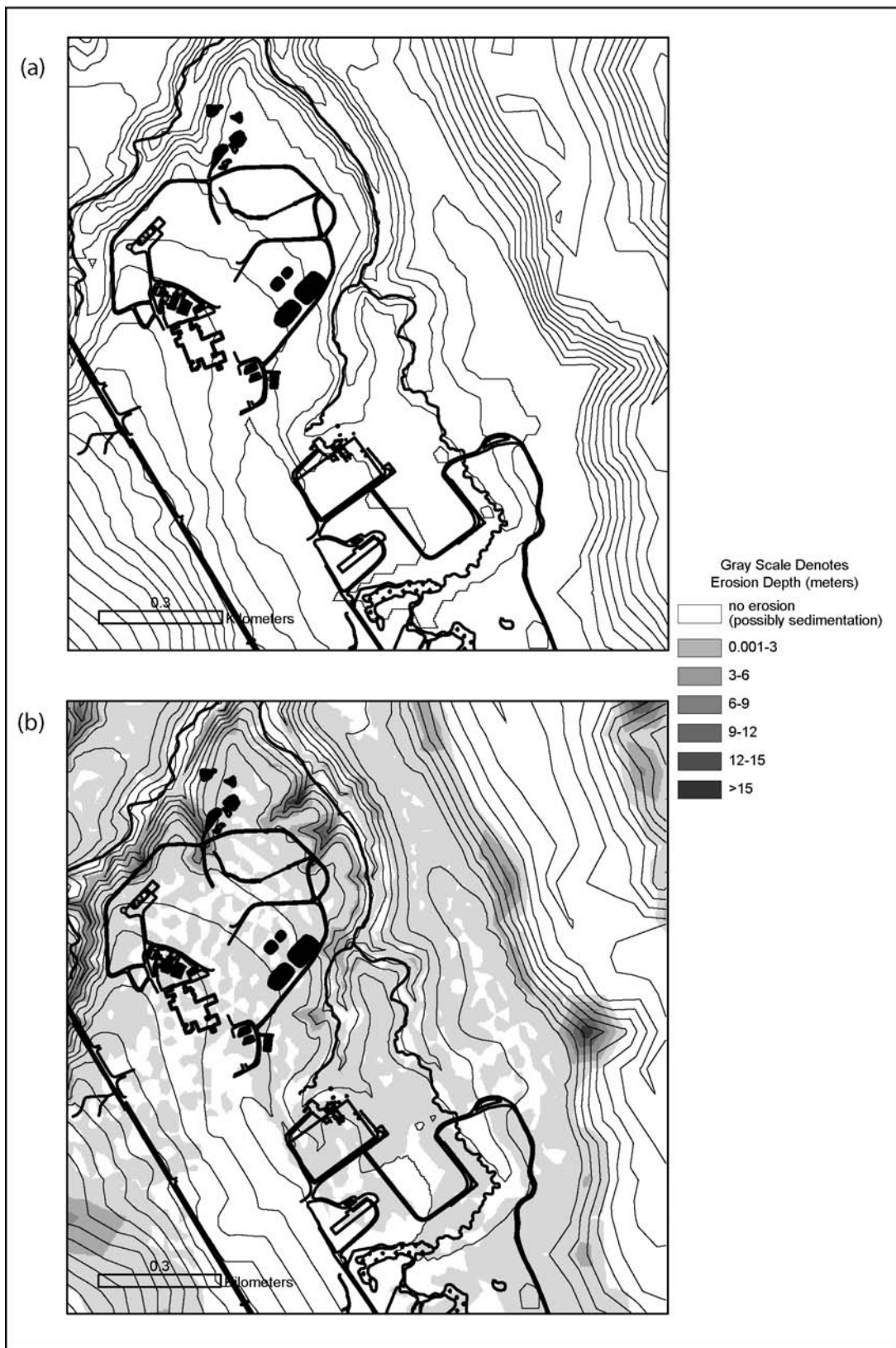
Figure F–20 Maps Showing (a) Current Topography at the Western New York Nuclear Service Center Site, and (b) Topography and Erosion Pattern Predictions at 10,000 Years as Computed by CHILD ([b] No Action Alternative No-Cap Scenario)

As noted in Figure F–20, a version of the No Action Alternative no cap scenario was run using the calibration topography, rather than the observed topography, as a starting point. The erosion patterns computed in this run (not shown) differ in detail but involve similar erosion depths and similar patterns of gully propagation. This suggests that the issue of "model shock" discussed previously has only a minor impact on the results.

In the Sitewide Close-In-Place Alternative soft-cap scenario (**Figure F–21** [c]), the erosion patterns are broadly similar to those of the no-cap scenario with the exception of the northern and western parts of the SDA-NDA area. In the presence of a soft-capped tumulus on the South Plateau, drainage that presently feeds the NDA Gully is diverted to the south, and the small gully running between the SDA and NDA becomes a zone of sediment accumulation. The infilling results from down-slope creep of the mound material, which accumulates along the bases of the burial mounds and within this channel. Modeled erosion depth on the South Plateau mounds is on the order of 0.1 to 1.7 meters (0.33 to 5.58 feet). Erosion depths greater than a meter are found in two locations. One is at the north end of the SDA. The other is at the western corner of the NDA mound, which is undermined by erosion along Erdman Brook at this location. On the north-plateau mound, erosion depths range from 0.01 to 0.7 meters (0.03 to 2.30 feet), with the greatest depths along the convex rim of the mound.

Erosion patterns in the Sitewide Close-In-Place Alternative hard-cap scenario (Figure F–21 [d]) are very similar to those for the soft-cap scenario, indicating that hillslope mass-movement processes drive the vast majority of mound erosion in both scenarios. The biggest difference between the cap and no-cap scenarios is the presence or absence of gully erosion in the gap between the NDA and SDA and at the western end of the NDA. In the no-cap scenario, drainage accumulated on the South Plateau flows around the south end of the NDA, then turns northward to run between the SDA and NDA toward Erdman Brook. This drainage path erodes a gully-like feature along the boundary between the SDA and NDA (the NDA Gully). In the Sitewide Close-In-Place Alternative cap scenarios, this drainage, together with the headwaters of Erdman Brook, is diverted around the south side of the SDA where it generates about a meter of erosion.

In summary, the CHILD model scenarios predict that the areas most prone to erosion are the existing gullies, the east and west rims of the North Plateau, and the three Creek valleys (Franks, Erdman, and Quarry). In the No Action Alternative no-cap scenario, the model predicts gully erosion along the NDA-SDA boundary. In the Sitewide Close-In-Place Alternative cap scenarios, this is prevented by the diversion of upper Erdman Brook around the south end of the SDA. The chief mode of cap erosion is soil creep, which generates up to about a meter of erosion on the cap rims and corners over the evaluated 10,000-year timeframe.

F.3.2.6.4   Forward Modeling: Results from SIBERIA

In both the No Action Alternative (no-cap) and Sitewide Close-In-Place Alternative soft-cap scenarios, SIBERIA predicts the greatest depth erosion in the NP-3 gully, on the western flank of lower Franks Creek (**Figure F–22**). Both cases also show concentrated erosion around the EQ-1 gully. In the No Action Alternative no-cap scenario, significant erosion also occurs in the NDA Gully along the boundary between the SDA and NDA. In the Sitewide Close-In-Place Alternative soft-cap scenario, the drainage feeding this gully is diverted around the NDA cap and, as in the CHILD cap scenarios, the NDA Gully area undergoes aggradation rather than erosion. One difference between the two models is that SIBERIA predicts drainage diversion into Erdman Brook, while in CHILD much of this drainage is diverted around the south end of the SDA. The difference may simply reflect the fact that the SIBERIA runs were limited to the present-day Franks Creek catchment, and therefore all drainage is constrained to remain within the boundaries of this catchment.
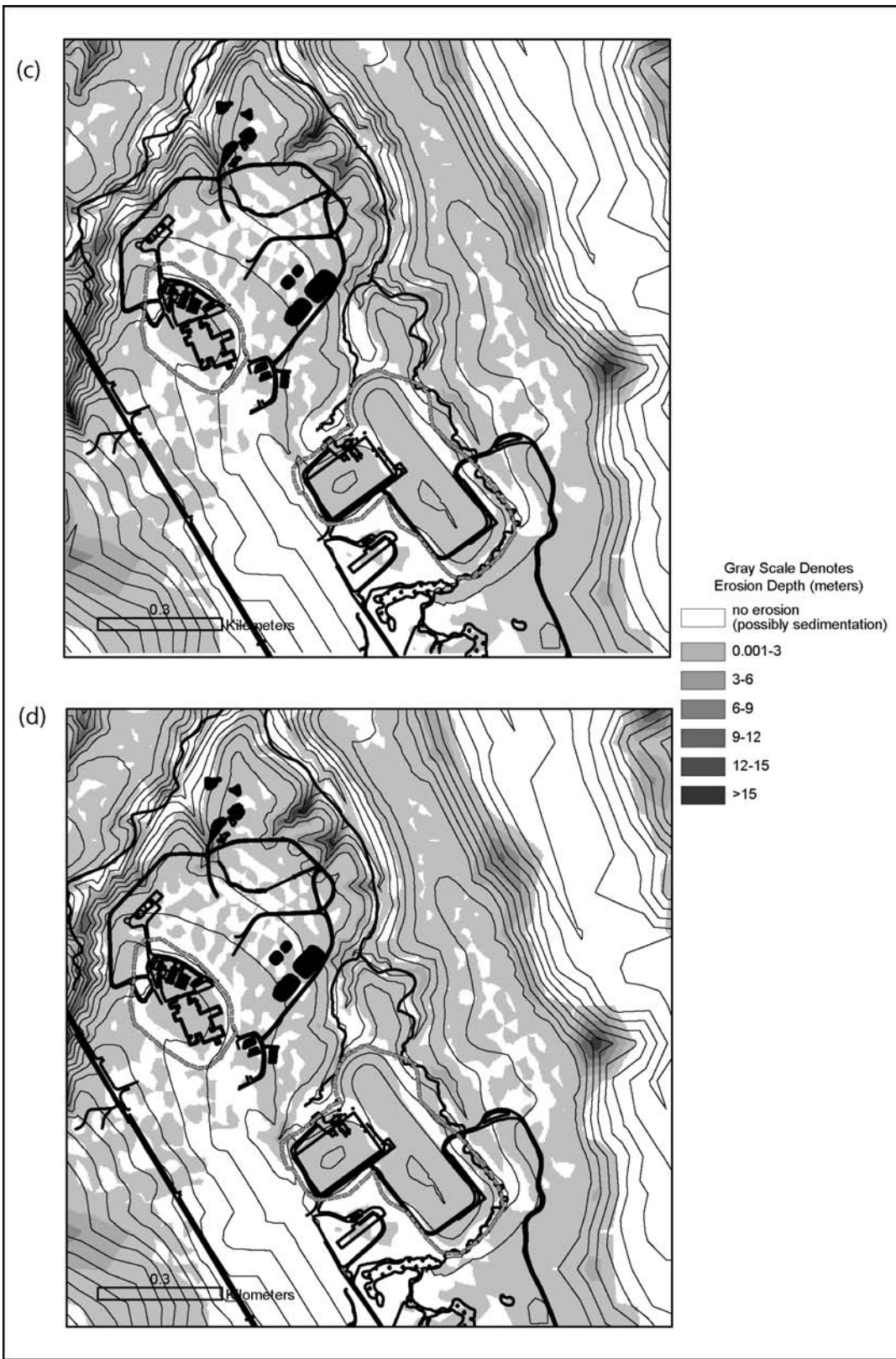
Figure F–21 Maps Showing (c-d) Topography and Erosion Pattern Predictions at 10,000 Years as Computed by CHILD for the Sitewide Close-In-Place Alternative ([c] Soft-Cap Scenario, [d] Hard-Cap Scenario)
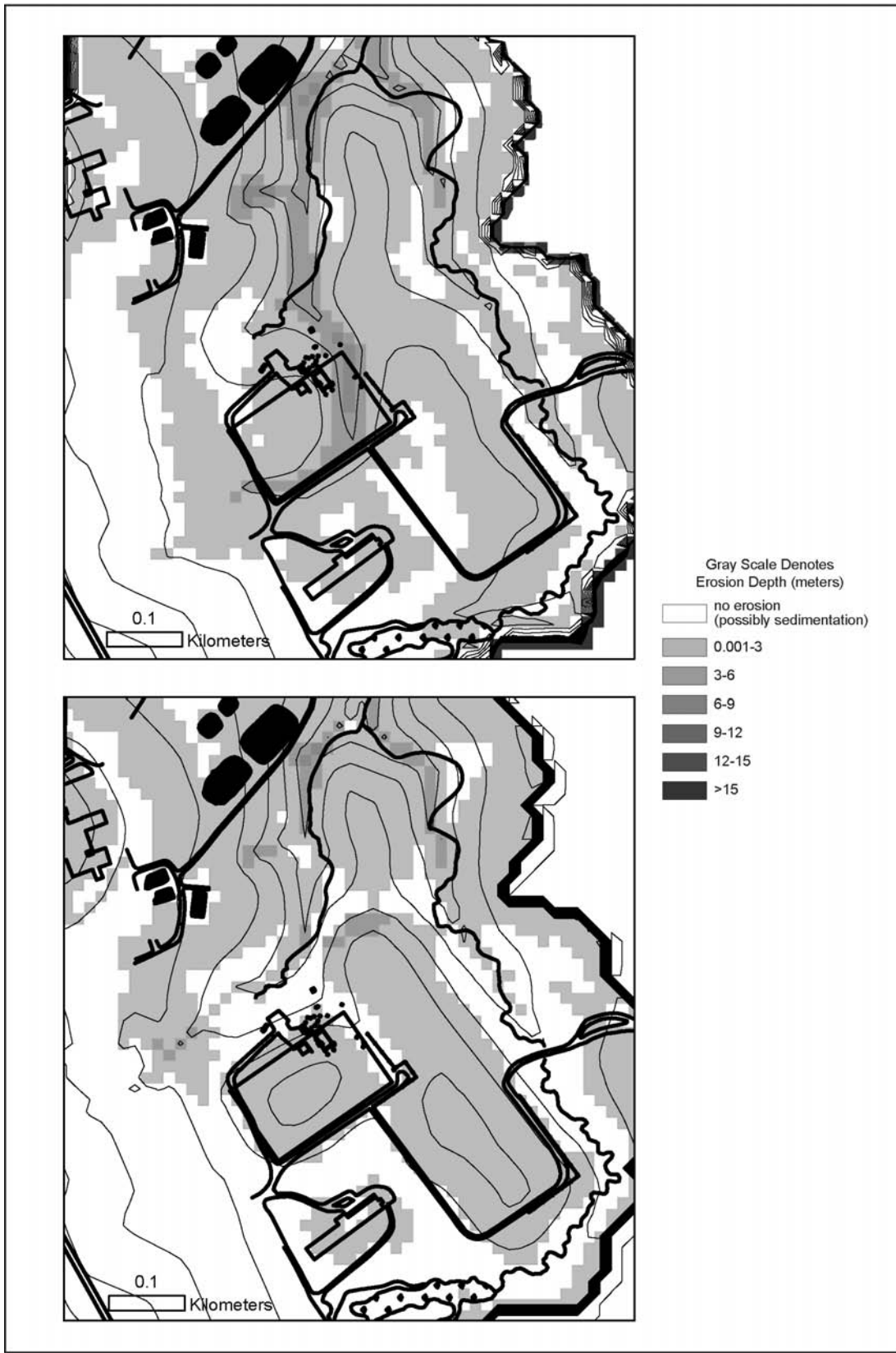
**Figure F–22 Erosion Patterns Computed by SIBERIA for the
Sitewide Close-In-Place Alternative No-Cap (top) and Soft-Cap (bottom) Scenarios**

F.3.2.6.5   Forward Modeling: Discussion and Interpretation

The calibrated CHILD and SIBERIA models predict broadly similar patterns and rates of erosion over the evaluated 10,000-year timeframe. The model calculations support the view that gully propagation represents the greatest erosional threat to the north and south plateaus. Existing gullies, such as NP-3, are predicted to deepen significantly and advance headward. Both models show significant erosion along the NDA Gully in the No Action Alternative no-cap scenario, but drainage diversion away from this gully in the Sitewide Close-In-Place Alternative cap scenarios. Maximum erosion depths locally exceed 15 meters (49.2 feet) within the most active gullies with advances of up to 220 meters (722 feet) over the 10,000 period, which is equivalent to a long-term advance rate of 0.02 meters (0.066 feet) per year. Of the two plateaus, the North Plateau site is generally stable, with computed erosion depths generally no greater than about a meter (3.28 feet), which is equivalent to a rate of 100 millimeters (0.328 feet) per 1,000 years. The South Plateau appears to be more vulnerable in all model runs, with up to three or four meters (9.8 to 13.1 feet) of erosion in the no-cap scenarios and lesser amounts in the cap scenarios, which is equivalent to a rate of 980 to 1,310 millimeters per 1,000 years. These rates are compared to the erosion frame measurements and the short-term modeling predictions in **Table F–21**.

Table F–21 Comparison of SIBERIA/CHILD Erosion Rates on the Plateaus to Short-Term Modeling Estimates and Erosion Frame Measurements

Model Name	Average Elevation Change (meters per 10,000 years)	Average Elevation Change (millimeters per 1,000 years)
SIBERIA/CHILD North Plateau	0 - 1	0 - 100
SIBERIA/CHILD South Plateau	3 - 4	300 - 400
Erosion Frames	0 - 14 [a]	0 - 1,400 [a]
USLE	0.128	12.8
SEDIMOT II	0.11	11
CREAMS	6.9	690
WEPP	4.08	408

[a] Range is representative of sheet and rill erosion on overland flow areas as well as mass wasting on hillslopes.

There are a number of sources of uncertainty that should be taken into consideration when interpreting these findings. Perhaps the most significant concerns the assumption that climate will not significantly change over the forecast period. There are two potential weaknesses to this assumption. The first and most obvious is the possibility that the future climate may differ substantially from the present one. Climate has a direct or indirect control on all of the landscape-forming processes at the West Valley Site. Rainfall frequency and magnitude directly impact erosion and sediment transport by running water, and indirectly influence the nature of the vegetation. Biota are linked with a number of transport processes, and can influence rates of soil mixing, surface resistance to overland flow, and land-surface hydrology, among other effects. In addition, the temperature regime can impact rates of hillslope soil motion by, for example, influencing the frequency and magnitude of frost heave within the soils. The complexity of biologic-hydrologic-geomorphic feedbacks makes it difficult to generalize about how future changes in climate might impact erosion rates or patterns; much depends on the particular suite of processes and materials present, and on the particular nature of changes in precipitation and/or temperature. Assessment of the potential impact of future climate change on erosion patterns would require the construction and analysis of scenarios with varying climate states.

The second assumption regarding climate lies in the calibration method. In calibrating models based on post-glacial landscape development, the implicit assumption was made that the climate during that time period is comparable to the present climate, at least to the extent that it reflects rainfall, runoff, and soil creep processes. This assumption introduces some degree of error in the analysis, because climate in this portion of North

America is known to have varied to some extent over the post-glacial period. Thus, even if future climate remained unchanged relative to the present day, some uncertainty in model forecasts would result from the imperfect knowledge of environmental conditions during the calibration period. Assessing the degree of error introduced by these uncertainties would require some form of probabilistic or scenario-based calibration and forward propagation analysis.

Without a formal uncertainty analysis, it is difficult to place quantitative bounds on the projected erosion rates and patterns. However, some confidence may be gained from the fact that two rather different models point toward generally similar erosion patterns. In particular, the agreement between the models in terms of locations of focused erosion suggests that these spatial patterns are likely to be robust. To further improve confidence in the performance of these models, it would be necessary to conduct a comprehensive study of the sensitivity of their predictions to errors and uncertainties in the input parameters and boundary conditions.

F.3.2.6.6 Forward Modeling: Use of the Results in the Long-Term Performance Assessment

As discussed above, landscape evolution modeling predicts that extension and deepening of gullies has the greatest potential for disturbance of waste located at the West Valley Site. The range of potential impacts can be investigated using the simplified, single gully model described in Appendix G, Section G.5. In this model concept, the rate of soil loss from a gully with a triangular cross-section in both horizontal and vertical planes may be characterized using the stable angle between the ground surface and sides of the gully and the rates of advance and downcutting of the gully. Site-specific data supporting an estimate of stable angle of 21 degrees is presented in Appendix F, Section F.2.3.1. The rates of development of gullies are reported to have high initial values that decrease with time with possible ultimate re-filling of the gully (Nachtergaele et al. 2002). Site-specific estimates of the initial rate of gully advance of 0.4 to 0.7 meters (1.31 to 2.30 feet) per year are discussed in Section F.2.3.3. Site-specific estimates of initial rate of downcutting range from 0.05 meters (0.16 feet) per year from longitudinal profile measurements along Franks Creek (Section F.2.2) to 0.01 meters (0.03 feet) per year from OSL measurements along Buttermilk Creek (Section F.2.2). Gully downcutting rates based on the landscape evolution modeling are on the order of 0.0015 meters (0.0049 feet) per year consistent with the estimated long-term downcutting rate of 0.001 meters (0.003 feet) per year along Buttermilk Creek (Section F.2.2). Estimates of human health impact developed using the single gully model and the higher of these estimates of rates of gully advance and downcutting are presented in Appendix H.

F.4   References

ACE (U.S. Army Corps of Engineers), 1993 and 2002, *Users Manual for the Hydraulic Design Package for Channels (SAM)*, Draft, U.S. Army Corps of Engineers, Waterways Experiment Station, Vicksburg, Mississippi, April 2.

Albanese, J. R., S. L. Anderson, R. H. Fakundiny, S. M. Potters, W. G. Rogers, and L. F. Whitbeck, 1984, *Geologic and Hydrologic Research at the Western New York Nuclear Service Center, West Valley, New York*, U.S. Nuclear Regulatory Commission, NUREG/CR-3782, Washington, DC, June.

Anderson, R. S., Finkel, R. C., Repka, J. L., 1997, Cosmogenic dating of fluvial terraces, Fremont River, Utah, Earth and Planetary Science Letters, v. 152, Issue 1-4, pp. 59-73.

Bogaart, P. W., Tucker, G. E., de Vries, J. J., 2003, Channel network morphology and sediment dynamics under alternating periglacial and temperate regimes: a numerical simulation study, Geomorphology, v. 54, Issue 3-4, pp. 257-277.

Boothroyd, J. C., B. S. Timson, and R. H. Dana, Jr., 1979, *Geomorphic and Erosion Studies at the Western New York Nuclear Service Center, West Valley, New York*, U.S. Nuclear Regulatory Commission, NUREG/CR-0795, Washington, DC, December.

Boothroyd, J. C., B. S. Timson, and L. A. Dunne, 1982, *Geomorphic Processes and Evolution of Buttermilk Valley and Selected Tributaries, West Valley, New York*, Fluvial Systems and Erosion Study, Phase II, U.S. Nuclear Regulatory Commission, NUREG/CR-2862, July.

Brownlie, W. R., 1981, Predictions of Flow Depth and Sediment Discharge in Open Channels, Report No. KH-R-43A, California Institute of Technology, Report No. KH-R-43A, November.

Camelbeek T., Martin, H., Vanneste K., Meghraoui M., Verbeeck K., and Brondeel M., 2001, Geomorphic evidence of active faulting in slow deformation area: the exemple of the Lower Rhine Embayment, Seismic Workshop, Han sur Lesse, 13-17 March 2001, Volume 31-34.

Chow, V. T., D. R. Maidment, and L. W. Mays, 1988, *Applied Hydrology*, McGraw-Hill Publishing Company, New York.

Clevis, Q., Tucker, G. E., Lock, G., Lancaster, S. T., Gasparini, N. M., and Desitter, A., 2006, A simple algorithm for the mapping of TIN data onto a static grid: applied to the stratigraphic simulation of river meander deposits: Computers and Geosciences, v. 32.

Collins, D. B. G., R. L. Bras, and G. E. Tucker, 2004, Modeling the effects of vegetation-erosion coupling on landscape evolution. Journal of Geophysical Research, Vol. 109.

Copeland, R. R., D. S. Bledenharn, and J. C. Fischenich, 2000, *Channel-Forming Discharge*, U.S. Army Corp of Engineers, ERDC/CHL CHETN-VII-5, December.

Crosby, B. T., Gasparini, N. M., Whipple, K. X., Wobus, C. W., 2007, Formation of fluvial hanging valleys: Theory and simulation, Journal of Geophysical Research, Vol. 112.

Dames and Moore, Inc., 1987, *Application of the CREAMS Computer Model to a Portion of the West Valley Demonstration Project Site*, CIN0193:SEA-69, July 29.

Dietrich, W. E., Bellugi, D., Heimsath, A. M., Roering, J. J., Sklar, L., and Stock, J. D., 2003, Geomorphic transport laws for predicting landscape form and dynamics, *in* Wilcock, P. R., and Iverson, R., eds., Prediction in geomorphology, Washington, DC, American Geophysical Union.

Doyle, M. W., D. Shields, K. F. Boyd, P. B. Skidmmore, and D. Dominick, 2007, Channel-Forming Discharge Selection in River Restoration Design, J. Hydr. Engrg. Volume 133, pp. 831-837, July.

Dunne T., and R. Black, 1970, Partial area contributions to storm runoff in a New England watershed, *Water Resources Research*, 6, 1297-1311.

Dunne, T., 1978, Field studies of hillslope flow processes, Hillslope Hydrology.

Eagleson, P.S., 1978, Climate, soil, and vegetation: 2. the distribution of annual precipitation derived from observed storm sequences: Water Resources Research, v. 14, p. 713-721.

Elliot, W. J., A. M. Liebenow, J. M. Laflen, and K. D. Kohl, 1989, A Compendium of Soil Erodibility Data from WEPP Cropland Soil Field Erodibility Experiments 1987 and 1988, NSERL Report No. 3, The Ohio State University, and USDA Agricultural Research Service.

Ellis, K. G., H. T. Mullins, and W. P. Patterson, 2004, Deglacial to middle Holocene (16,600 to 6000 calendar years BP) climate change in the northeastern United States inferred from multi-proxy stable isotope data, Seneca Lake, New York: Journal of Paleolimnology, v. 31, p. 343-361.

Fairbanks, R. G., R. A. Mortlock, T. C. Chiu, L. Cao, A. Kaplan, T. P. Guilderson, T. W. Fairbanks, A. L. Bloom, P.M. Grootes, and M.-J. e Nadeau, 2005, Radiocarbon calibration curve spanning 0 to 50,000 years BP based on paired ^{230}Th/^{234}U/^{238}U and ^{14}C dates on pristine corals, Quaternary Science Reviews, v. 24, p. 1781-1796.

Fakundiny, R. H., 1985, Practical applications of geological methods at the West Valley low-level radioactive waste burial ground, western New York: Northeastern Environmental Science, v. 4, p. 116-148.

Flores-Cervantes, J. H., R. L. Bras, and E. Istanbulluoglu, 2006, Development of gullies on the landscape: A model of headcut retreat resulting from plunge pool erosion, Journal of Geophysical Research, v. 111.

Foster, G. R., 1982, "Modeling the Erosion Process", in *Hydrologic Modeling of Small Watersheds*, C. T. Haan, H. P. Johnson, and D. L. Brakensiek (eds).

Galbraith R., and G. Laslett, 1993, Statistical models for mixed fission track ages, Nuclear tracks and radiation measurements, ISSN 0969-8078.

Gasparini, N. M., R. L. Bras, and K. X. Whipple, 2007, Predictions of steady state and transient landscape morphology using sediment-flux-dependent river incision models, Journal of Geophysical Research, v. 112.

Goldenfeld, N., and L. P. Kadanoff, 1999, *Science*, Vol. 284, pp. 87–89, April 2.

Gomez, B., and M. Church, 1989, An assessment of bed load sediment transport formulae for gravel bed rivers: Water Resources Research, v. 25, p. 1161-1186.

Hancock, G. R., K. G. Evans, G. R. Willgoose, D. R. Moliere, M. J. Saynor, and R. J. Loch, 2000, Medium term erosion simulation of an abandoned mine site using the SIBERIA landscape evolution model. *Australian Journal of Soil Research* 38:249-263.

Hancock, G., and G. Willgoose, 2001a, *The Production of Digital Elevation Models for Experimental Model Landscapes,* Earth Surface Processes and Landforms 26, 475-490 (2001).

Hancock, G., and G. Willgoose, 2001b, *Use of a Landscape Simulator in the Validation of the SIBERIA Catchment Evolution Model: Declining Equilibrium Landforms*, Department of Civil, Surveying, and Environmental Engineering, University of Newcastle Callaghan, "Water Resources Research," Volume 37, No. 7, Pages 1981-1992, New South Wales, Australia, July.

Hancock, G. R., G. R. Willgoose, and K. G. Evans, 2002, *Testing of the Siberia Landscape Evolution Model Using The Tin Camp Creek, Northern Territory, Australia, Field Catchment*, Earth Surface Processes, Landforms 27, 125-143 (2002).

Hancock G. R., 2003a, The effect of catchment aspect ratio on geomorphological descriptors, In *Prediction in Geomorphology*, Peter Wilcock and Richard Iverson editors, American Geophysical Union monograph, Washington.

Hancock G. R., 2003b, The use of landscape evolution models in mining rehabilitation design. *Journal of Geotechnical and Geoenvironmental Engineering*, in review.

Hancock G. R., 2004, The use of landscape evolution models in mining rehabilitation design, Environmental Geology, 46, 561-573.

Hoffman, V. C., 1980, *Geotechnical Analysis of Soil Samples and a Study of a Research Trench at the Western New York Nuclear Service Center, West Valley, New York*, New York Geological Survey Publication No. NYSGS/24.01.030.

Hanks T. C., 1998, Dating and Earthquakes, Review of Quaternary Geochronology.

Hawk, K. L., 1992, Climatology of station storm rainfall in the continental United States: parameters of the Bartlett-Lewis and Poisson rectangular pulses models, unpublished M.S. thesis, Department of Civil and Environmental Engineering, Massachusetts Institute of Technology, 330 pp.

Holcombe, T. L., L. A. Taylor, D. F. Reid, J. S. Warren, P. A. Vincent, and C. E. Herdendorf, 2003, Revised Lake Erie postglacial lake level history based on new detailed bathymetry: Journal of Great Lakes Research, v. 29, p. 681-704.

Howard, A. D., 1980, Thresholds in River Regimes, in Thresholds in Geomorphology, edited by D. R. Coates and J. D. Vitek, pp. 227-258, Allen and Unwin, Concord, Massachusetts.

Howard, A. D., and G. Kerby, 1983, Channel changes in badlands: Geological Society of America Bulletin, v. 94, p. 739-752.

Howard, A., W. Dietrich, and M. Seidl, 1994, Modeling Fluvial Erosion on Regional to Continental Scales: Journal of Geophysical Research, v. 99, p. 13,971- 13,986.

Ibbit, R. P., G. R. Willgoose, and M. J. Duncan, 1999, *Channel Network Simulation Models Compared with Data from the Ashley River, New Zealand*, "Water Resources Research," Volume 35, Number 12, Pages 3975-3890, New Zealand, December.

Ijjasz-Vasquez, E. J., R. L. Bras, and G. E. Moglen, 1992, Sensitivity of a basin evolution model to the nature of runoff production and initial conditions: Water Resources Research, v. 28, p. 2733-2742.

Istanbulluoglu, E., R. L. Bras, H. Flores-Cervantes, and G. E. Tucker, 2005, Implications of bank failures and fluvial erosion for gully development: Field observations and modeling, Journal of Geophysical Research, v. 110.

Julian, J. P., and R. Torres, 2006, Hydraulic erosion of cohesive riverbanks, Geomorphology, v. 76, Issue 1-2, pp. 193-206.

Kirkby, M. J., and L. J. Bull, 2000, Some factors controlling gully growth in fine-grained sediments: a model applied in southeast Spain, Catena, v. 40, Issue 2, pp. 127-146.

Kirkby, M. J., 1995, Modelling the links between vegetation and landforms, Geomorphology, Volume 13, Issue 1-4, pp. 319-335.

LaFleur, R. G., 1979, *Glacial Geology and Stratigraphy of Western New York Nuclear Service Center and Vicinity, Cattaraugus and Erie Counties, New York*, New York State Education Department, U.S. Geological Survey Open File Report 79-989, Albany, New York.

Lancaster, N., J. R. Miller, and J. Sloan, 2001, Response and recovery of the Eel River, California, and its tributaries to floods in 1955, 1964, and 1997, Geomorphology, v. 36, Issue 3-4, pp. 129-154.

Lancaster, S. T., G. E. Grant, and S. K. Hayes, 2003, Effects of Wood on Debris Flow Runout in Small Mountain Watersheds, Submitted to Water Resources Research.

Leopold, L. B., M. G. Wolman, and J. P. Miller, 1964, Fluvial Processes in Geomorphology: San Francisco, W. H. Freeman and Co., 522p.

Madden, E. B., 1993, Modified Laursen Method for Estimating Bed-Material Sediment Load.

Mahan, S. A., 2007, *Informal Memo from USGS Luminescence Dating Lab*, U.S. Geologic Survey, March 15.

Martin, Y., and M. Church, 2000, *Diffusion in Landscape Development Models: On The Nature Of Basic Transport Relations,* Earth Surface Processes and Landforms, Volume 22, Pages 273–279.

Martin, Y. and M. Church, 2003, *Earth Surface Processes and Landforms*, V25, 1011-1024.

Meyer, P. D., and G. W. Gee, 1999, *Information on Hydrologic Conceptual Models, Parameters, Uncertainty Analysis, and Data Sources for Dose Assessments at Decommissioning Sites*, NUREG/CR-6656, U.S. Nuclear Regulatory Commission, Washington, DC, November.

Middleton, G. V., and J. B. Southard, 1984, Mechanics of Sediment Movement: Short Course 3, Society of Economic Paleontologists and Mineralologists.

Millar, R. G., 2004, Theoretical regime equations for mobile gravel-bed rivers with stable banks, Geomorphology, v. 64, Issue 3-4, pp. 207-220.

Muller, E. H., and P. E. Calkin, 1993, Timing of Pleistocene glacial events in New York State, Canadian Journal of Earth Sciences, v. 30, Issue 9, pp. 1829-1845.

Mullins, H. T., E. J. Hinchey, R. W. Wellner, D. B. Stephens, W. T. Anderson Jr., T. R. Dwyer, and A. C. Hine, 1996, Seismic stratigraphy of the Finger Lakes: a continental record of Heinrich Event H-1 and Laurentide ice sheet instability. In: Mullins, N. Eyles, eds. Subsurface Geologic Investigations of New York's

Finger Lakes: Implications for Late Quaternary Deglaciation and Environmental Changes, Geological Society of America special paper 311 p.

Mulvihill, C. I., A. G. Ernst, and B. P. Baldigo, 2005, *Regionalized Equations for Bankfull Discharge and Channel Characteristics of Streams in New York State: Hydrologic Region 6 in the Southern Tier of New York*, U.S. Geological Survey, SIR 2005-5100.

Nachtergaele, J., J. Poesen, D. Oostwoud Wijdenes, and L. Vandekerckhove, Geomorphology, 46, 2002, p. 223-239.

Nash, D. B., 1984, Morphologic Dating of Fluvial Terrace Scarps and Fault Scarps near West Yellowstone, Montana, *GSA Bulletin*, V.95; no.12; p. 1413-1424.

Nicks, A., and G. Gander, 1997, *Cligen Weather Generator,* U.S. Department of Agriculture, Agricultural Research Service Laboratory, Durant, Oklahoma.

Niviere, B., G. Marquis, and J. C. Maurin, 1998, Morphologic Dating of Slowly Evolving Scarps using a Diffusive Analogue: *Geophysical Research Letters*, V.25, p. 2325-2328.

Niviere, B., S. Carretier, M. Giamboni, and T. Winter, 2005, Do river profiles record along-stream variations of low uplift rate?, Journal of Geophysical Research, v. 111, no. F2.

Oehm, B., and B. Hallett, 2005, Rates of soil creep, worldwide: weak climatic controls and potential feedback, Zeitschrift Fur Geomorphologie.

O'Neal, M. A., J. Putkonen, and T. C. Orloff, 2005, Degradation of Unconsolidated Landforms, Geological Society of America, Paper No. 133-4.

Prosser, I. P., and P. Rustomji, 2000, Sediment transport capacity relations for overland flow: Progress in Physical Geography, v. 24, p. 179-193.

Rodriguez-Iturbe, I., and A. Rinaldo, 1999, *Fractal River Basins*, Cambridge University Press, Cambridge, United Kingdom.

Roering, J. J., J. W. Kirchner, and W. E. Dietrich, 1999, Evidence for nonlinear, diffusive sediment transport on hillslopes and implications for landscape morphology: Water Resources Research, v. 35, p. 853-870.

Roering, J. J., K. M. Schmidt, J. D. Stock, W. E. Dietrich, and D. R. Montgomery, 2003, Shallow landsliding, root reinforcement, and the spatial distribution of trees in the Oregon Coast Range, Canadian Geotechnical Journal, v. 40, p. 237-253.

Rosenbloom, N. A., and R. S. Anderson, 1994, Hillslope and channel evolution in a marine terraced landscape, Santa Cruz, California: Journal of Geophysical Research, B, Solid Earth and Planets, v. 99, p. 14, 013-14, 029.

Snyder, N. P., K. X. Whipple, G. E. Tucker, and D. J. Merritts, 2002, Interactions between onshore bedrock-channel incision and nearshore wave-base erosion forced by eustasy and tectonics: Basin Research, v. 14, p. 105-127.

Solyom, P. B., and Tucker, G. E., 2004, Effect of limited storm duration on landscape evolution, drainage basin geometry, and hydrograph shapes: Journal of Geophysical Research, v. 109, p. 13.

Stock, J. D., and D. R. Montgomery, 1999, Geologic constraints on bedrock river incision using the stream power law: Journal of Geophysical Research B: Solid Earth, v. 104, p. 4983-4993.

Summerfield, M. A., 1986, Tectonic geomorphology: macroscale perspectives, Progress in Physical Geography, v. 10, no. 2, pp. 227-238.

Tomkin, J. H., M. T. Brandon, F. J. Pazzaglia, J. R. Barbour, and S. D. Willett, 2003, Quantitative testing of bedrock incision models for the Clearwater River, NW Washington State: Journal of Geophysical Research B: Solid Earth, V. 108, p, ETG 10-1-10-19.

Tucker, G. E., 2004, Drainage basin sensitivity to tectonic and climatic forcing: implications of a stochastic model for the role of entrainment and erosion thresholds: Earth Surface Processes and Landforms, v. 29, p. 401-422.

Tucker, G. E., and K. X. Whipple, 2002, Topographic outcomes predicted by stream erosion models: Sensitivity analysis and intermodel comparison: Journal of Geophysical Research B: Solid Earth, v. 107, p. doi:10.1029/2001JB000162.

Tucker, G. E., and R. L. Bras, 1998, Hillslope processes, drainage density, and landscape morphology: Water Resources Research, v. 34, p. 2751-2764.

Tucker, G. E., and R. L. Bras, 2000, A stochastic approach to modeling the role of rainfall variability in drainage basin evolution: Water Resources Research, v. 36, p. 1953-1964.

Tucker, G. E., and R. Slingerland, 1997, Drainage basin responses to climate change: Water Resources Research, v. 33, p. 2031-2047.

Tucker, G. E., S. T. Lancaster, N. M. Gasparini, and R. L. Bras, 2001a, The Channel-Hillslope Integrated Landscape Development (CHILD) Model, in *Landscape Erosion and Evolution Modeling,* edited by R. S. Harmon and W. W. Doe III, Kluwer Academic/Plenum Publishers, pp. 349-388.

Tucker, G. E., S. T. Lancaster, N. M. Gasparini, R. L. Bras, and S. M. Rybarczyk, 2001b, An Object-Oriented Framework for Hydrologic and Geomorphic Modeling Using Triangulated Irregular Networks, *Computers and Geosciences,* 27(8), pp. 959-973.

USDA (U.S. Department of Agriculture), 1976, *Procedures for Determining Rates of Land Damage, Land Depreciation, and Volume of Sediment Produced by Gully Erosion*, Soil Conservation Service, Technical Release No. 32.

USDA (U.S. Department of Agriculture), 1984, *User's Guide for the CREAMS Computer Model*, Technical Release No. 72, Soil Conservation Service.

USDA (U.S. Department of Agriculture), 1986, *Urban Hydrology for Small Watersheds,* Soil Conservation Service, Technical Release No. 55, June.

USDA (U.S. Department of Agriculture), 1995, *USDA − Water Erosion Prediction Project (WEPP) Hillslope Profile and Watershed Model Documentation*, NSERL Report No. 10, National Soil Erosion Research Laboratory, West Lafayette, IN.

USDA (U.S. Department of Agriculture), 2004, Cattaraugus County soil survey downloaded from the NRCS soils data mart located at http://soildatamart.nrcs.usda.gov/Survey.aspx?County=NY009.

van der Beek, P. and P. Bishop, 2003, Cenozoic river profile development in the Upper Lachlan catchment (SE Australia) as a test quantitative fluvial incision model: Journal of Geophysical Research B: Solid Earth, v.108, p. ETG 11-1-11-27.

Weltz, M. A., H. D. Fox, S. Amer, F. B. Pierson and L. J. Lane, 1992, "Erosion Prediction on Range and Grazing Lands: A Current Perspective", *in Grazingland Hydrology Issues: Perspectives for the 21st Century*.

Werner, B. T., 1999, Complexity in Natural Landform Patterns, *Science*, Vol. 284, pp. 102–103, April 2.

Whipple, K. X., N. P. Snyder, and K. Dollenmayer, 2000, Rates and Processes of Bedrock Incision by the Upper Ukak River since the 1912 Novarupta Ash Flow in the Valley of Ten Thousand Smokes, Alaska: Geology (Boulder), V.28, p. 835-838.

Whipple, K. X., and G. E. Tucker, 2002, Implications of sediment-flux dependent river incision models for landscape evolution, *Journal of Geophysical Research,* v. 107, no. B2, DOI 10.1029/2000JB000044.

Willgoose, G. R., 1989, *A Physically Based Channel Network and Catchment Evolution Model*, Ph.D. Dissertation, Massachusetts Institute of Technology, April.

Willgoose G. R., R. L. Bras, and I. Rodriguez-Iturbe, 1991, "A physical explanation of an observed link area-slope relationship," *Water Resources Research*, 27(7):1697-1702.

Willgoose, G., 1994, *A Physical Explanation for an Observed Area-slope-elevation Relationship for Catchments with Declining Relief,* Department of Civil Engineering and Surveying, University of Newcastle, "Water Resources Research," Volume. 30, Number 2, Pages 151-159, Newcastle New South Wales, Australia, February.

Willgoose, G., 2005, Mathematical modeling of whole landscape evolution: Annual Review of Earth and Planetary Sciences, v. 33, p. 443-459.

Wischmeier, W. H., and D. D. Smith, 1978, *Predicting Rainfall Erosion Losses – A Guide to Conservation Planning*, U.S. department of Agriculture, Agriculture Handbook No. 537.

Wolman, M. G. and J. P. Miller, 1960, "Magnitude and Frequency of Forces in Geomorphic Processes", *Journal of Geology*, Vol. 68, pp. 54–74.

WVNS (West Valley Nuclear Services Company, Inc.), 1993a, *Environmental Information Document, Vol. III, Hydrology: Part 3 of 5, Erosion and Mass Wasting Processes*, WVDP-EIS-009, Rev. 0, West Valley, New York, February.

WVNS (West Valley Nuclear Services Company, Inc.), 1993b, *Environmental Information Document, Vol. III, Hydrology: Part 1, Geomorphology of Stream Valleys*, WVDP-EIS-009, Rev. 0.

WVNS (West Valley Nuclear Services Company, Inc.), 1993c, *Environmental Information Document, Vol. III, Hydrology: Part 2, Surface Water Hydrology*, WVDP-EIS-009, Rev. 0, West Valley, New York, January.

WVNS (West Valley Nuclear Services Company, Inc.), 1993d, *Environmental Information Document, Vol. III, Hydrology: Part 4 of 5, Groundwater Hydrology and Geochemistry*, WVDP-EIS-009, Rev. 0, West Valley, New York, February.

WVNS (West Valley Nuclear Services Company, Inc.), 1993e, *Environmental Information Document, Vol. XI, Ecological Resources of the Western New York Nuclear Service Center*, WVDP-EIS-010, Rev. 0, West Valley, New York.

WVNS (West Valley Nuclear Services Company, Inc.), 1993f, *Environmental Information Document, Vol. III, Hydrology: Part 3 of 5*, Erosion and Mass Wasting Processes, WVDP-EIS-009, Rev. 0, West Valley, New York, January.